CHAPTER 3

MATERIALS AND EXPERIMENTAL METHOD

It has been established in recent years that polymer-based composites reinforced with a small percentage of strong fillers can significantly improve the mechanical, thermal and barrier properties of the pure polymer matrix. Moreover, these improvements are achieved through conventional processing techniques without any detrimental effects on process ability, appearance, density and aging performance of the matrix. Now-a-day's hybrid polymers, which are the hybrid structure of inorganic-organic nano-composite materials are being used to impart the combination of scratch resistance with dirt-repellent effect, high transparency, special barrier properties or antimicrobial function to the material.

From the available literature and the best possible commercial applicability of polymer/SiO_2 nanocomposite product, the entire study is based on effect of SiO_2 nano particles on different polymers used in textiles. In the present study selection of material has been made on the bases of commercial viability and utility of particular polymer in specific form, like polyamide in film form, polypropylene in filament form and polyester in fabric form.

The experimental plan was based on application of silica nano particles to different textiles in various forms viz. film, filament and fabric. The prepared polymer silica nanocomposite textiles were analyzed by standard techniques for evaluating changes in structural and mechanical properties and compared with respective pure material.

For effective evaluation the experimental work was conducted in three parts;

Part – I: deals with preparation of polymer (polyamide) silica nanocomposite film and its evaluation in terms of structural and mechanical behavior. The selection of PA silica nanocomposite film was made on the bases of its commercial applicability as packaging material.

Part – II: In this part, filament containing different proportions of silica nanoparticles were prepared using melt spinning pilot plant. The evaluation of prepared polymer (polypropylene) silica nanocomposite filaments was evaluated in terms of

improvement in their structural and mechanical properties and compared with pure filament. This was selected on the basis of wide applicability of polypropylene in technical textile.

Part – III: Polymer silica nanocomposite fabrics were prepared by incorporating different proportions of silica nano particles to polymeric (polyester) fabric by pad-dry-cure method. The prepared composite fabric was analyzed in terms of change in their structural and mechanical properties and compared with pure polymeric fabric.
The main purpose of selecting polyester fabric with nano silica particles was to investigate the structural and mechanical properties to consider it as high performance textiles.

3.1 MATERIALS

3.1.1 Film

Polymer Chips: Material used in the experiment was polyamide chips procured from reputed company of India having following specifications.

Table 3.1 Specifications Polyamide chips

Type	Viscosity (poise)	H_2O (ppm)	TiO_2 (%)	Chip Size (mm)
Semi Dull (SD)	2.47± 0.03	≤ 800	0.29 ± 0.05	2.5 D x 2.5 L

ppm: parts per million

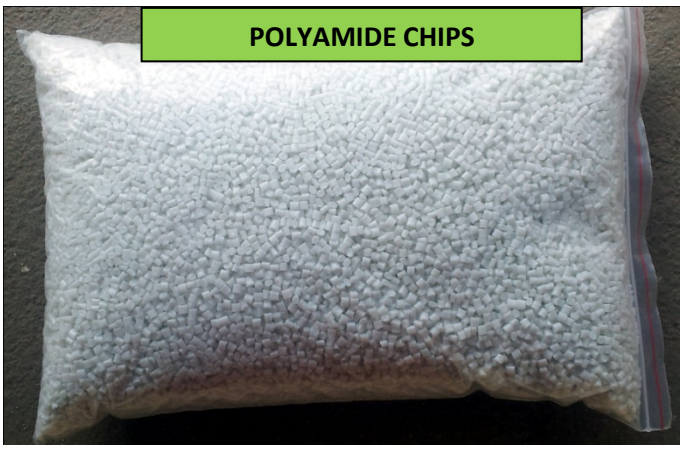

Figure 3.1 Polyamide chips

Chemicals:

Silica (SiO_2) nano particles with average size less than 100 nm were procured from a reputed international company, having specifications as mentioned below.

Table 3.2 SiO_2 Specifications

Particle size	< 100 nm
Molecular weight	60.08 Mw
Surface Area	175-225 m^2/g
pH	9
Melting point	>1600°C
Density	2.2 to 2.6 g/ml at 25°C
Bulk density	0.068 g/ml

Formic acid LR (Laboratory reagent grade) supplied by reputed local supplier. All the chemicals and chips were used in the experiment without any further purification.

3.1.2 Filament

Polymer Chips: The polymer used for the manufacturing of nanocomposite filaments was polypropylene homopolymer chips were supplied by one of the reputed company of India. The polymer is fibre grade polymer with 16 MFI (melt flow index).

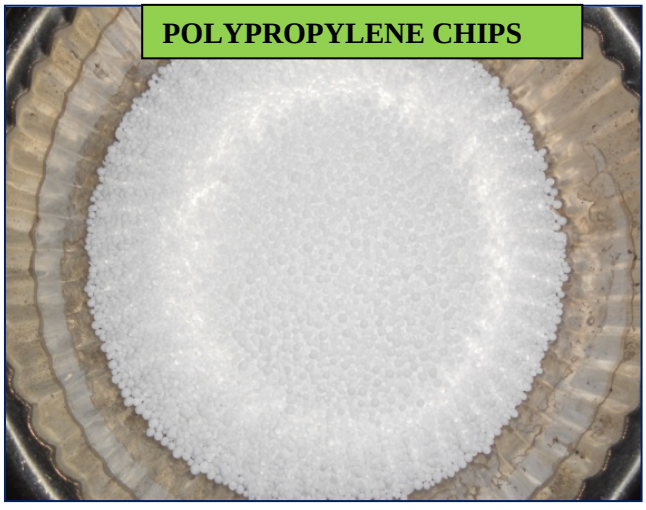

Figure 3.2 Polypropylene chips

3.1.3 Fabric

Polymeric fabric: Polyester fabric was mild scoured (5% soap Lisaapol L, 2% soda ash and boiled for 15 min.) before use. Table 3.3 shows the specifications of polyester fabric.

Table 3.3 Fabric specifications

Sample	Material Specification					
	Denier/fil.		Fabric Setting	Weave	GSM	Thickness (mm)
	Warp	Weft	Ends/cm, Pick/cm			
100% Polyester	128/36	146/36	36/28	Plain	109.7	0.21

Chemicals:

Polyacrylamide, Lissapol L were used for this experiment without further purification. The chemicals are of laboratory reagent grade supplied by reputed supplier.

3.2 EQUIPMENTS FOR EXPERIMENTAL WORK

Various equipments used at different stages of the work are mentioned below;

3.2.1 Equipments used for preparation of nanocomposite materials

3.2.1.1 Magnetic stirrer with heater (for preparation of film)

Specifications: High speed magnetic stirrer with temperature range of 40 to 120°C.

3.2.1.2 Melt spinning pilot plant (for preparation of filament)

Specifications: Melt spinning pilot plant was manufactured by reputed manufacturer of Vadodara, Gujarat with following specifications:

Table 3.4 Melt spinning pilot plant specifications

Make	AEC/25-4/MUL
Denier range	50 to 2000
Product	POY, FOY and FDY
Extruder	Four zone extruder with 25mm diameter of screw
	L/D ratio of screw: 30
	Screw rpm: 0 to 50
	Barrel with 75mm outer diameter and 25mm inner diameter
	Four heating zone with individual temperature control
	Maximum output capacity: 10 kg/hr.
	Ceramic perforated heater
Melt pressure regulator	350 bar maximum
Metering pump assembly	3 C.C. metering pump of rectangular type design with single inlet and outlet.
	3 Kw one temperature control zone with cartridge type heater
Spinning Head	Stainless steel
	02 pack body
	02 distribution plates

	3 Kw Cartridge heater
Quenching Chamber	MOC stainless steel
	Honey comb type S.S. chamber
	Water chilling unit of 1 ton capacity with temperature range from 5°C to 20°C.
	Blower with 400 CFM
Spin finish pump	Capacity: 0.08 cc/rev
Godets	Two godets with hard crome mirror finish
	Godet with cold and hot facility: 0 to 200°C
	Godet dia: 125 mm, 150mm length, 3500 mpm speed
Winder	speed: upto 3500 mpm
Spinneret cleaning oven	Ultrasonic cleaning oven for cleaning the spinneret: 500°C

3.2.1.3 Equipment used for preparation of polymeric nanocomposite fabric

3.2.1.3.1 Padding mangle with curing chamber

The specifications of the machine are given below:

- Padding mangel: Two bowl padding mangle with digital hydraulic pressure gauge
- Curing Chamber
- Pin type rail with to and fro facility
- Digital control of temperature 60 to 300°C and speed 30 sec to 180 sec. for 2 meter length of fabric.

3.2.2 Equipments for testing and analysis

To achieve the aim i.e. structural and mechanical changes in polymer silica nanocomposite, for testing these properties, equipments were classified into two groups:

1) Structural properties
2) Mechanical properties

1) Structural properties

- **Scanning Electron Microscope (SEM)** Model JSM-5610 LV Japan, used for analyzing surface morphology, size and shape; with Oxford Inca software for elemental analysis (EDX).
- **Fourier Transform Infrared Spectroscopy (FTIR)** FTIR Spectroscopy Nicolet iS10 FT-IR Spectrometer (Thermo Scientific, Japan) was used for analysis of chemical composition.
- **X-Ray diffraction (XRD)** Model X'Pert Pro PANalytical, Singapore for evaluation of crystalline/amourphous structure of prepared nanocomposite material.
- **Differential scanning calorimeter (DSC)** Model DSC 6000, Perkin Elmer, USA; for thermal analysis.
- **Melt flow Indexer (MFI)** Model from Hem-Tech Corporation, India; for determining melt flow index.

2) Mechanical Properties

- **Tensile strength Tester** (Lloyd LRX Model, U.K), for tensile tests of the samples.
- **Tearing Tester** Elmendorf tearing tester used for the study of tearing property of fabric.
- **Crease recovery tester** Shirley Crease Recovery tester used for the study of crease recovery angle of fabric.

3.3 EXPERIMENTAL METHODS

3.3.1 Part-I: Preparation of Polymer/SiO_2 nanocomposite film

Accurately weighed silica nano particles were suspended in formic acid under continuous stirring as shown in figure 3.3. The polyamide (PA) chips were added and mixture was heated to 60°C for 1 hr. The nanocomposite mixture was poured on a cleaned smooth petridish glass surface, compressed manually with another glass surface and solvent was allowed to evaporate up to dryness for 12 hrs at room temperature. Schematic presentation of polyamide/nano silica composite film preparation is shown in figure 3.4.

Figure 3.3 Magnetic stirrer with heater

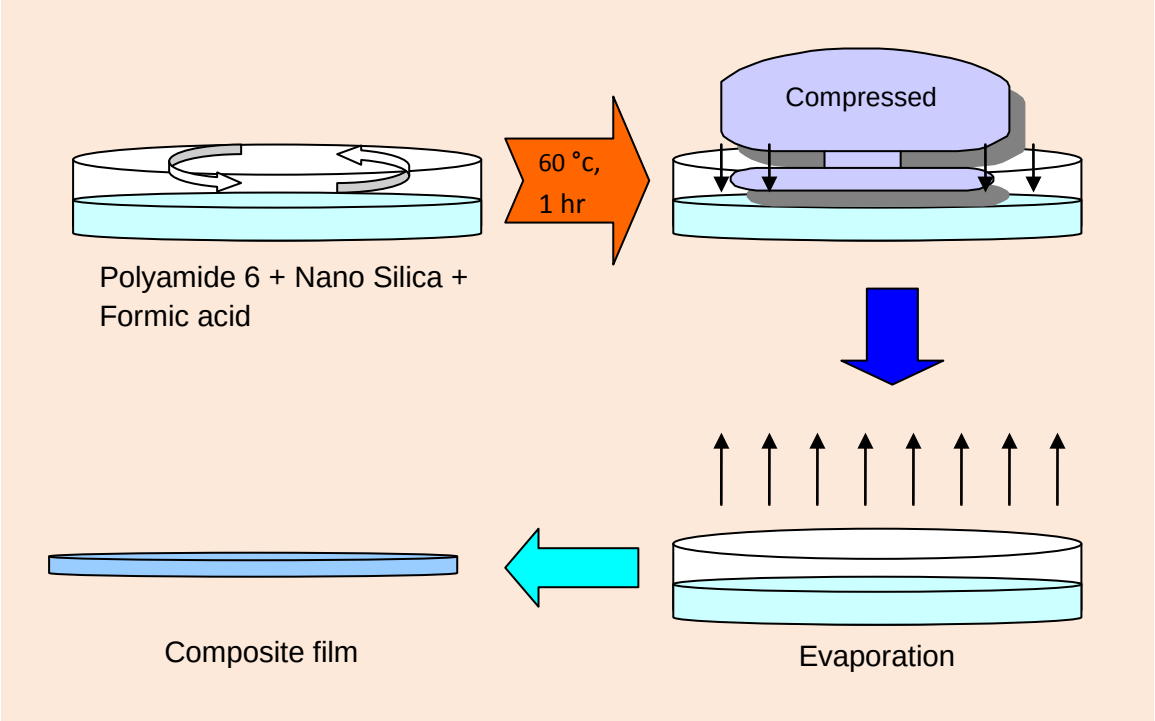

Figure 3.4 Schematic diagram of polyamide silica nanocomposite film preparation

Different formulations used to prepare polyamide silica nanocomposite film are given in table 3.5.

Table 3.5 Compositions of nanocomposites preparation by formic acid mixing

Sample	Silica (gm)	Silica (wt %)	Polyamide (gm)	Formic Acid (ml)
PA	0.00	0.0	10	100
NPA1	0.01	0.1	10	100
NPA2	0.03	0.3	10	100
NPA3	0.05	0.5	10	100
NPA4	0.07	0.7	10	100
NPA5	0.10	1.0	10	100

PA: polyamide, NPA: Nano silica loaded polyamide

3.3.2 Part-II: Preparation of Polymer/SiO_2 nanocomposite filament

Manufacturing of the Polypropylene / SiO_2 nanocomposite filaments were done in two stages: a) mixing of polypropylene (PP) granules with SiO_2 nanoparticles through twin screw extruder; b) extrusion of the nanocomposite filaments by melt spinning on pilot plant.

The SiO_2 nanoparticles were mixed with polypropylene chips in various concentrations of 0.10%, 0.30%, 0.50%, 0.70%, 1.00%, 1.25% and 1.50% on the basis of weight of PP chips. These values were selected to study the influence of increase in SiO_2 nanoparticles in PP structure on its performance. The mixing of the two components was done in twin screw extruder to get homogeneous mixture. The mixture of polypropylene with SiO_2 nanoparticle chips was then fed into the hopper of the melt spinning pilot plant as shown in figure 3.5. Monofilament yarn with above mentioned percentages of SiO_2 concentrations were spun at optimized spinning conditions on melt spinning pilot machine. The extruded filaments were passed through a water bath containing chilled water having temperature 4˚C. Finally the filaments were wound on to package. A control sample of pure PP was also manufactured at the same spinning parameters for comparative study with the PP / SiO_2 nanocomposite filaments. The prepared samples are shown in figure 4.14. The pilot plant parameters were optimized experimentally by taking pilot trials. The optimized parameters were used throughout the study to retain consistent and desired quality of yarn. The parameters optimized and used for the study are appended in table 3.6.

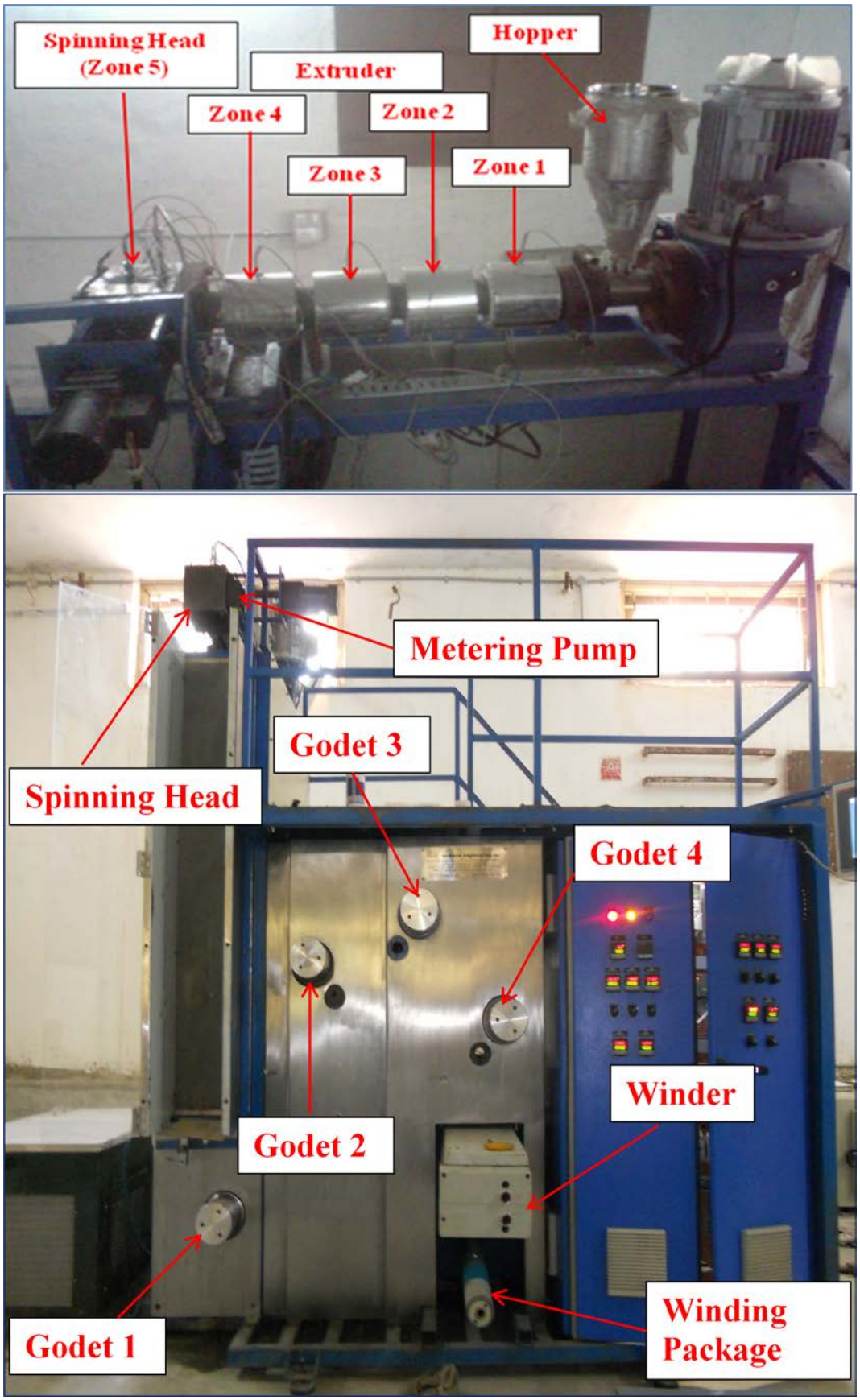

Figure 3.5 Melt spinning pilot plant

Table 3.6 Spinning Parameters

ZONES		**PARAMETERS**
Extruder Temperature	Zone 1	165 ˚C
	Zone 2	200 ˚C
	Zone 3	210˚C
	Zone 4	215˚C
Spinning Head	Zone 5	235˚C
Metering Pump	Zone 6	230˚C
Godet Temperature	Godet 1	R.T*
	Godet 2	R.T*
	Godet 3	R.T*
	Godet 4	R.T*
Extruder Pressure		40 bar
Metering Pump Speed		5 rpm
Godet Speed	Godet 1	0 mpm
	Godet 2	0 mpm
	Godet 3	300 mpm
	Godet 4	400 mpm
Winder	Friction Roller	400 mpm
	Grooved Roller	250 mpm

*R.T = Room Temperature

Different formulations used to prepare polypropylene silica nanocomposite filaments are given in table 3.7.

Table 3.7 Compositions of polypropylene SiO_2 nanocomposite filament

Sr. No.	Sample	Silica (wt %)
1	**PP**	0.0
2	**NPP1**	0.1
3	**NPP2**	0.3
4	**NPP3**	0.5
5	**NPP4**	0.7
6	**NPP5**	1.0
7	**NPP6**	1.25
8	**NPP7**	1.50

PP: polypropylene, NPP: Nano silica loaded polypropylene

3.3.3 Part-III: Preparation of Polymer/SiO_2 nanocomposite fabric

3.3.3.1 Preparation of silica nano padding liquor

Nano silica particles were applied to polyester fabric samples using pad-dry-cure method. The coating solutions were prepared using 1gpl, 2.5gpl, and 5gpl concentration. For 1 gpl solution, 0.1 gm nano particles were added in 100 ml water with 5 gm Lissapol L surfactant and 10gm polyacrylamide binder. The mixture was then stirred using magnetic stirrer at 250 rpm for 30 minutes at 60^oC temperature. Likewise all concentration solutions were prepared.

3.3.3.2 Application to fabric

Polyester fabric sample (size : 40cm x 50cm) immersed in padding liquor at room temperature for 10 minutes and then passed through a two bowl laboratory padding mangle, which was running at a speed of 15 rpm with a pressure of 1.75 Kg/cm^2 using

2-dip 2-nip padding sequence at 70% expression for polyester fabric. The padded substrates were dried at 80^{o}C for 5-6 minutes. Finally cured at 140^{o}C temperature for 3 minutes, in a preheated curing chamber.

Figure 3.6 Two bowl padding mangle with stenter

Different formulations used to prepare polyester silica nanocomposite fabrics are given in table 3.8.

Table 3.8 Compositions of polyester SiO_2 nanocomposite fabric

Sr. No.	SAMPLE	COMPOSITIONS
1	PT	Polyester fabric without SiO_2
2	NPT1	Polyester fabric with 1 gpl SiO_2
3	NPT2	Polyester fabric with 2.5 gpl SiO_2
4	NPT3	Polyester fabric with 5 gpl SiO_2

PT: polyester, NPT: Nano silica loaded polyester

3.3.4 Testing and Analysis

3.3.4.1 Structural Properties

3.3.4.1.1 Scanning Electron Microscopy (SEM)

Scanning Electron Microscopy Model JSM 5610LV, Version 1.0, Jeol, Japan as shown in figure 3.8, was used to characterize the nano particles shape and size. The elemental analysis (EDX) of prepared pure and silica nanocomposite film, filament and fabric were performed on scanning electron microscope (SEM) using Oxford Inca Software for elemental analysis. The instrument reports the presence of elements in pure and oxide state qualitatively. SEM image was formed using transmitted electrons (instead of the visible light) which can produce magnification up to 1,00,000 X with resolution up to 100A^{o}. Stabilized solution of copper nano coated aluminum sheet was dried and illuminated under scanning electron microscope. Scanned images with different magnification and resolution were recorded on computer.

The pure and silica nanocomposite film, filament and fabric were placed on carbon coated aluminum sheet and illuminated under scanning electron microscope. Scanned images with different magnification and resolution recorded on computer. The scanning electron microscopy has the great advantage of its much larger depth of focus.

Figure 3.7 Scanning electron microscope

3.3.4.1.2 Fourier Transform Infrared Spectroscopy (FTIR)

The chemical composition of the control sample and nanocomposite filaments was evaluated using FTIR Spectroscopy, Nicolet IS10 FT-IR Spectrometer (Thermo Scientific). FTIR is a technique which is used to obtain an infrared spectrum of absorption, emission, photoconductivity or Raman scattering of a solid, liquid or gas. A FTIR spectrometer simultaneously collects spectral data in a wide spectral range (400 to 4000 cm^{-1}). This confers a significant advantage over a dispersive spectrometer which measures intensity over a narrow range of wavelengths at a time. The photograph of FTIR instrument and its working principle is shown in figure 3.8.

Figure 3.8 FTIR Spectrometer instrument

3.3.4.1.3 X-Ray diffraction (XRD)

The characterization of treated and untreated samples was done using PANalytical XRD as shown in figure 3.9. The XRD of all the samples was done within the 2θ range of 5˚ to 80˚ at the scan speed of 3˚ per minute, using Cu-K_α radiation of wavelength 1.5406Å. The diffraction profiles were obtained for individual samples. The X-Ray Diffractometer X'pert Pro PANalytical, Singapore make was used. Here in all XRD graphs the X axis represents 2θ values and Y axis represents intensity of the material.

Figure 3.9 X-Ray diffractometer

3.3.4.1.4 Differential scanning calorimeter (DSC)

The thermal analysis of the prepared samples was performed using differential scanning calorimeter model 6000, Perkin Elmer, USA shown in figure 3.10.

The sample preparation was done by cutting the sample into small piece and weighing them accurately. The weighed sample was placed in aluminium pan and sealed. In DSC the given sample and the reference material (which does not undergo any transition in the temperature range of interest, here empty pan were taken as reference material) were kept in separate crucibles in the same furnace which is heated at programmed heating rate. There was an extra heater provided just below the crucible

carrying the sample, which operates on the instructions received from the device measuring the temperature difference (ΔT) between the sample and the reference, to maintain the ΔT as zero. Thus the DSC records the extra heat (ΔH) supplied per unit time to the sample crucible as a function of the overall temperature of the furnace.

The DSC of the samples was carried out under the heat – cool – heat mode as given below:

- 1st Heating – Heating from 30˚C to 180˚C (for Polypropylene), 30˚C to 300˚C (for Polyamide and Polyester); Rate of heating - 10˚C/ min
- Cooling - From 180 ˚C to 30˚C (for Polypropylene), 300˚C to 30˚C (for Polyamide and Polyester); Rate of cooling - 10˚C/ min
- 2nd Heating – Heating from 30˚C to 180˚C (for Polypropylene), 30˚C to 300˚C (for Polyamide and Polyester); Rate of heating - 10˚C/ min

Nitrogen gas was used as the purge gas for the above experiment. Pressure of about 3 bars was maintained for the gas flow of 20 ml/ min in the instrument.

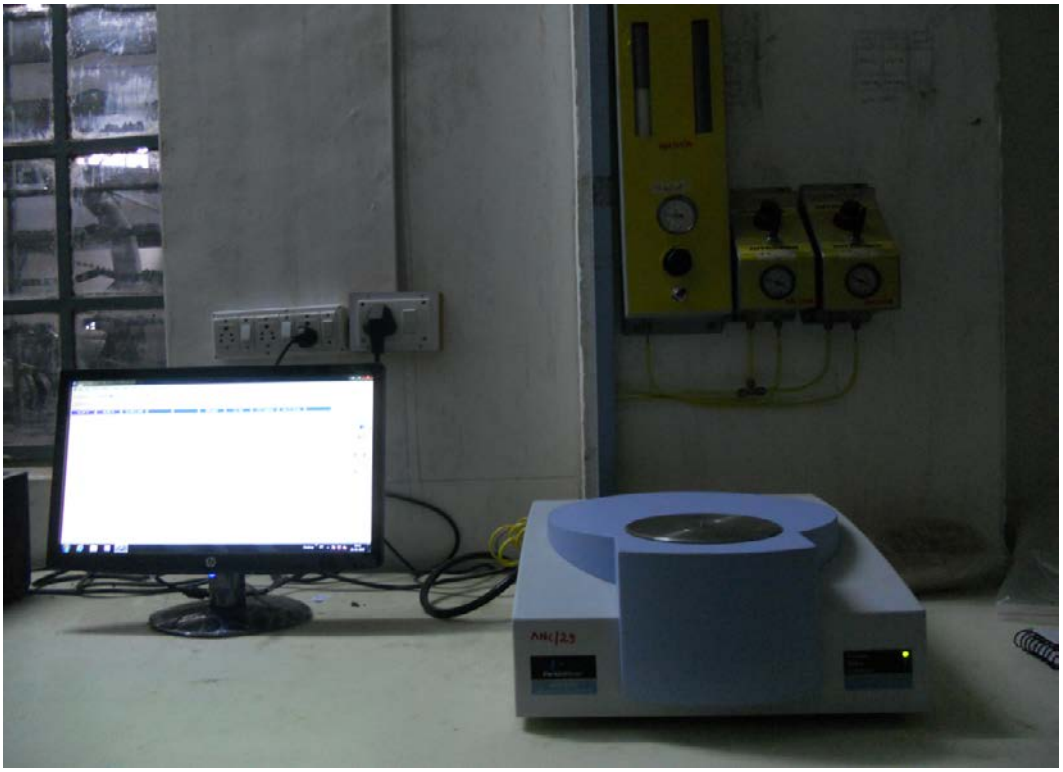

Figure 3.10 Differential Scanning Calorimeter

The thermograph obtained after the test was analyzed and the results were interpreted. The crystallinity percent (X) of studied samples was also calculated using the following equation.

$$X = \left(\frac{\Delta H}{(1-w_f)\Delta H^*}\right) \times 100 \quad \text{.....Equation 3.1}$$

Where,

X = Crystallinity %

w_f = weight fraction of nanocomposite filler,

ΔH = measured melting enthalpy,

ΔH^* = extrapolated value of enthalpy corresponding to 100% crystalline polyamide and polypropylene are 230.1 and 209 J/g respectively [138, 139].

3.3.4.1.5 Rheological measurement (Melt flow index-MFI)

The Melt Flow Index (MFI) of the polymer chips was measured as per ASTM D1238 standard. The MFI was measured using an Extrusion Plastometer manufactured by HEM-TECH CORPORATION shown in figure 3.11. It is a dead-weight piston plastometer consisting of a thermostatically controlled heated steel cylinder with a die at the lower end and a weighted piston operating within the cylinder.

The apparatus was set at 230˚C, on attaining the set temperature polymer chips were fed from the top portion of cylinder. The polymer chips were kept for around 5 minutes for melting. After the specified time, the piston rod was inserted in the cylinder and a weight of 2.16 kg was placed above the piston for loading. On attaining a uniform polymer extrusion from the die, the timer was started and the polymer was collected. The timer was stopped when there was discontinuity in polymer extrusion. The collected polymer was weighed and the MFI was calculated as per following equation.

Weight of polymer in "x" seconds = w gram

So, weight of polymer in 600 seconds = $\frac{w \times 600}{x}$ gram .....Equation 3.2

So, MFI = weight of polymer (in gram) extruded in 10 minutes.

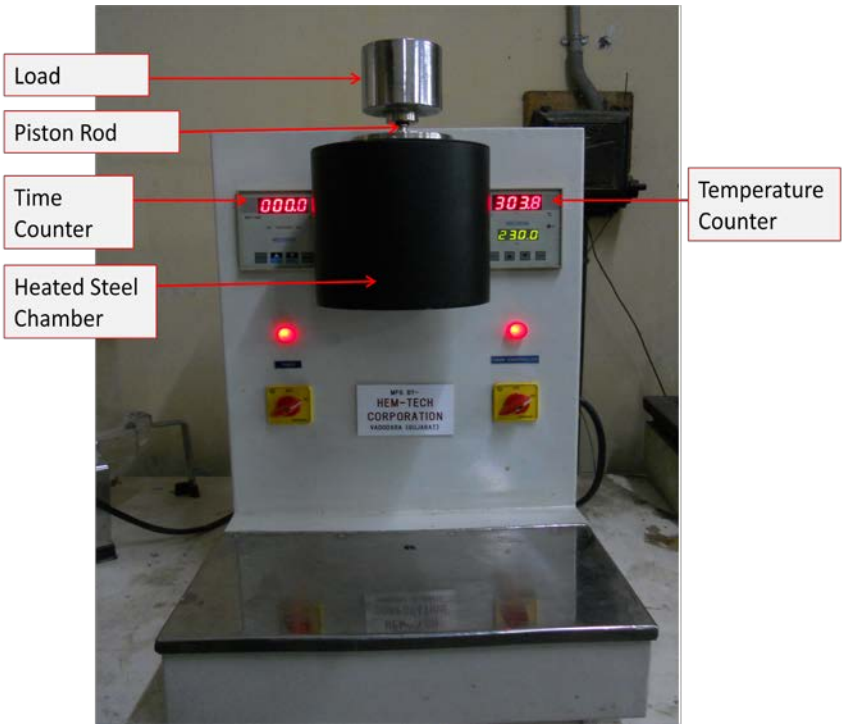

Figure 3.11 Melt Flow Indexer

3.3.4.2 Mechanical Properties

3.3.4.2.1 Tensile strength Tester

Tensile strength in terms of stress and strain of polymer/silica nano composite film, filament and fabric were tested for comparing the effect of incorporation of silica nano particles. Measurements of this physical property was performed on tensile tester (Model: LRX, Lloyd, UK.) in accordance with ASTM D882-02, which works on constant rate of elongation (CRE) principle as shown in figure 3.12. The capacity of the instrument is 0.5 – 2500N while the rate of extension can be varied from 0.1 - 1000 mm/min.

The test was conducted with following specifications:

Film:

- Gauge Length: 20 mm, Width: 25.4 mm, Rate of Extension: 50 mm/min

Filament:

- Gauge Length: 50 mm, Rate of Extension: 100 mm/min,

Fabric:

- Gauge Length: 80 mm, Width: 20 mm, Rate of Extension: 100 mm/min

Figure 3.12 Lloyd LRX tensile strength tester

3.3.4.2.2 Tearing Tester

The tearing strength of treated and untreated fabric samples were measured on falling pendulum type tearing strength (Elmendorf) apparatus as per ASTM-D-1424-1996, shown in figure 3.13. The fabric specimen having a size 6 inches x 3 inches (cut slit of 2 cm) was fixed between the two clamps. When the pendulum was in the raised position, then it was released. The fabric gets teared off across its width. The force required for tearing the fabric, was indicated by the pointer on scale. The testing was carried out in standard atmospheric condition, the tearing strength of fabric measured separately for warp and weft direction. The tearing strength was calculated using following equation.

$$F = R.S. \times \frac{C.S.}{100} \quad \text{.....Equation 3.3}$$

Where,

F = Tearing force in gf

R.S. = Scale reading

C.S. = Full scale capacity in gf

Figure 3.13 Elmendorf tearing tester

3.3.4.2.3 Crease recovery tester

Shirley Crease Recovery tester principle was used for the measurement of crease recovery angle after creasing under standard load as shown in figure 3.14. Standard weight of 2 kilogram was applied for one minute for crease formation to the strips conditioned at standard atmosphere.

Three Specimens each in warp and three weft way were taken, each of size 2 inch x 1 inch were tested. Average of three was considered. The test was performed as per AATCC test method 66-2003, AATCC Technical Manual /2006, page: 95.

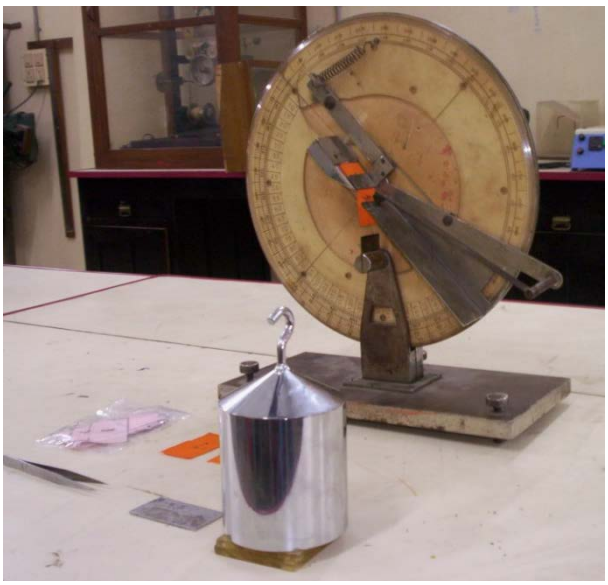

Figure 3.14 Crease recovery tester

CHAPTER 4

RESULTS AND DISCUSSION

This chapter is divided into three parts for avoiding the complexity of the discussion. Part-I deals with polymer (polyamide) silica nanocomposite film, part-II deals with polymer (polypropylene) silica nanocomposite filament and part-III deals with polymer (polyester) silica nanocomposite fabric. The prepared polymer silica nanocomposite textiles were analyzed by standard techniques for evaluating changes in structural and mechanical behavior and compared with respective pure material.

4.1 PART – I: POLYMER SILICA NANOCOMPOSITE FILM

Silica nanoparticles at 0.1%, 0.3%, 0.5%, 0.7% & 1.0% concentration level were mixed with polyamide chips in formic acid as solvent with constant stirring at 250 rpm. The mixture was heated at 60 °C for 1 hr., finally the polymer/nanocomposite mixture were poured in flat glass dish and allowed the solvent to evaporate, which resulted in terms of distribution of SiO_2 nano particles throughout the film as shown in figure 4.1. The effect on the structural and mechanical properties has been presented in this section. The nomenclature used during the discussion for the samples prepared is given in following table 4.1.

Table 4.1 Nomenclature of Polyamide silica nanocomposite films

Sr. No.	Sample	Silica (gm)
1	**PA**	Pure Polyamide film
2	**NPA1**	Polyamide film with 0.1% addition of SiO_2
3	**NPA2**	Polyamide film with 0.3% addition of SiO_2
4	**NPA3**	Polyamide film with 0.5% addition of SiO_2
5	**NPA4**	Polyamide film with 0.7% addition of SiO_2
6	**NPA5**	Polyamide film with 1.0% addition of SiO_2

PA: polyamide, NPA: Nano silica loaded polyamide

a) Pure Polyamide film

b) PA+0.1% nano silica

c) PA+0.3% nano silica

d) PA+0.5% nano silica

e) PA+0.7% nano silica

f) PA+1.0% nano silica

Figure 4.1 Polyamide untreated (a) and treated (b to f) films

4.1.1 STRUCTURAL ANALYSIS

4.1.1.1 Surface morphological analysis through SEM

Figure 4.2 a) shows the SEM micrograph of pure polyamide film. Figure 4.2 (b to f) shows the nanocomposite films with 0.1%, 0.3%, 0.5%, 0.7% and 1.0% concentration of silica nano particles in polyamide matrix prepared from dissolution mixing method. In figure 4.2 b), c) and d) the uniform distribution of nano particles is observed. Figure 4.2 e) shows the some non-uniform distribution of SiO_2 nano particles. Figure 4.2 f) shows the agglomeration of silica nanoparticles and detoriation of film in terms of its continuity, the holes have been observed in the film.

a)

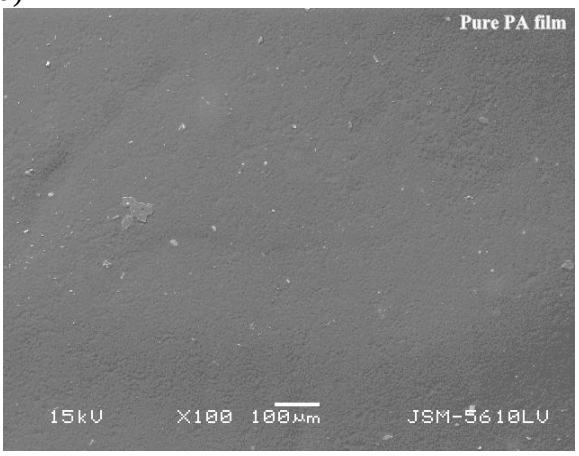

b)

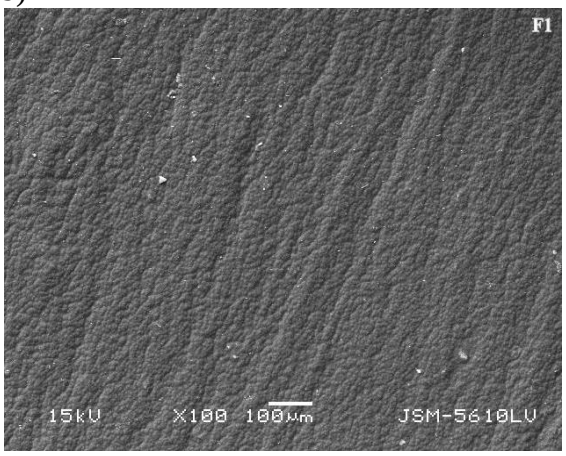

c)

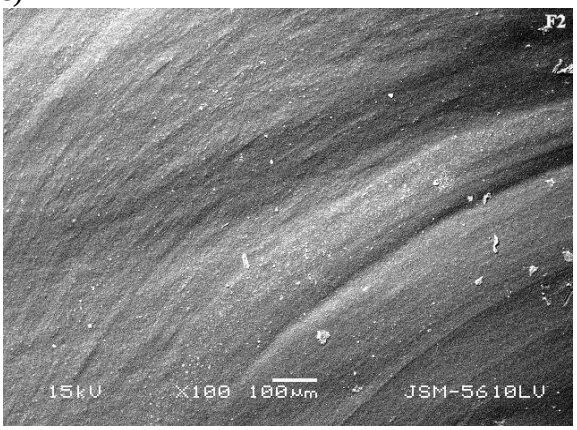

d)

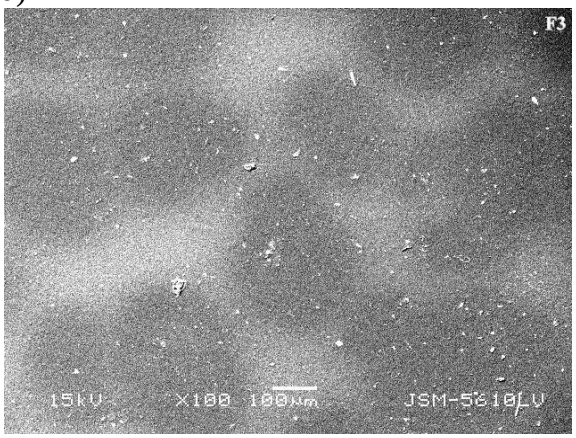

e) f)

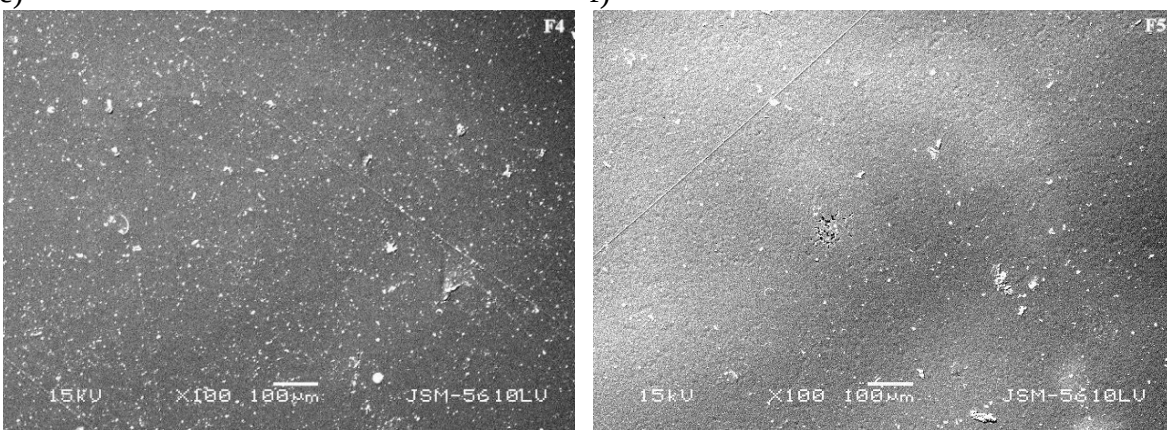

Figure 4.2 SEM micrographs of pure polyamide and polyamide/SiO_2 nanocomposite films, a) pure polyamide film, b) polyamide+0.1% nano SiO_2, c) polyamide+0.3% nano SiO_2, d) polyamide+0.5% nano SiO_2, e) polyamide+0.7% nano SiO_2, f) polyamide+ 1.0% nano SiO_2.

4.1.1.2 FTIR spectral analysis

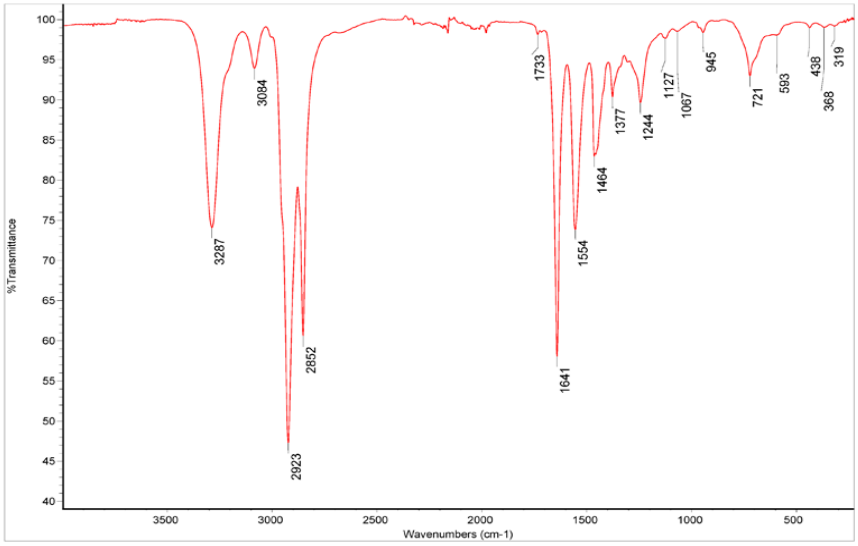

a) Pure Polyamide film

The chemical compositions of the pure polyamide and polyamide/silica nanocomposite films were evaluated using FTIR Spectroscopy. Table 4.2 and figure 4.3 (a) represents the IR characterization absorption peak of pure polyamide film, from which it can be seen that the peaks associated were hydrogen bonded N-H stretching at 3287 cm^{-1} [140], C-H stretching at 3084 cm^{-1}, asymmetric stretching vibrations of C-H [141] at 2923 cm^{-1}, Symmetric stretching vibrations of C-H [141]

bonds at 2852 cm^{-1}, peak 1733 cm^{-1} [142] corresponding to the carboxyl groups, C=O [140] stretching at 1641 cm^{-1}, N-H bending at 1554 cm^{-1}, the presence of these modes suggests presence of a polyamide., CH_2 symmetric bending vibration-scissoring type at 1464 cm^{-1}, CH_3 bending at 1377 cm^{-1}, inplane C-H bending at 1244 cm^{-1}, C-H stretching at 1127 cm^{-1}, O-H stretching at 1067 cm^{-1}, C-H stretching at 945 cm^{-1} and CH_2 bending vibrations-rocking type observed at 721 cm^{-1}.

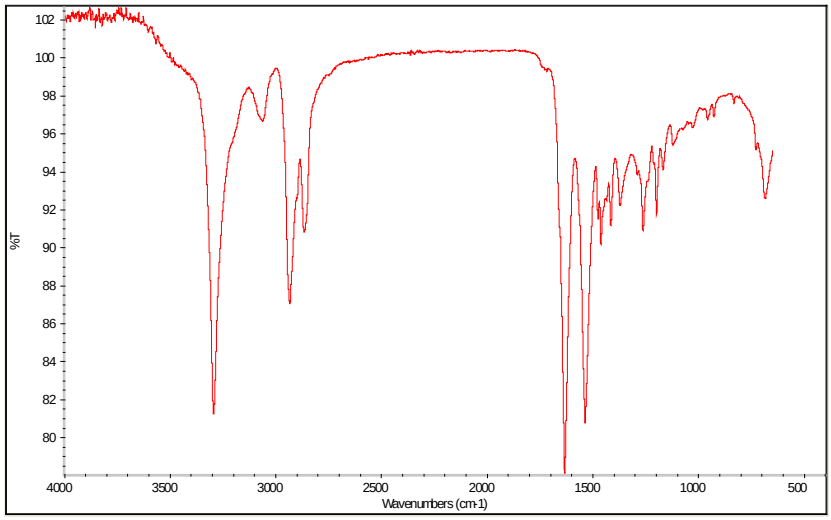

b) Polyamide and 0.1% SiO_2 film

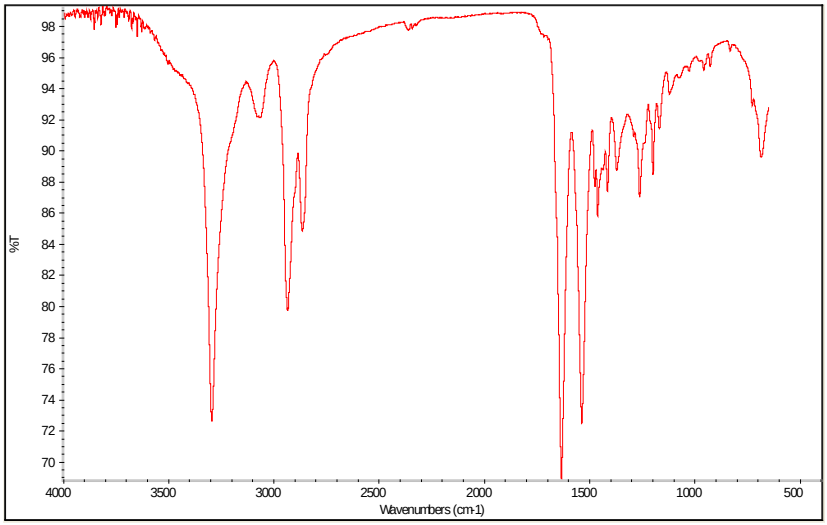

c) Polyamide and 0.3% SiO_2 film

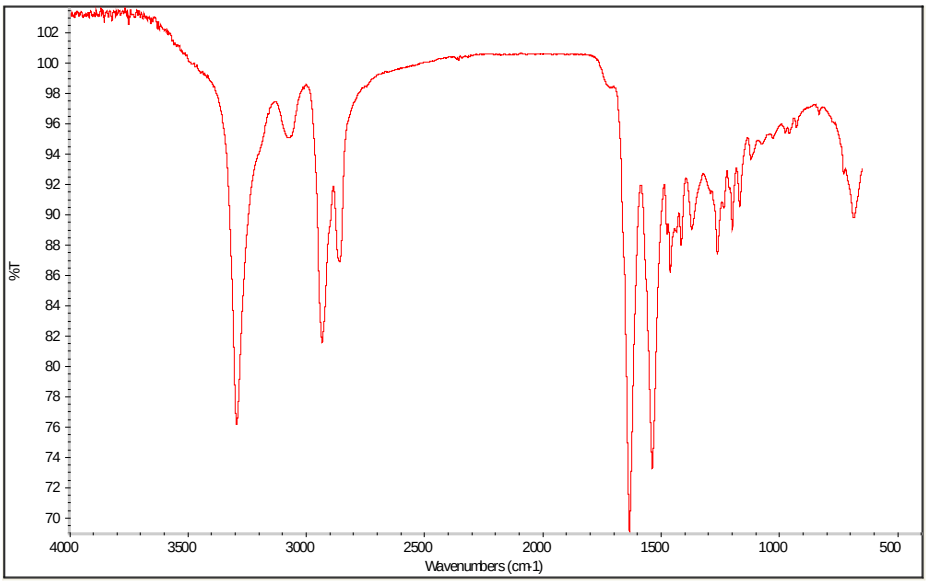

d) Polyamide and 0.5% SiO_2 film

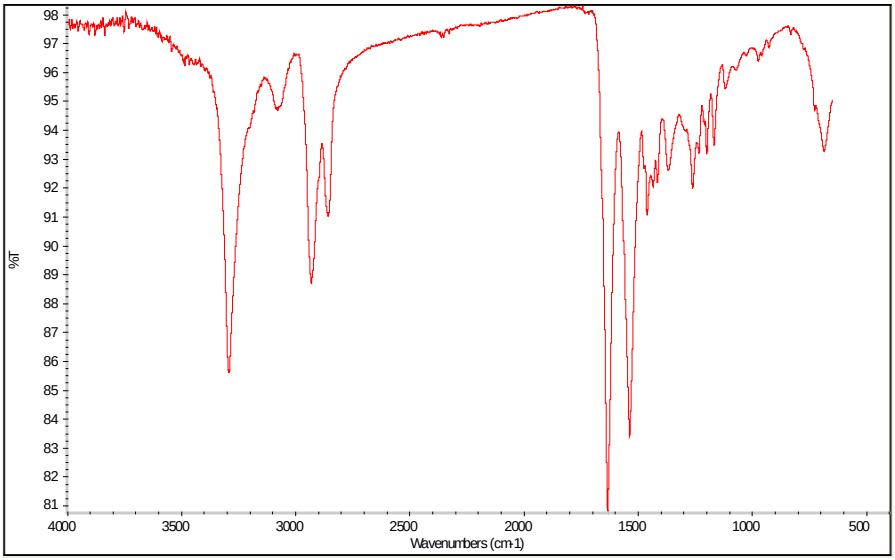

e) Polyamide and 0.7% SiO_2 film

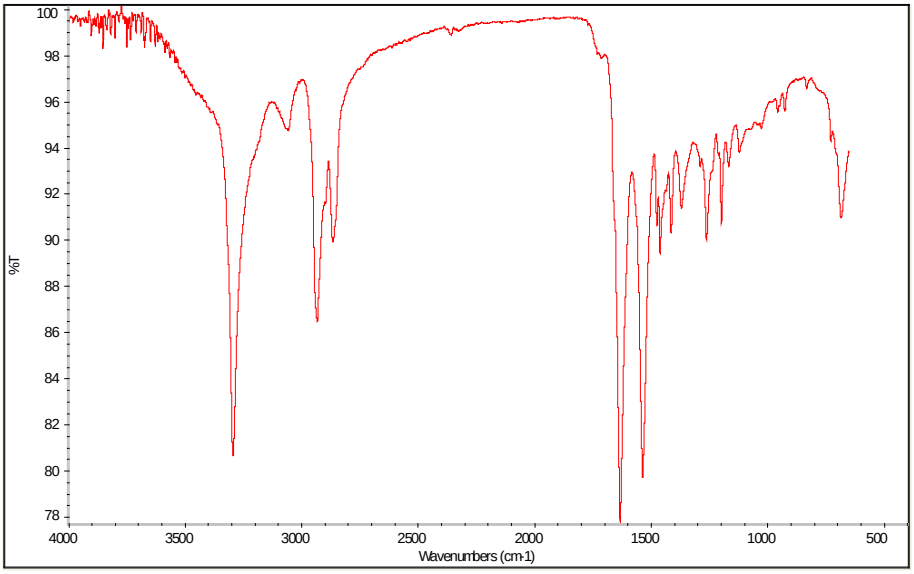

f) Polyamide and 1.0% SiO_2 film

Figure 4.3 IR absorption peaks of pure polyamide (a) and polyamdie/Silica nanocomposite films (b to f).

Peaks shown by pure polyamide film are identical in all nanocomposite films as shown in figure 4.3 (b to f), additionally the nanocomposite films showed the peaks of silica around 840 cm^{-1} corresponds to Si-O [143] bending vibration, absorption peak belonging to the Si-OH [141] bond appears at 920 cm^{-1}, band around 1098 cm^{-1} correspond to asymmetric stretching vibration of Si-O-Si [144] band. Due to addition of silica nano particles in polyamide in different concentrations, the FTIR peaks showed the increased stretching vibrations of O-H in the range of 3600 to 3900 cm^{-1} in all spectrographs of nanocomposite films, also C-O stretches observed at 1160 cm^{-1} and 1210 cm^{-1}, C-H bend at 1410 cm^{-1} as shown in figure 4.3 (b to f).

Table 4.2 FTIR characterization peaks of pure polyamide and polyamdie / Silica nanocomposite films

Groups	Wavenumber (cm^{-1})					
	PA	**NPA1**	**NPA2**	**NPA3**	**NPA4**	**NPA5**
CH2 bending vibrations-rocking type	721	721	721	721	721	721
C-H bending	945	945	945	945	945	945
O-H stretching	1067	1067	1067	1067	1067	1067
C-H stretching	1127	1127	1127	1127	1127	1127
Inplane CH bending	1244	1244	1244	1244	1244	1244
CH_3 bending	1377	1377	1377	1377	1377	1377
CH_2 symmetric bending vibration-scissoring type	1464	1464	1464	1464	1464	1464
N-H bending	1554	1554	1554	1554	1554	1554
C=O stretching	1641	1641	1641	1641	1641	1641
Carboxyl group	1733	1733	1733	1733	1733	1733
Symmetric vibrations of C-H	2852	2852	2852	2852	2852	2852
Asymmetric vibrations of C-H	2923	2923	2923	2923	2923	2923
C-H stretching	3084	3084	3084	3084	3084	3084
N-H stretching	3287	3287	3287	3287	3287	3287
Si-O bending vibration	-	840	840	840	840	840
Absorption peak belonging to the Si-OH bond	-	920	920	920	920	920
Asymmetric stretching vibration of Si-O-Si band	-	1098	1098	1098	1098	1098
C-O stretches	-	1160	1160	1160	1160	1160
C-O stretches	-	1210	1210	1210	1210	1210
C-H bend	-	1410	1410	1410	1410	1410
Stretching vibrations of O-H	-	3600 to 3900	3600 to 3900	3600 to 3900	3600 to 3900	3600 to 3900

4.1.1.3 X-ray diffraction Analysis

The X-ray diffraction patterns were taken on X'pert Pro PANalytical x-ray diffractometer. The XRD of both the fabrics was done within the 2θ range of 10° to 30° at the scan speed of 3° per minute at 25°C temperature, using Cu-K_α radiation of wavelength 1.5406Å. The diffraction profiles were obtained for individual samples. The XRD patterns are given in figure 4.4 and 4.5 for PA and NPA4 samples i.e. pure polyamide film and 0.7% nano silica in polyamide film respectively. The combined XRD patterns of both the samples are shown in figure 4.6.

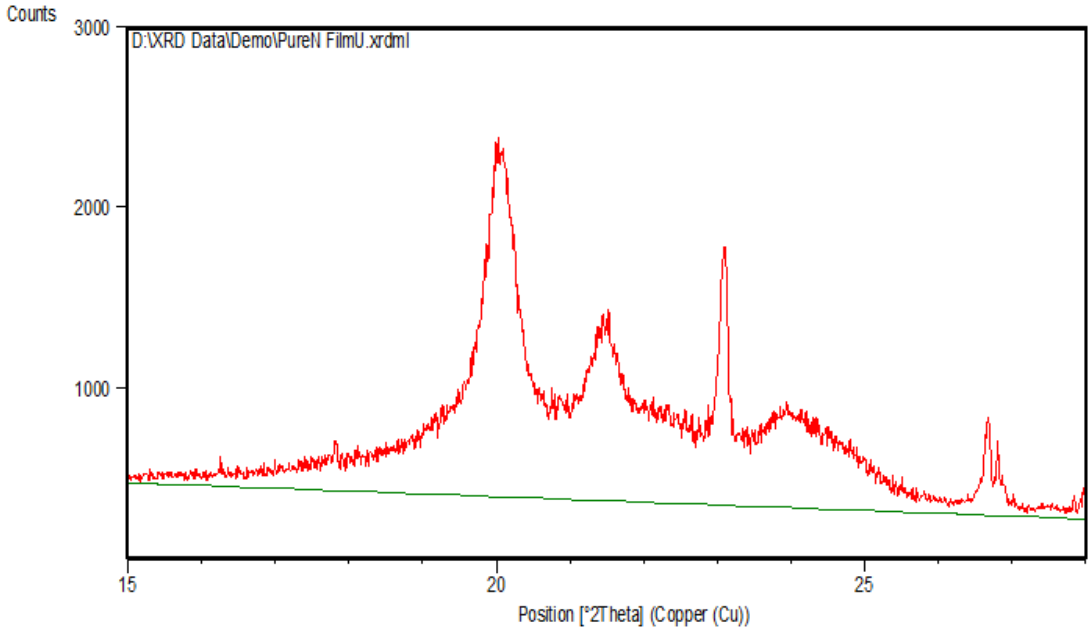

Pos. [°2θ]	Height [cts]	d-spacing [Å]	Area [cts*°2θ]	Rel. Int. [%]
20.047	1662	4.42562	1277.34	100
21.520	659	4.12788	763.61	39.643
23.082	1114	3.85021	214.55	67.021
23.99	316	3.70665	314.68	19.025
26.669	396	3.33987	70.64	23.805

Figure 4.4 XRD pattern of pure polyamide film (PA)

XRD pattern of PA sample shows sharp and broad features with reasonably high intensity. Four prominent peaks are observed. The pattern exhibits a certain degree of amorphicity. However, the characteristic peaks are well defined and quite intense. The peak at 2θ value of 20.047° has the highest intensity followed by 23.082°, 21.510° & 26.669° and these peaks are of polyamide polymer [145].

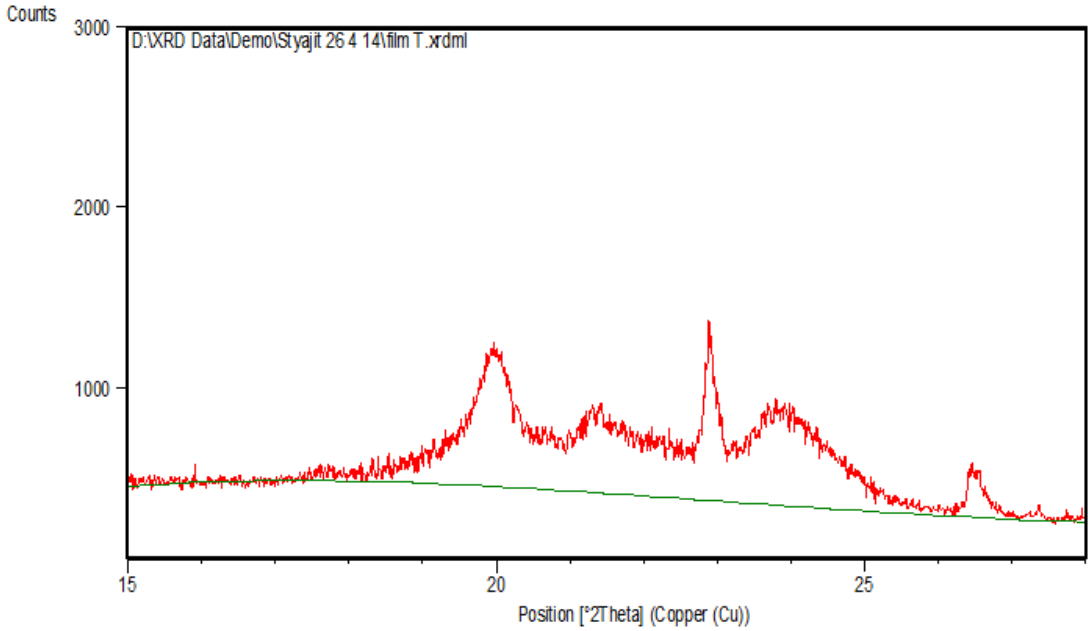

Pos. [°2θ]	Height [cts]	d-spacing [Å]	Area [cts*°2θ]	Rel. Int. [%]
19.952	671	4.44653	774.26	99.68
21.54	357	4.12165	703.96	53.06
22.90	672	3.88029	162.01	100
23.95	500	3.71303	1032.55	74.44
26.505	286	3.36024	67.60	42.42

Figure 4.5 XRD pattern of polyamide silica nanocomposite film (NPA4)

The incorporation of silica nano particles lead to the development of some kind of force which drifts the atomic planes, such that the d-value increases. From the figure it can be seen that the crystallinity of the treated sample is of lower order compared to the untreated samples. However, the SEM micrographs show the incorporation of silica nano particles within the film. These particles might disperse the x-rays incident on the film. This may be reason for decrease in the peak intensity of the treated film and not the crystallinity of the film itself. Due to addition of nano silica in polyamide, the peak intensity is reduced from 2400, 1428, 1750, 1000 and 850 to 1250, 900, 1380, 920 and 580 respectively. This may be due to diffraction or deviation of x-rays by the nano silica particles. Hence, the number of x-rays reaching the detector might be less. The d-values for the observed diffraction peak of silica is in close agreement with those reported for corresponding standard samples as reported in JCPDS data file no. 84-0384. One of the peaks corresponding to d-value of 4.4414 Å is in complete agreement.

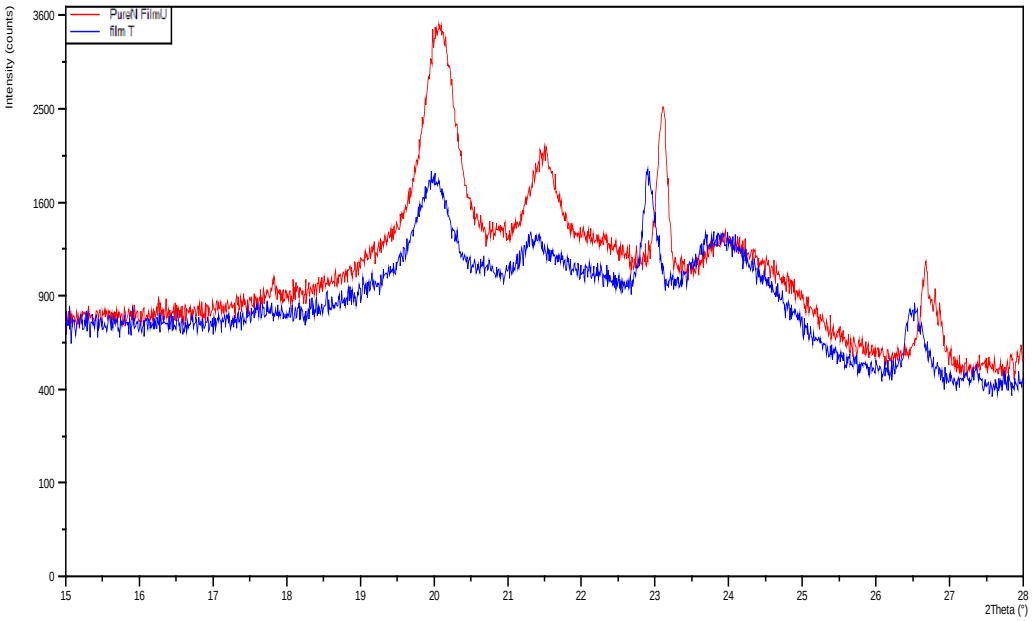

Figure 4.5 Combined XRD patterns of PA and NPA4 samples

4.1.1.4 Thermal analysis

The effect on thermal property due to incorporation of silica nano particles in polyamide film is studied through differential scanning calorimetry (DSC). The silica nano particles were added in different proportions as 0.1%, 0.3%, 0.5%, 0.7% and 1.0% on weight bases. The thermal behavior of pure and nanocomposite film is shown in figure 4.7 and the results are given in table 4.3.

Table 4.3 Enthalpy (ΔH) of pure polyamide and polyamide/silica nanocomposite film

Sample	% Concentration of nano SiO_2	Melting Temperature (°C)	Enthalpy (ΔH) (J/g)	% Change in Enthalpy (ΔH)	Crystallinity %
PA	0.0	214.24	30.00	0	13.04
NPA1	0.1	217.8	64.85	116.17	28.21
NPA2	0.3	215.64	52.89	76.30	23.05
NPA3	0.5	218.31	49.55	65.17	21.64
NPA4	0.7	215.14	46.58	55.27	20.39
NPA5	1.0	209.31	22.87	-23.77	10.04

Figure 4.7 (a) shows the differential scanning calorimetry (DSC) curve of pure polyamide film. Here the pure polyamide film sample was heated at 10°C/min rate upto 300°C, in which it shows the melting temperature of the film as 214.24°C and the total heat required to melt i.e. enthalpy (ΔH) is 30 J/g, the % crystallinity calculated on the bases of enthalpy is 13.04%. DSC curves for polyamide sometime exhibits three or two or one peak. In this experimental work pure polyamide film exhibited two peaks; the reason may be the polyamide has different forms of lamellar thickness like α, γ, and δ forms [146].

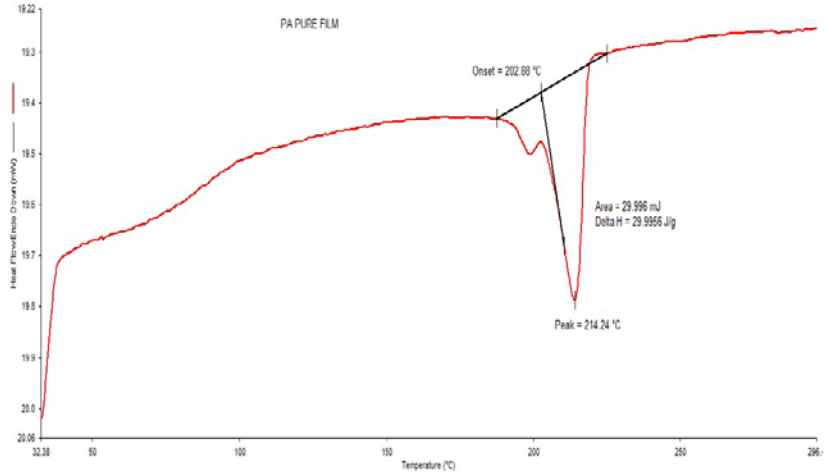

a) DSC curve of Pure Polyamide film

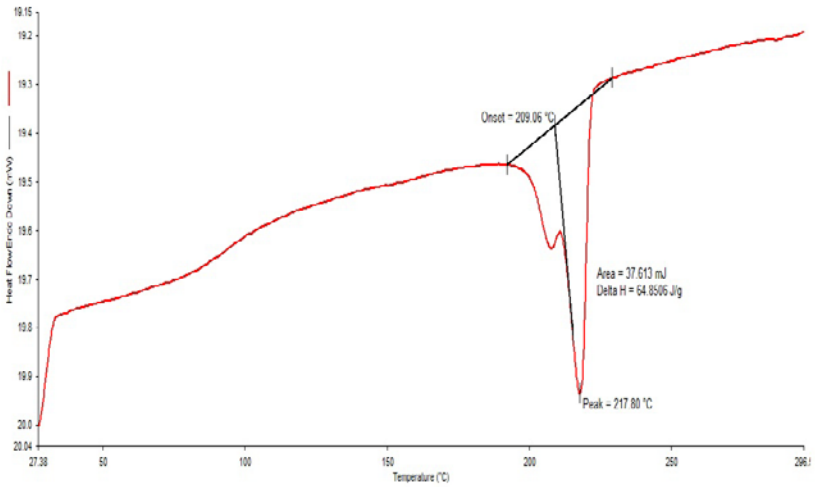

b) DSC curve of Polyamide and 0.1% SiO_2 film

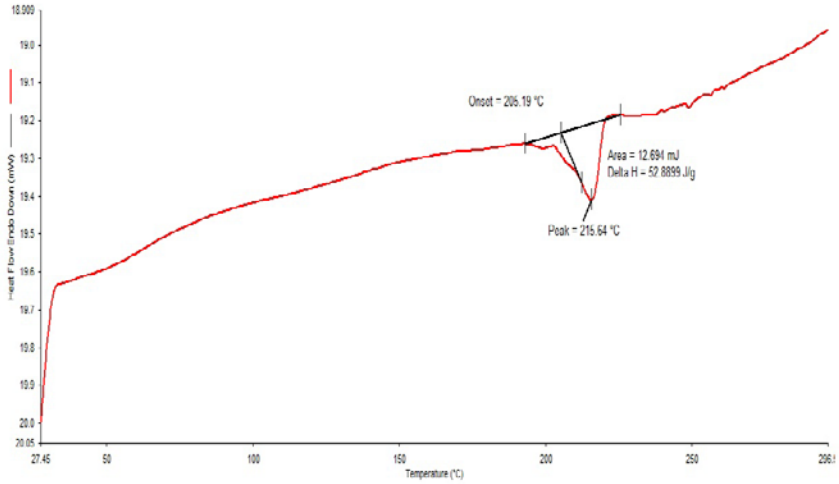

c) DSC curve of Polyamide and 0.3% SiO_2 film

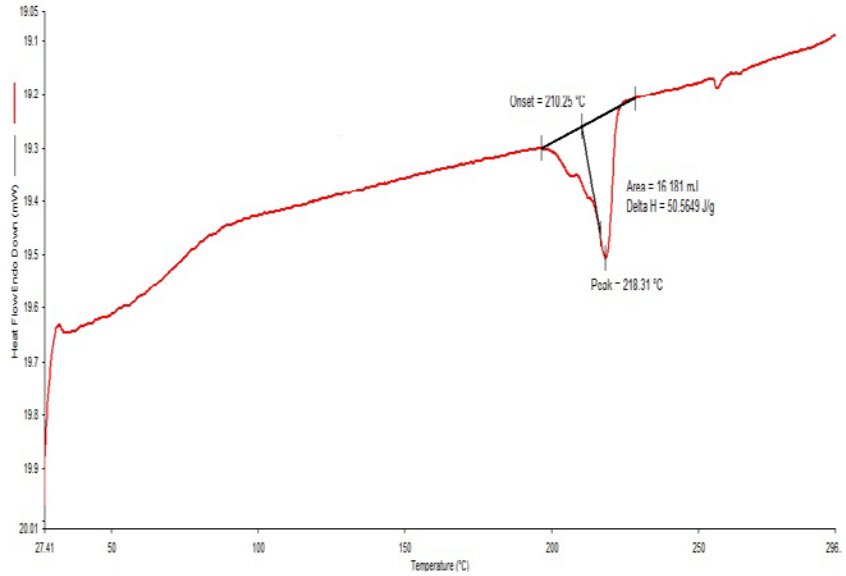

d) DSC curve of Polyamide and 0.5% SiO_2 film

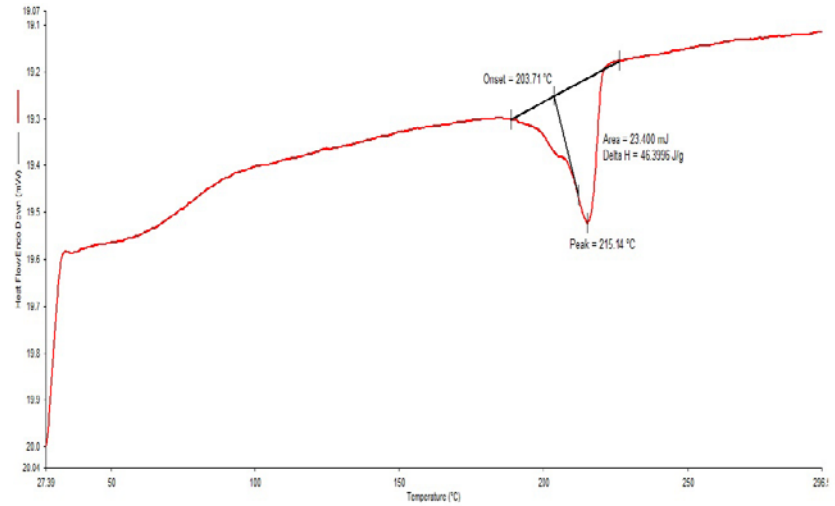

e) DSC curve of Polyamide and 0.7% SiO_2 film

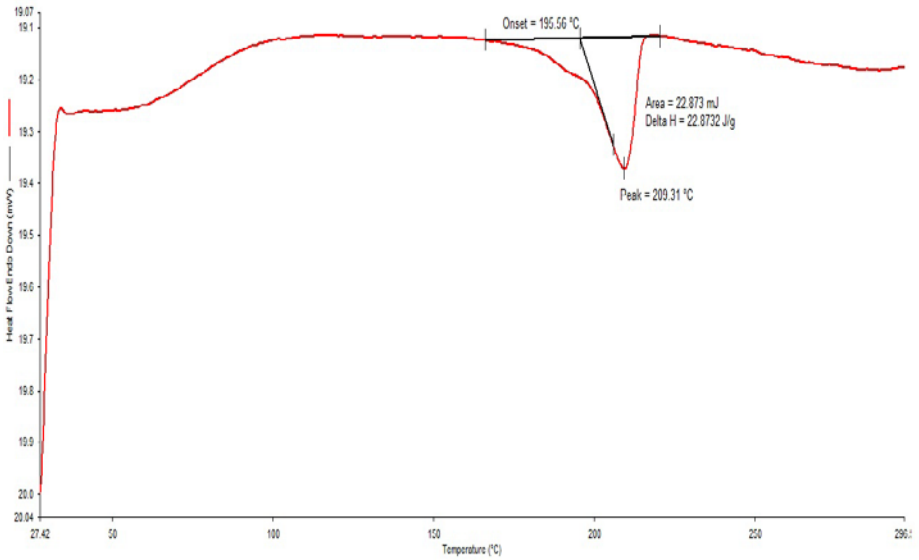

f) DSC curve of Polyamide and 1.0% SiO_2 film

Figure 4.7 DSC curves of pure polyamide (a) and polyamide silica nanocomposite films (b to f)

The NPA1 i.e. 0.1% concentration of nano silica sample also exhibited two similar peaks like pure polyamide sample, but NPA2 and NPA3 samples exhibited three peaks, this means that the change is taking place in lamellar thickness of polyamide structure due to addition of nano silica by 0.3% and 0.5% concentrations. Further addition of nano material by 0.7% in polyamide i.e. NPA4 sample exhibits two peaks and in sample NPA5 i.e. 1%, these peaks are getting merged into one peak. This means that with further increase in nano silica concentrations i.e. 0.7% and 1%, there is again change in structure take place.

Figure 4.7 (b to f) show the DSC curves of nanocomposite films of polyamide and SiO_2 nano particles at different concentration levels like 0.1%, 0.3%, 0.5%, 0.7% and 1.0%. The melting temperature, enthalpy and % crystallinity of all films is given in table 4.3. The melting temperature of pure polyamide film is 214.24°C and there is no significant effect on melting temperature due to addition of silica nano particles, except the 1.0% silica nanocomposite polyamide film, where there is significant drop in melting temperature i.e. 209.31°C. This reduction in melting temperature may be due to degradation of the film i.e. holes are observed in SEM micrographs of the film (figure 4.2 (f)). This has also reflected in less enthalpy required to melt this film as

compare to pure polyamide film. The results show that there is a significant difference in ΔH between virgin PA and PA/silica nanocomposite films. At higher concentration of silica nano particles in PA matrix, indicating that silica in agglomerate form was not able to alter the thermal behavior of PA. On the other hand, lower concentration of nano silica in dissolution mixed PA/silica nanocomposite has a higher ΔH value than virgin PA. In this case, silica size is reduced into a nanoscopic level, hence inducing better thermal stability of the film [147]. In PA/silica nanocomposite films two melting peaks observed, but these two peaks are getting merged into one as the concentration of nano silica particles is increasing, which is clearly seen in NPA5 sample.

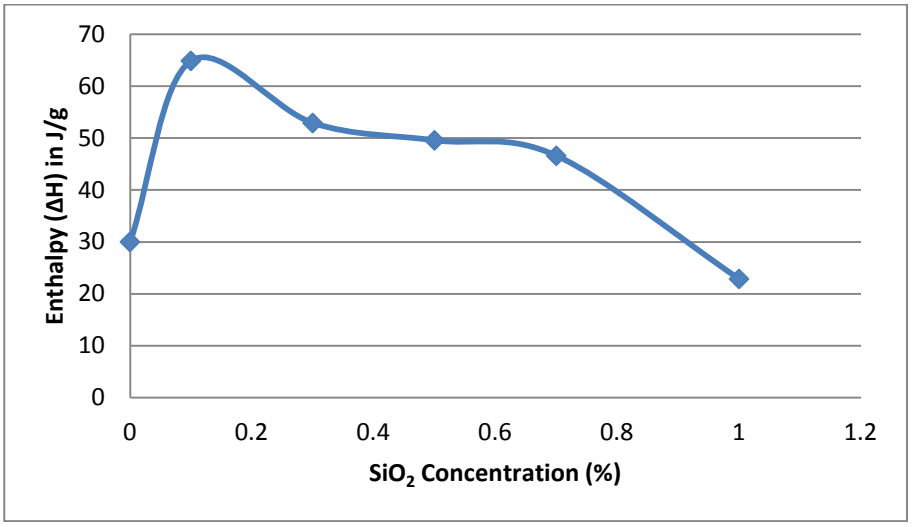

Figure 4.8 Percentage change in Enthalpy (ΔH) of polyamide/silica nanocomposite film

The percentage change in enthalpy of silica treated nanocomposite film is found more than virgin polyamide by 116.17%, 76.30%, 65.17% and 55.27% for 0.1%, 0.3%, 0.5% and 0.7% concentrations respectively. The same trend is seen in case of crystallinity of film. In less concentration of nano silica would be giving better stability to the film as compare to higher concentration of silica nano particles. Overall the enthalpy required to melt the nanocomposite films is higher than pure polyamide film. But in case of 1% concentration of nano silica, the enthalpy required to melt the film has found less than pure film i.e. 22.87 J/g. This may be due to the high concentration of nano silica particles which may cause agglomeration of nano particles and not allowing to form continuous structure of polyamide and damaged the film, which can be clearly seen from the SEM micrographs.

4.1.2 MECHANICAL PROPERTIES

The effect on mechanical properties i.e. tensile, young's modulus and work of rupture due to incorporation of silica nanoparticles in polyamide film is studied here. The silica nanoparticles were added in different proportions as 0.1, 0.3, 0.5, 0.7 and 1.0 percentage on weight bases.

4.1.2.1 Tensile property

The tensile test was performed on Llyod LRX tensile testing machine and the stress strain curve of various samples tested are summarized in table 4.4 and shown in figure 4.9 below.

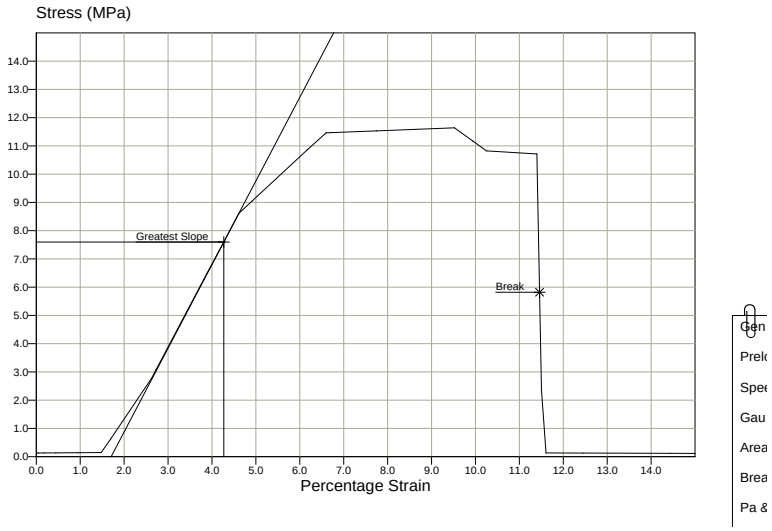

a) Pure polyamide film

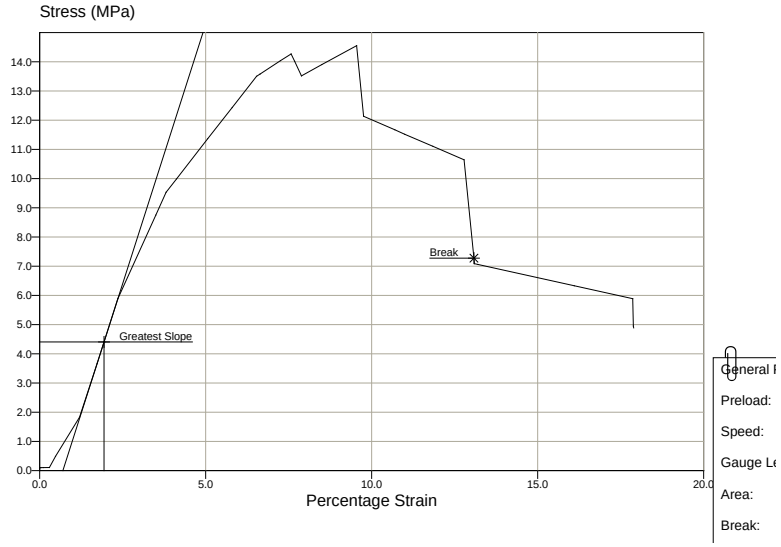

b) Polyamide and 0.1% SiO_2 film

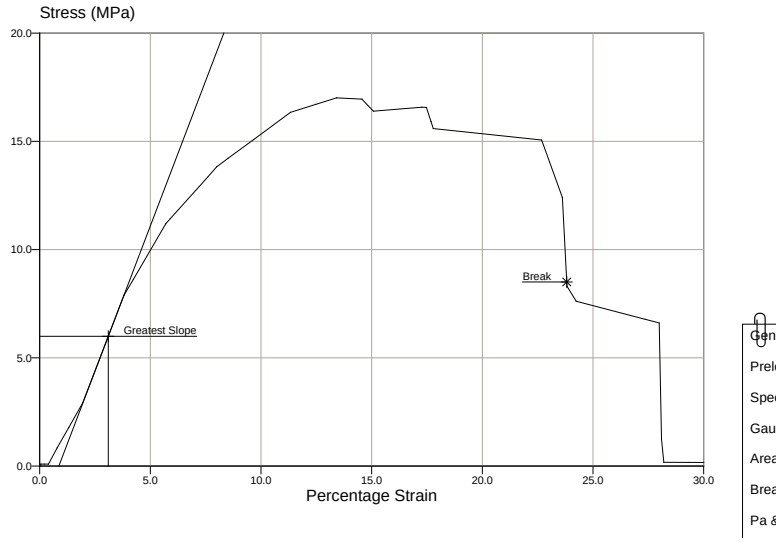

c) Polyamide and 0.3% SiO_2 film

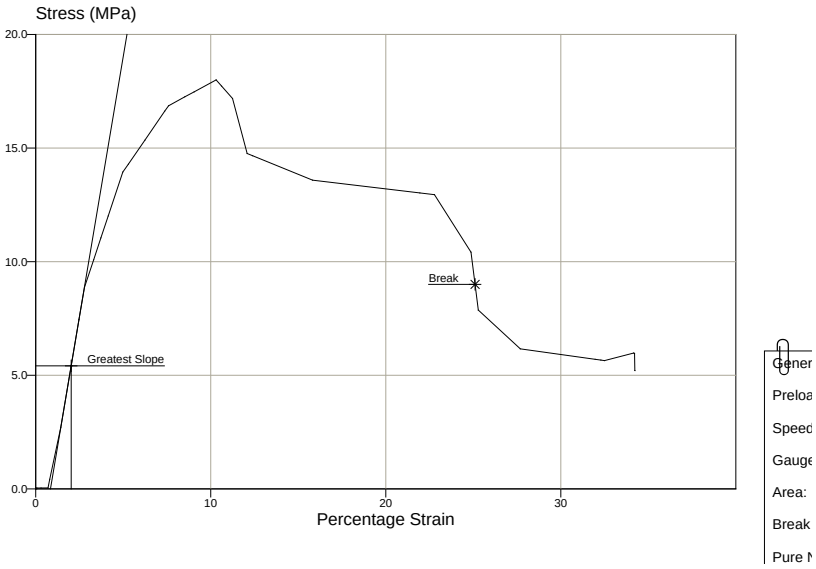

d) Polyamide and 0.5% SiO_2 film

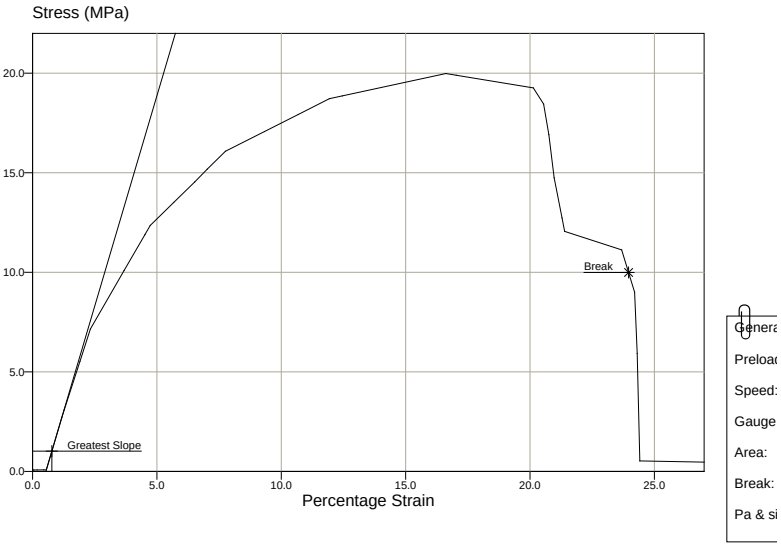

e) Polyamide and 0.7% SiO_2 film

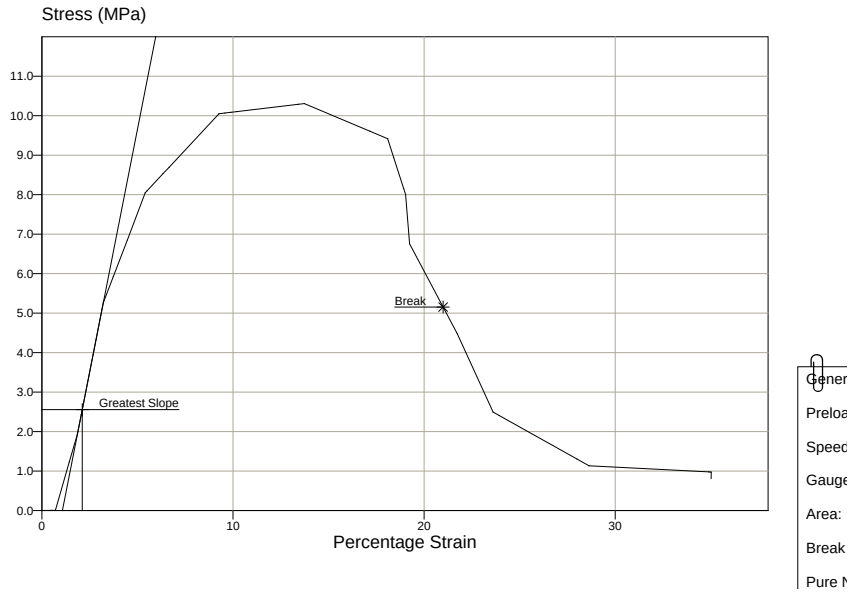

f) Polyamide and 1.0% SiO_2 film

Figure 4.9 Stress strain behavior of pure polyamide (a) and polyamide/Silica nanocomposite films (b to f).

The results given in table 4.4 and stress strain curves in figure 4.9 revels that the obtained nanocomposite film exhibits an increase in specific strength with an increase in percent silica loading (silica loading of 0.1 wt % to 0.7 wt % respectively), it may be due to the phenomenon of reinforcement effect at nanoscopic level. However, the composite film at higher concentration of nano silica exhibits the erratic trend of tensile strength value due to the phase separation problem arising from particles' agglomeration. Also SEM result is showing the detoriation of film for 1.0 % concentration of SiO_2 nano particles in terms of its continuity, as film becomes brittle and breaks easily i.e. holes have been observed in the film in SEM micrographs figure 4.2 (f). Good mechanical property results are obtained at 0.7% loading of nano silica polyamide film and then it shows decrease in mechanical property. Such changes in mechanical properties i.e. tensile strength, elongation and stiffness was also observed by Hagenmueller, et al., 2003; Poncharal, et al., 1999; Stegmaier, 2006; Kalarikkal, Sankar, and Ifju, 2006 [12-15].

Table 4.4 Effect of SiO_2 nano silica on tensile property of nanocomposite films

Sample	% Concentration of nano SiO_2	Thickness in Mm	Maximum Load in gf	Elongation %	Area = Width x thickness in mm^2	Specific strength in gm/mm^2
PA	0.0	0.0427	1418.4	12.02	1.0694	1326.35
NPA1	0.1	0.03	1098.8	9.52	0.75	1465.07
NPA2	0.3	0.0819	3484.3	13.41	2.0486	1700.82
NPA3	0.5	0.0444	2102.8	14.37	1.115	1885.92
NPA4	0.7	0.0491	2463.6	16.39	1.2291	2004.39
NPA5	1.0	0.0472	1244.2	14.48	1.1805	1053.96

Width=25.4 mm, Gauge Length=20 mm

The stress (specific strength) is found increasing by 10.55%, 28.15%, 42.11% and 51.04% for 0.1%, 0.3%, 0.5% and 0.7% concentration of nano silica in polyamide film respectively as compare to pure polyamide film. This may be due to increase in concentration and uniform distribution of nano particles in polymer matrix, which can be seen from the SEM micrographs. Above 0.7% concentration, it is observed that the stress property decreases by 20.62% for 1% concentration of nano silica in polyamide film as compare to pure polyamide film. This may be due to agglomeration of nano silica in polymer matrix, which is making the film brittle and so it gets broken easily and thus reducing the stress of polyamide silica nano composite film, which has also caused damage to the film. Small holes on the surface of the film can be seen in SEM micrographs figure 4.2 (f).

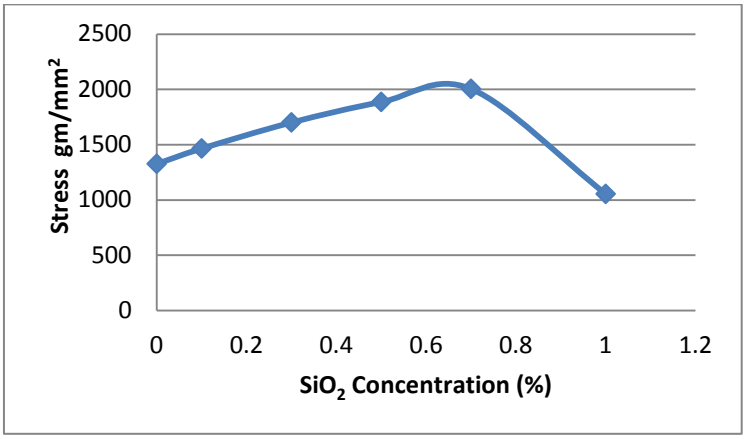

Figure 4.10 Effect of nano silica on stress property of film

4.1.2.2 Young's modulus and work of rupture

The table 4.5 and figure 4.11 and 4.12 show the young's modulus and stiffness properties of virgin polyamide film and nano silica loaded polyamide films, the young's modulus is directly proportional to the stiffness property. Here the young's modulus is calculated on the bases of Meredith's method. The virgin polyamide film is showing lower young's modulus and stiffness i.e. 136.25 gf/mm^2 and 11.10 KN/m respectively than the polyamide silica loaded nanocomposite films i.e. 173.68 & 26.21, 161.15 & 30.54, 250.11 & 30.89 and 230.39 & 31.69 respectively for 0.1%, 0.3%, 0.5% and 0.7% concentration of nano silica particles in polyamide film, except 1% concentration film i.e. 78.05 & 16.59. The young's modulus is found increased with addition of silica nano particles and also there is further overall rise in young's modulus with increase in percentage loading of silica nano particles i.e. upto 0.7% concentration and above this i.e. at 1% concentration of silica nano particles, the drop in young's modulus is observed which is 66.12% from the value of young's modulus of 0.7% concentration sample. Similarly, the stiffness property is also increasing with the increase in concentration of nano silica in polyamide i.e. upto 0.7% and thereafter at 1% concentration of nano silica the stiffness is decreased by 47.65% from the maximum value.

Table 4.5 Effect of nano silica on young's modulus, stiffness and work of rupture

Sample	Concentration of nano SiO_2 (%)	Young's Modulus (gf/mm^2)	Stiffness (KN/m)	Work of rupture at maximum load (gf.mm)
PA	0.0	136.25	11.10	1023.0
NPA1	0.1	173.68	26.21	2708.0
NPA2	0.3	161.15	30.54	6695.1
NPA3	0.5	250.11	30.89	3343.0
NPA4	0.7	230.39	31.69	7228.0
NPA5	1.0	78.05	16.59	2778.9

It is observed that up to 0.7% of filler loading, the composite film gives better results compared to pure polyamide film, but as the loading of silica increased above 0.7%, the film becomes brittle and breaks easily, which also can be seen from the SEM

microphotograph in figure 4.2 (f). Overall the stiffness of the nano silica loaded polyamide films are showing rise except 1% concentration. The 1.0% nano silica loaded polyamide film would not be allowing the material to become compact due to agglomeration of the nano particles and becoming more brittle, which would be hindering the development of compact structure, which is also supported by the reduction in enthalpy required to melt the 1% concentration nano silica polyamide nanocomposite film in DSC as shown in figure 4.7 (f).

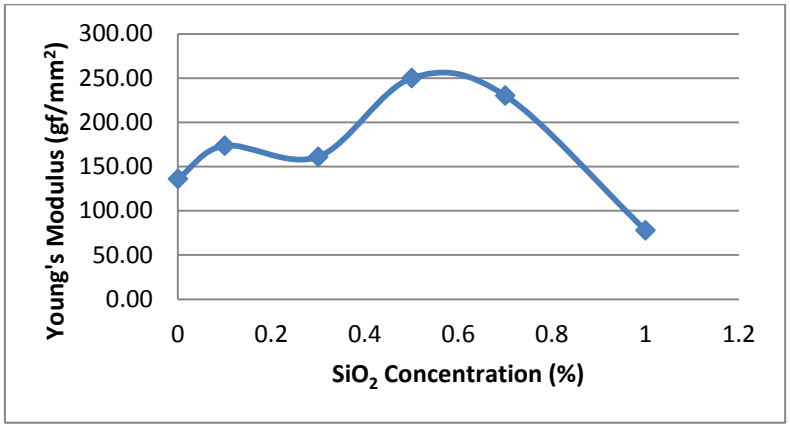

Figure 4.11 Effect of nano silica on young's modulus of treated and untreated polyamide films

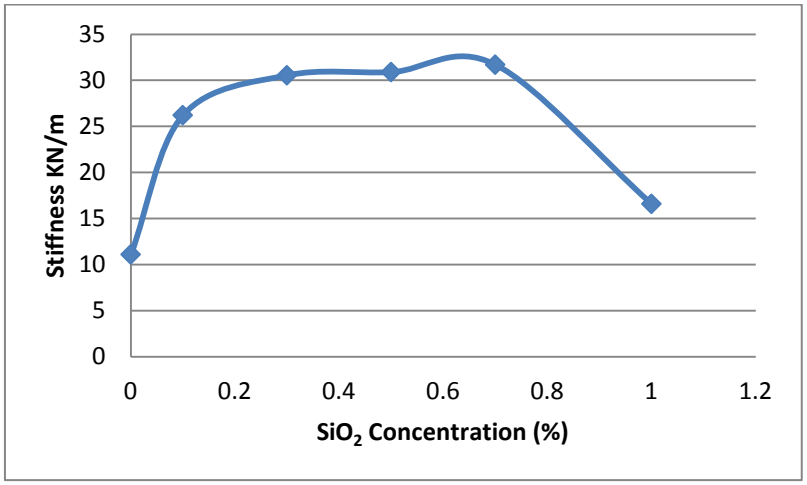

Figure 4.12 Effect of nano silica on stiffness of treated and untreated polyamide films

The work of rupture is a measure of the "toughness" of the material. It is the energy or work required to break the specimen. The area under the load-elongation curve represents the work done in stretching the material to breaking point. The work of

rupture value indicates the resistance of the material to sudden shock [148]. Table 4.5 and figure 4.13 show the work at maximum load of virgin polyamide film and nano silica loaded polyamide films. The work required to break the virgin polyamide film is 1023 gf.mm which is less as compare to nano silica treated polyamide nanocomposite films. Overall, the work of rupture is found increased with addition of silica nano particles and also there is further rise with increase in loading of silica nano particles i.e. 2708, 6695.1, 3343 and 7228 gf.mm, except 0.5% loading sample has shown the drop in work of rupture but overall the work is higher than pure polyamide film. Further, the 1% concentration sample is also showing the drop in work of rupture i.e. 2778.9 gf.mm, but here also the work is higher than the virgin polyamide film. The other properties of this sample, like enthalpy, young's modulus and stiffness are also showing the drop, and the reason could be the agglomeration induced brittleness in film, which can also be seen from the SEM micrographs.

Here also, it is observed that up to 0.7% of filler loading, the composite film gives better results compared to pure polyamide film, but as the loading of silica increased above 0.7%, the film becomes brittle and breaks easily, it may be due to agglomeration of nano particles, which also can be seen from the SEM microphotograph in figure 4.2 (f). Overall the work of rupture of the nano silica loaded polyamide films are showing rise as compare to virgin film, except 1% concentration. The 1.0% nano silica loaded polyamide film would not be allowing the material to become compact due to agglomeration of the nano particles and becoming more brittle, which would be hindering the development of compact structure.

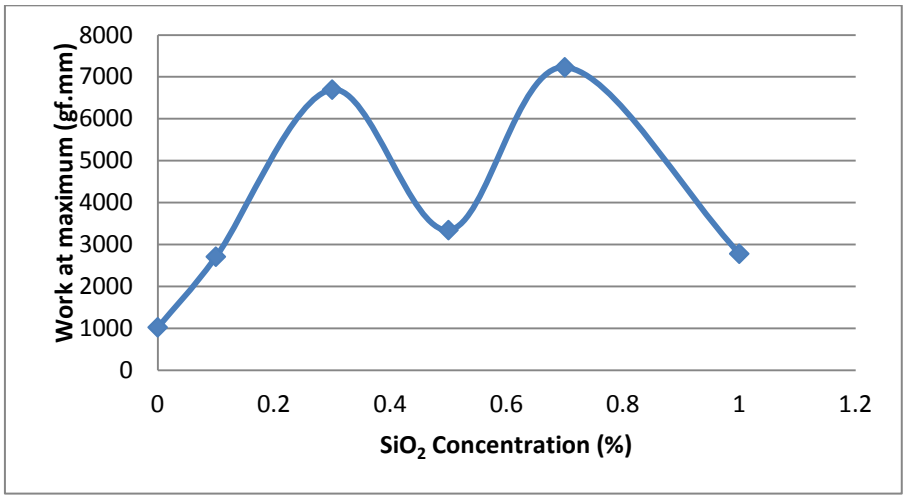

Figure 4.13 Effect of nano silica on work at maximum load of treated and untreated polyamide films

4.2 PART – II: POLYMER SILICA NANOCOMPOSITE FILAMENT

In this part, the basic polymer was changed from polyamide to polypropylene in filament form, and the concentration of silica nano particles is kept same as polyamide film. The filaments with different proportions of silica nanoparticles were prepared using pilot melt spinning plant. The evaluation of prepared polymer silica nanocomposite filaments was done in terms of their structural properties through SEM, FTIR, XRD and DSC techniques. Nanocomposite filaments were also evaluated for changes in their mechanical properties and compared with the filament prepared without addition of SiO_2 nano particles.

The present research deals with production of Polypropylene/SiO_2 nanocomposite filament yarn by melt spinning concept using pilot plant. The present research has been limited to the yarn stage only. Melt spinning deals with the addition of nanoparticles precisely on the weight basis and mixed in twin screw extruder. Then extrusion through melt spinning pilot machine. This can lead towards the production of nanocomposite yarn. Changes in structural and mechanical properties were evaluated using standard test methods.

First, pure polypropylene filament was spun; the melt flow index (MFI) of the procured polypropylene chips was measured on melt flow indexer. The measured MFI is near to the MFI claimed by the manufacturer of the polypropylene chips. The average measured value of MFI is 15.58 and the MFI value as per material specification is 16.

Polypropylene nanocomposite filament yarns were prepared with various concentrations of SiO_2 nanoparticles viz. 0.1%, 0.3%, 0.5%, 0.7%, 1.0%, 1.25% and 1.5%. The nomenclature used during discussion for the samples prepared is as follow.

Table 4.6 Nomenclature of polypropylene SiO_2 nanocomposite filaments

Sr. No.	SAMPLE	COMPOSITIONS
1	PP	Polypropylene without doping of SiO_2
2	NPP1	Polypropylene with 0.1% doping of SiO_2
3	NPP2	Polypropylene with 0.3% doping of SiO_2
4	NPP3	Polypropylene with 0.5% doping of SiO_2
5	NPP4	Polypropylene with 0.7% doping of SiO_2
6	NPP5	Polypropylene with 1.0% doping of SiO_2
7	NPP6	Polypropylene with 1.25% doping of SiO_2
8	NPP7	Polypropylene with 1.5% doping of SiO_2

PP: polypropylene, NPP: Nano silica loaded polypropylene

The prepared nanocomposite samples were compared with the sample prepared without SiO_2 nanoparticles, which is considered as control sample for further investigation. Prior pilot trials were undertaken to optimize the parameters involved during melt spinning for continuous spinning of filaments. Finally the control and the nanocomposite samples were prepared by using the optimized spinning parameters as given in table 3.6.

a) Pure polypropylene (PP)

b) Polypropylene and 0.1% SiO_2 filament (NPP1)

c) Polypropylene and 0.3% SiO_2 filament (NPP2)

d) Polypropylene and 0.5% SiO_2 filament (NPP3)

e) Polypropylene and 0.7% SiO_2 filament (NPP4)

f) Polypropylene and 1.0% SiO_2 filament (NPP5)

g) Polypropylene and 1.25% SiO_2 filament (NPP6)

h) Polypropylene and 1.5% SiO_2 filament (NPP7)

Figure 4.14 Polypropylene pure (a) and nanocomposite (b to h) filaments

4.2.1 STRUCTURAL ANALYSIS

4.2.1.1 Surface morphological analysis through SEM

The dispersion of SiO_2 nano particles on the surface of polypropylene filaments and inside the polymer matrix was observed by SEM micrographs. Figure 4.15 shows the SEM photograph of control sample, clear surface of filament can be seen at different magnifications. Figures 4.16 to 4.22 show the polypropylene filaments containing 0.1 to 1.5% SiO_2 nanoparticles by weight and figure 4.23 shows the cross sectional view of 0.7% concentration of SiO_2 nanoparticles prepared at melt spinning pilot plant.

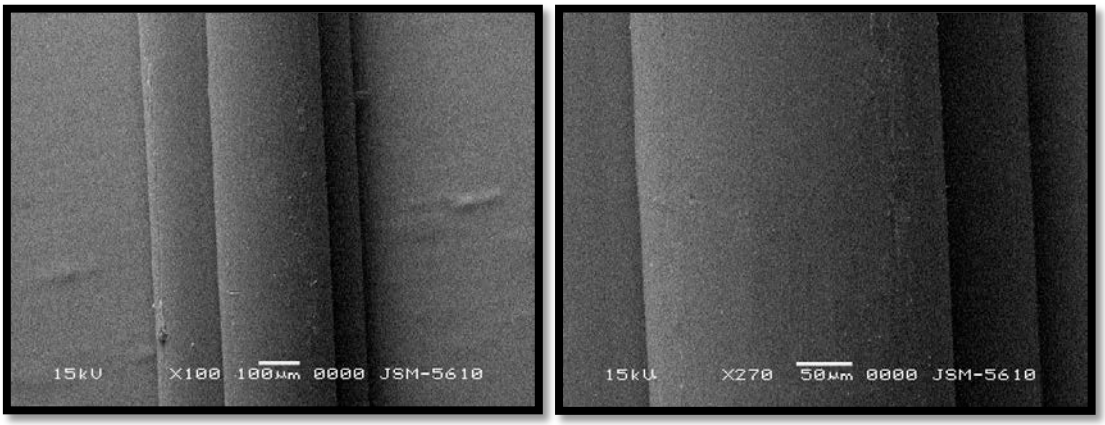

Figure 4.15 SEM photographs of Pure Polypropylene filaments (PP)

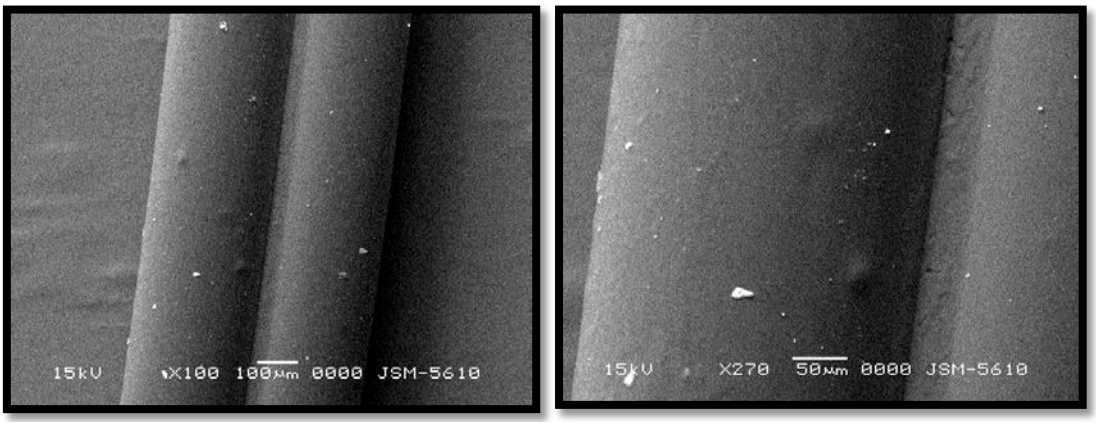

Figure 4.16 SEM photographs of PP filaments with 0.1% SiO_2 (NPP1)

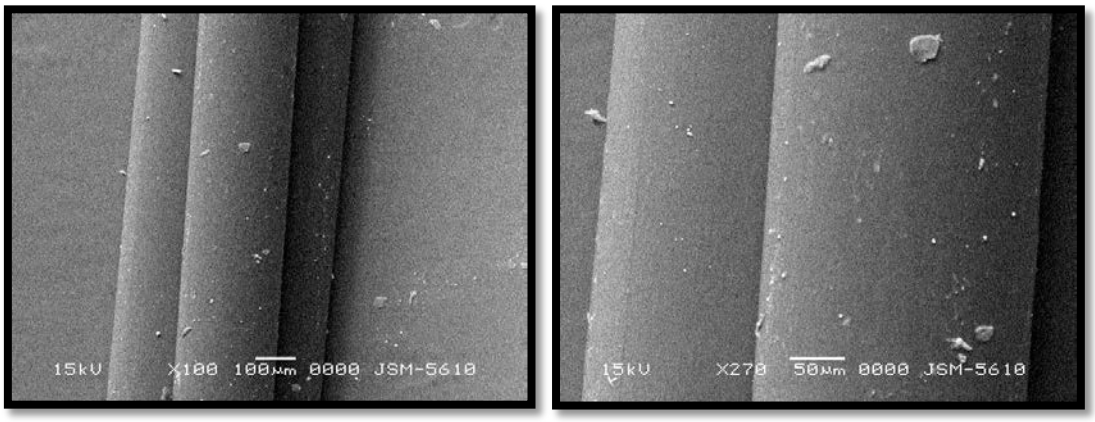

Figure 4.17 SEM photographs of PP filaments with 0.3% SiO_2 (NPP2)

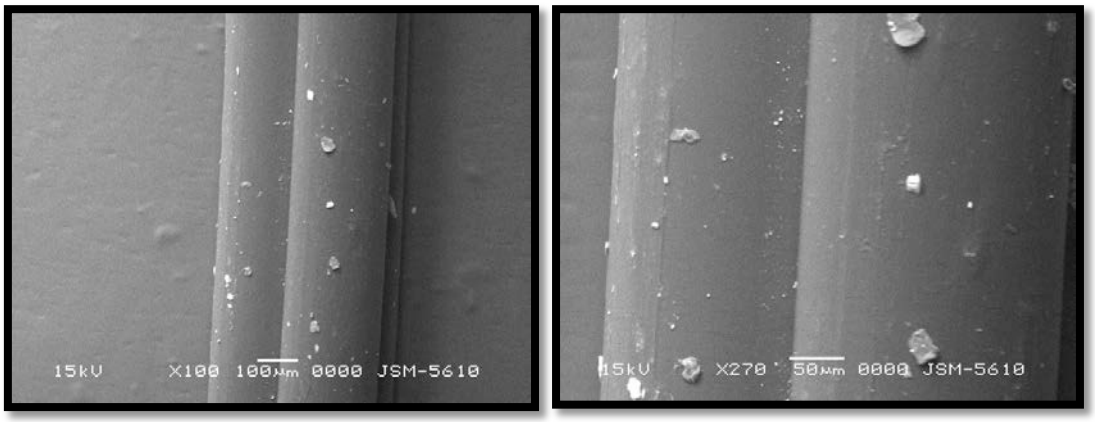

Figure 4.18 SEM photographs of PP filaments with 0.5% SiO_2 (NPP3)

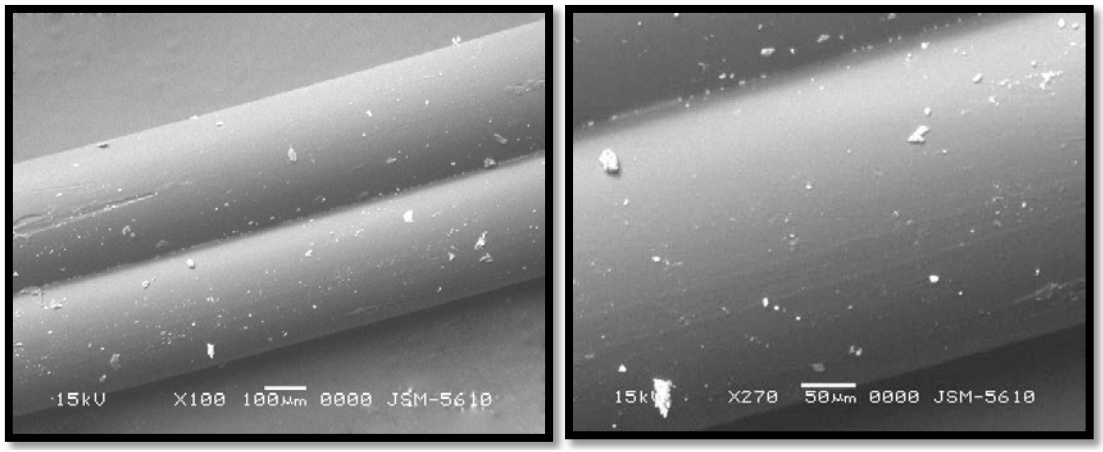

Figure 4.19 SEM photographs of PP filaments with 0.7% SiO_2 (NPP4)

The SEM micrographs confirm uniform distribution of nanoparticles. Some agglomeration of nano particles can be seen from 1% concentration. This agglomeration may be attributed to the increased concentration of SiO_2 nanoparticles and density difference of polypropylene and SiO_2. Polypropylene has density of 0.9

gm/cc and SiO_2 has density of 2.65 gm/cc [149]. The amount of agglomeration also increases with the increase in percentage concentration of SiO_2 nanoparticles.

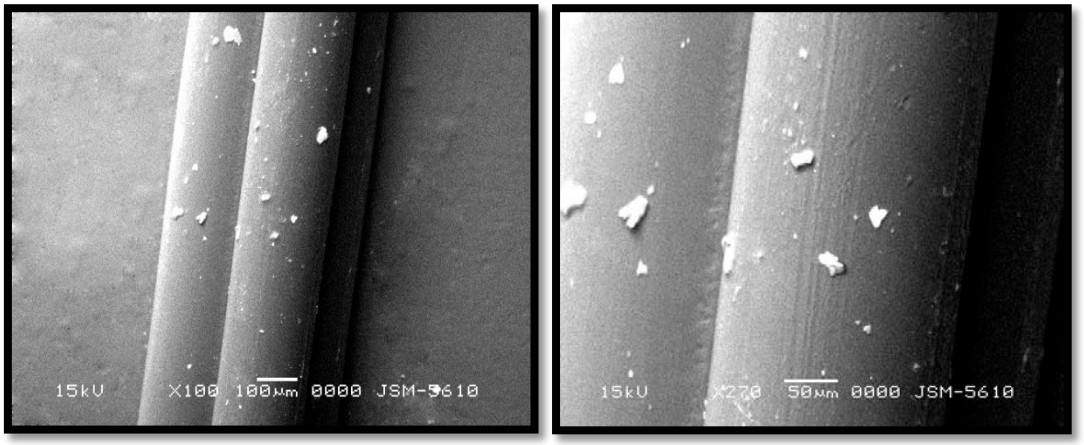

Figure 4.20 SEM photographs of PP filaments with 1.0% SiO_2 (NPP5)

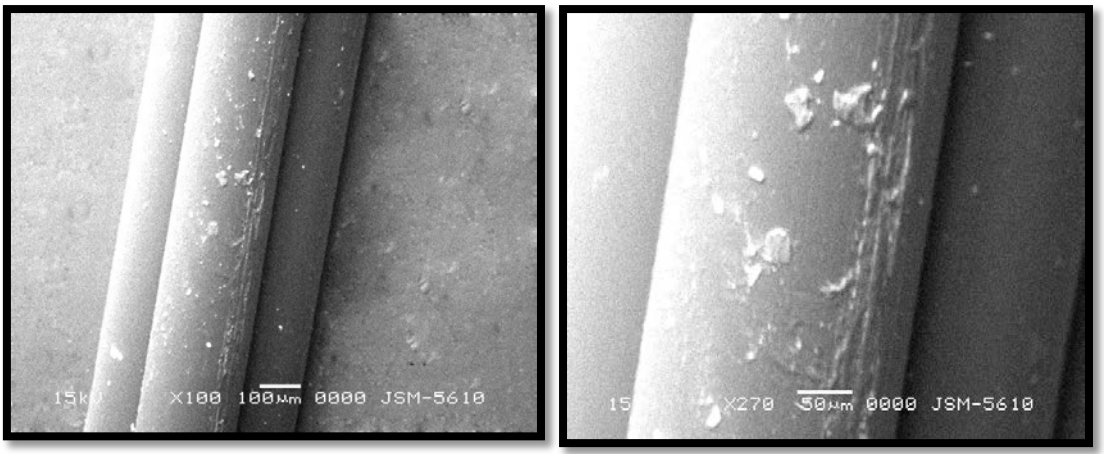

Figure 4.21 SEM photographs of PP filaments with 1.25% SiO_2 (NPP6)

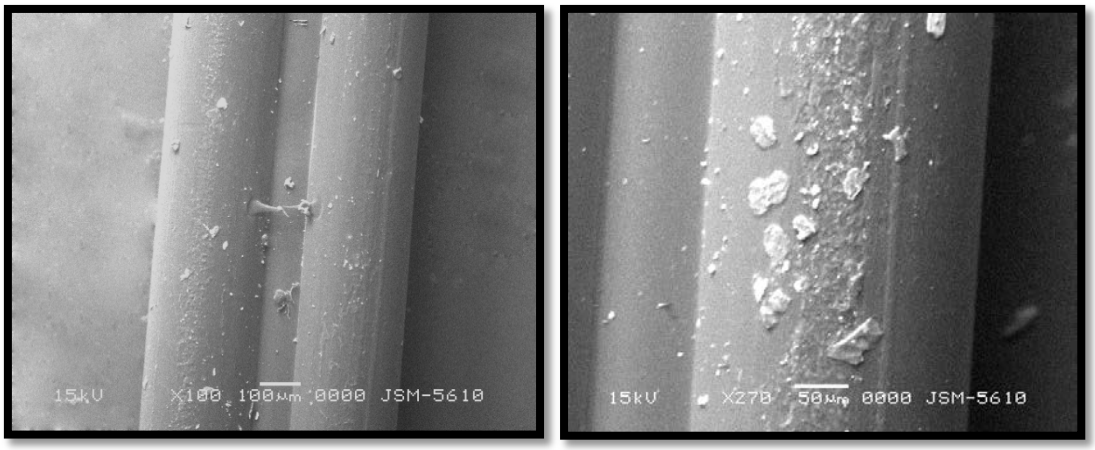

Figure 4.22 SEM photographs of PP filaments with 1.5% SiO_2 (NPP7)

The figure 4.23 shows the cross-sectional view of polypropylene silica nanocomposite filaments of 0.7% concentration of silica nano particles. In this view it can be seen that the distribution of the nanoparticles is throughout the structure of filament and also the distribution of nano particles is uniform.

The distribution of the nanoparticles within the structure has shown good uniformity for all the samples under consideration. Even number of nanoparticles induced within the structure has increased in direct proportion to SiO2 content. The photographs show that even with the increase in percentage of SiO2 content, good particle distribution was obtained.

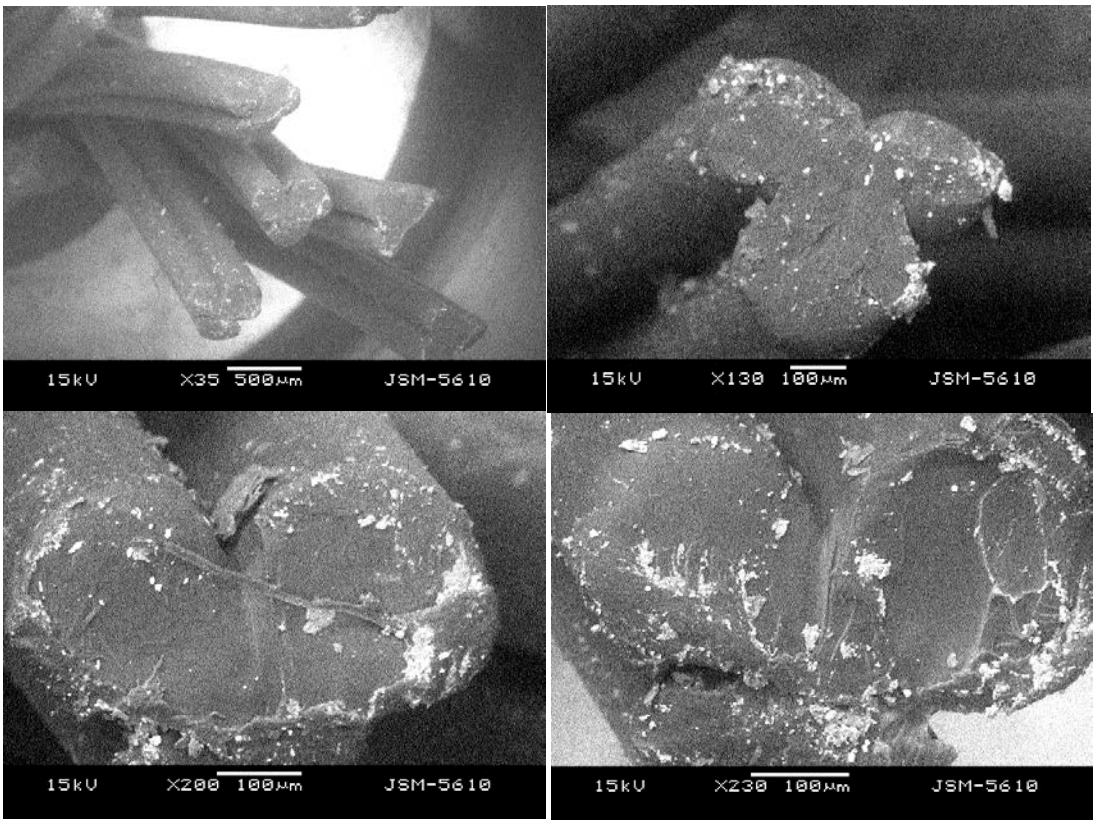

Figure 4.23 SEM cross-sectional photographs of PP filaments with 0.7% SiO_2 (NPP4)

4.2.1.2 Elemental analysis

The elemental analysis of pure polypropylene filament and polypropylene silica nanocomposite filament was performed on scanning electron microscope using Oxford-Inca software. The test results are shown in figure 4.24 and 4.25 and table 4.7 and 4.8. The presence of silica was confirmed by the elemental analysis curve, also the presence of oxygen in figure and table indicate that the silica is in the form of oxide or dioxide. Preparation of sample for testing as well as silicon dioxide nano particles may consist of impurities in final product like sodium, magnesium, chlorine, potassium, calcium and ferrous, as it has been reflected in elemental analysis. It may affect some properties of final product.

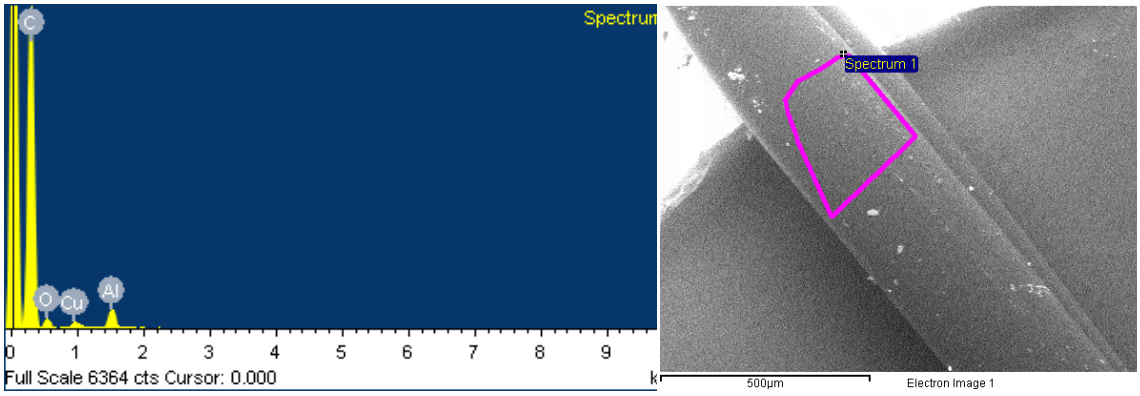

Figure 4.24 EDX spectrum of pure polypropylene filament

Table 4.7 Elemental analysis data of pure polypropylene filament

Element	Weight%	Atomic%
C K	87.50	92.05
O K	8.30	6.56
Al K	2.08	0.97
Cu L	2.11	0.42
Total	**100.00**	

K: Confirm, L: Probable

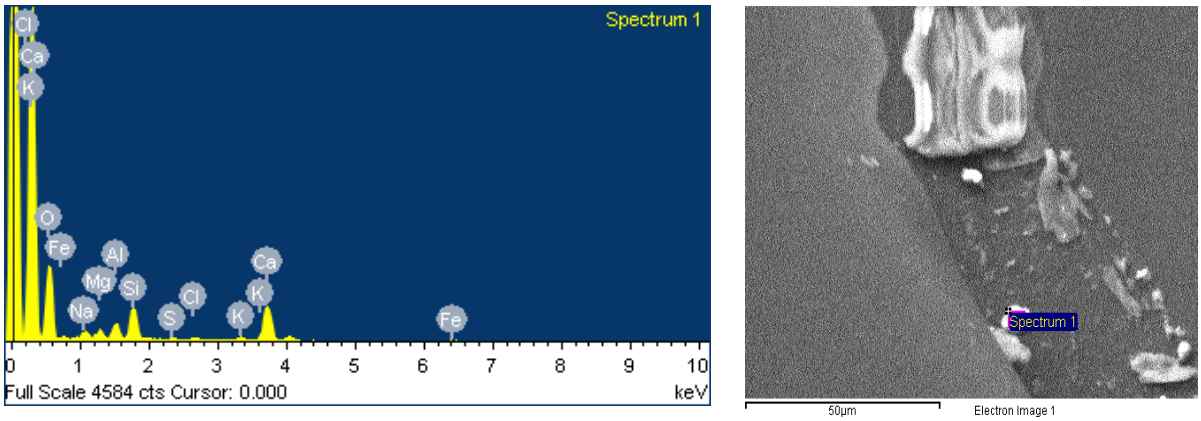

Figure 4.25 EDX spectrum of polypropylene silica nanocomposite filament

Table 4.8 Elemental analysis data of polypropylene silica nanocomposite filament

Element	Weight%	Atomic%
O K	60.17	75.42
Na K	2.99	2.61
Mg K	2.50	2.06
Al K	3.90	2.90
Si K	8.86	6.33
S K	0.58	0.36
Cl K	0.87	0.49
K K	1.52	0.78
Ca K	16.66	8.34
Fe K	1.97	0.71
Total	**100.00**	

4.2.1.3 FTIR spectral analysis

The chemical compositions of the control sample and polypropylene/SiO_2 nanocomposite filaments were evaluated using FTIR Spectroscopy. Figure 4.26 (a) represents the IR absorption peak of pure polypropylene whereas figure 4.26 (b to i) represent IR absorption peaks of different concentrations SiO_2 nanoparticles in polypropylene nanocomposite filaments.

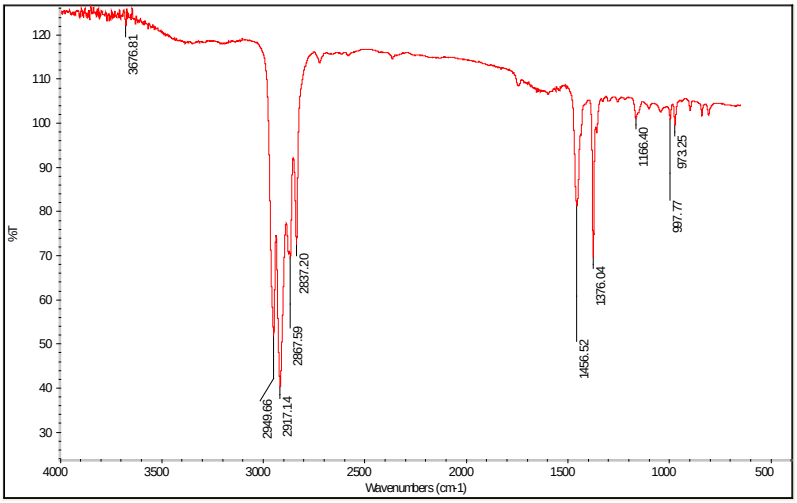

a) FTIR of Pure Polypropylene filaments (PP)

The chemical compositions of the pure polypropylene and polypropylene/silica nanocomposite filaments were evaluated using FTIR Spectroscopy. Figure 4.26(a) represents the IR characterization absorption peak of pure polypropylene filament, from which it can be seen that the major peaks associated were hydrogen bonded symmetric C-H stretching around 2949 cm^{-1}, asymmetric -CH stretching vibration at 2917 and 2867 cm^{-1} [140], C-H stretching vibrations [141] at 2837 cm^{-1}, C=O stretching is observed at 1750 $cm^{-1,}$ asymmetrical CH_2 bending [140] scissoring type at 1456 cm^{-1}, symmetrical CH bending [140] at 1376 cm^{-1}, the presence of polypropylene is confirmed at 973 cm^{-1} which is irrespective of it's tacticity, but at 997 and 1166 cm^{-1} it is confirmed that the tacticity of polypropylene polymer is iso-tactic. Very few O-H stretch and free vibrations peak is observed around 3676 cm^{-1}.

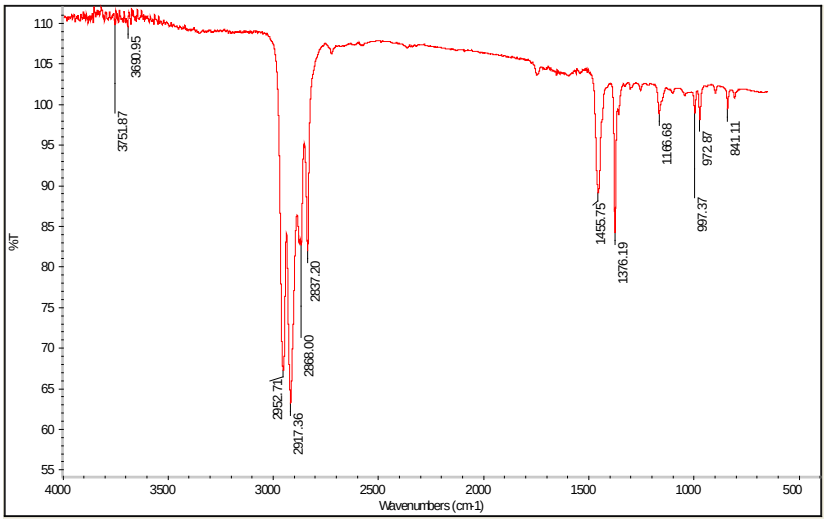

b) FTIR of PP filament with 0.10% SiO_2 (NPP1)

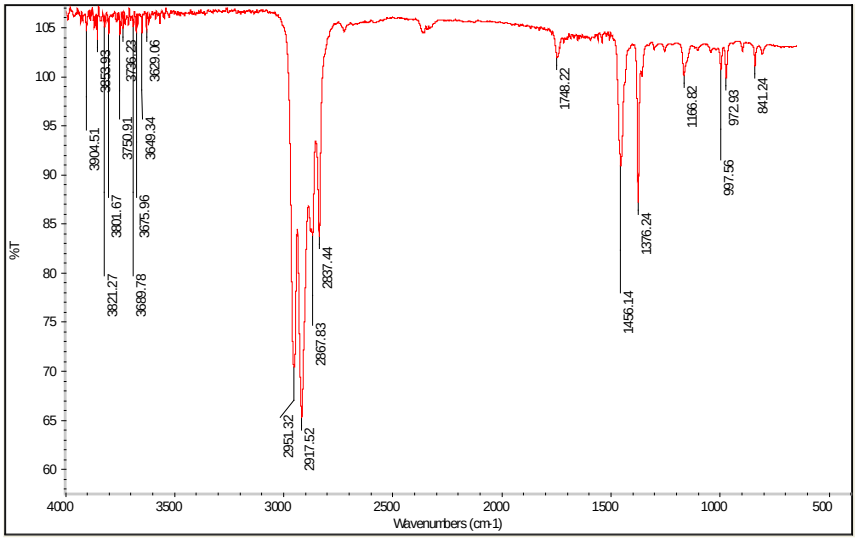

c) FTIR of PP filament with 0.30% SiO_2 (NPP2)

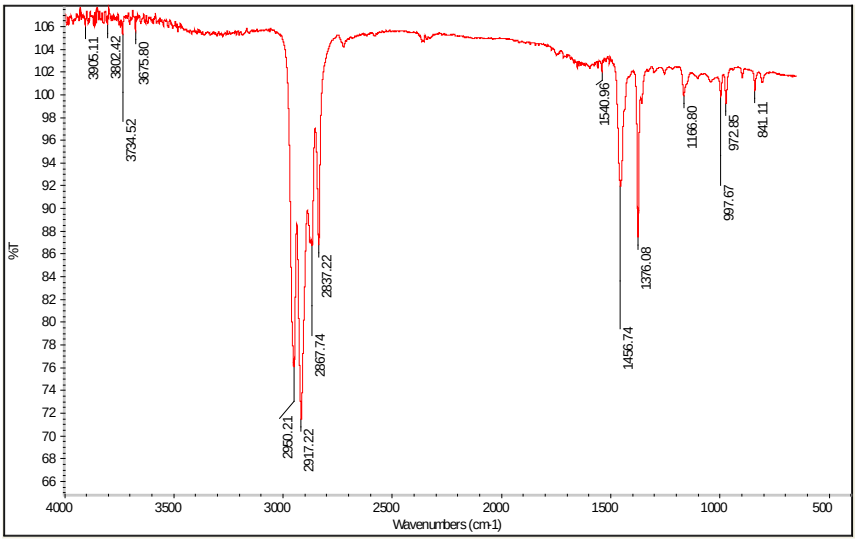

d) FTIR of PP filament with 0.50% SiO_2 (NPP3)

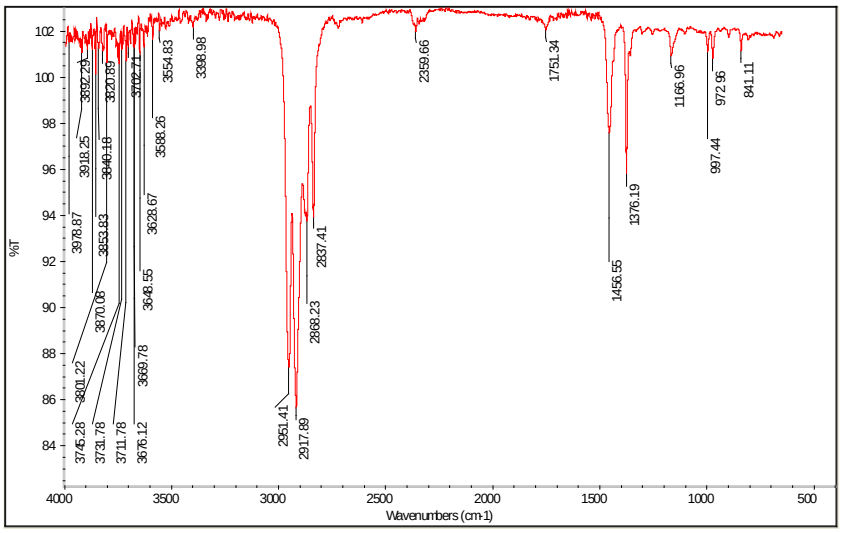

e) FTIR of PP filament with 0.70% SiO_2 (NPP4)

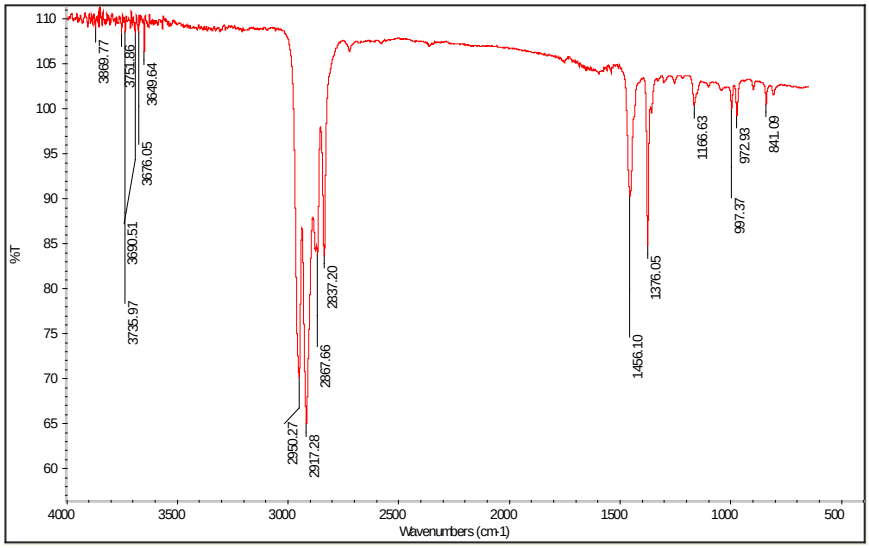

f) FTIR of PP filament with 1.00% SiO_2 (NPP5)

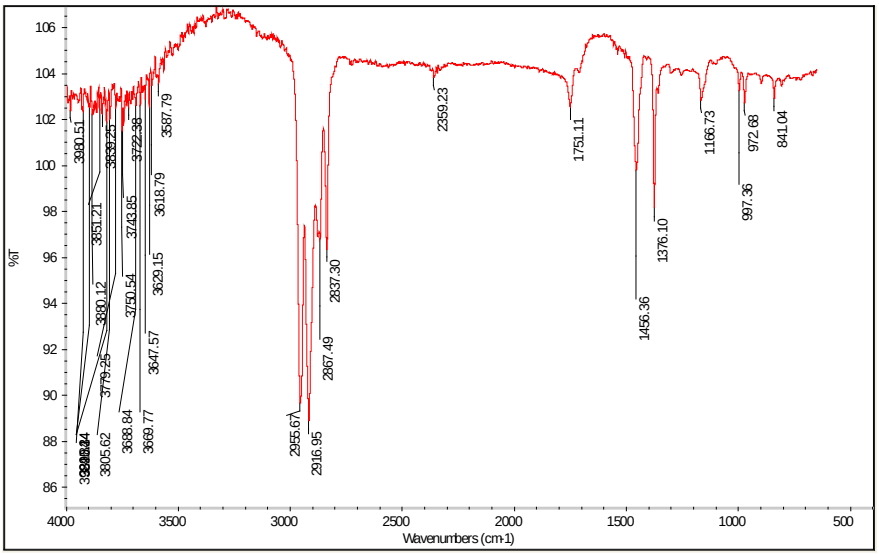

g) FTIR of PP filament with 1.25% SiO_2 (NPP6)

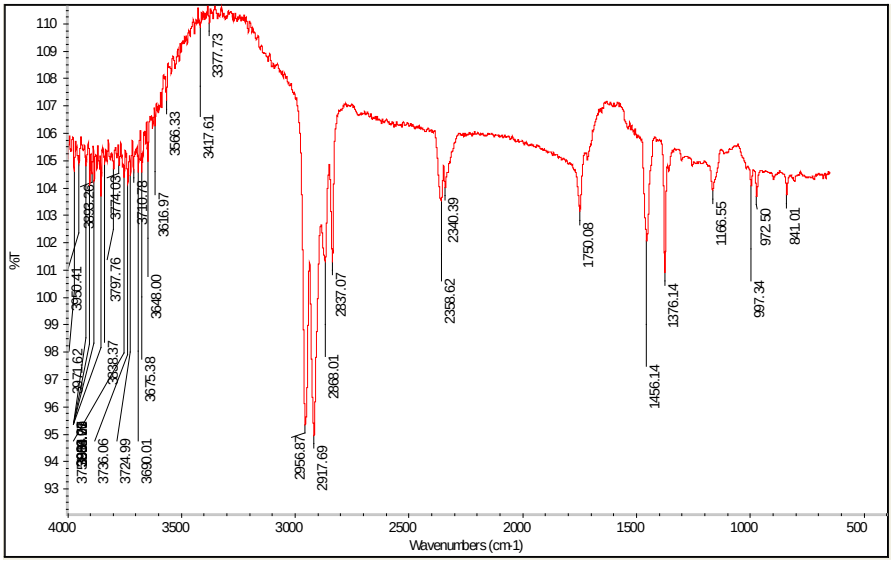

h) FTIR of PP filament with 1.50% SiO_2 (NPP7)

Figure 4.26 IR absorption peaks of pure polypropylene (a) and polypropylene/Silica nanocomposite filaments (b to h).

Peaks shown by pure polypropylene filaments are identical in all polypropylene silica nanocomposite filaments as shown in figure 4.26 (b to h as individual graphs; due to limitation of machine it was not possible to superimpose them), additionally all the nanocomposite filaments shown the peaks of silica at 841 cm^{-1} corresponds to Si-O [143, 150] bending vibration. Due to addition of silica nano particles in polypropylene in different concentrations, the FTIR peaks showed the increased stretching vibrations of O-H in the range of 3500 to 4000 cm^{-1} in all spectrographs of nanocomposite filaments, also the number of stretching vibrations in this range increased with increase in concentration of nano silica particles. Intramolecular H-bridges at 2359 cm^{-1} [151] increases as the concentration of silica in polypropylene nanocomposite filament increased, the reason may be silica would be getting bonded with hydrogen at higher concentration. The CO_2 peaks are found at 2340, 2359 cm^{-1} in the samples from 0.7% concentration of nano silica nanocomposite filaments. The reason could be the oxidation of the methyl group caused the formation of CO_2 and confined to small voids in the Si-O-Si network [152].

Table 4.9 FTIR characterization peaks of pure polypropylene and polypropylene / Silica nanocomposite filaments.

Groups	**Wavenumber (cm^{-1})**							
	PP	**NPP1**	**NPP2**	**NPP3**	**NPP4**	**NPP5**	**NPP6**	**NPP7**
Si-O bending vibration	-	841	841	841	841	841	841	841
Presence of polypropylene irrespective of tacticity	973	972	972	972	972	972	972	972
Iso-tactic polypropylene	997	997	997	997	997	997	997	997
Iso-tactic polypropylene	1166	1166	1166	1166	1166	1166	1166	1166
Symmetrical CH bending	1376	1376	1376	1376	1376	1376	1376	1376
Asymmetrical CH_2 bending-scissoring type	1456	1456	1456	1456	1456	1456	1456	1456
C=O stretching	1750	1750	1748	1750	1751	1750	1751	1750
CO_2 formation			2340		2340		2340	2340
Intramolecular H-bridges			2359	2359	2359	2359	2359	2358
-CH stretching vibration	2837	2837	2837	2837	2837	2837	2837	2837
Asymmetric -CH stretching vibration	2867	2868	2867	2867	2868	2867	2867	2868
	2917	2917	2917	2917	2917	2917	2916	2917
Symmetric -CH stretching vibration	2949	2952	2951	2950	2951	2950	2955	2956
O-H stretch and free vibrations	3500 to 4000	3500 to 4000	3500 to 4000	3500 to 4000	3500 to 4000	3500 to 4000	3500 to 4000	3500 to 4000

4.2.1.4 X-ray diffraction analysis

The X-ray diffraction patterns were taken on X'pert Pro PANalytical x-ray diffractometer. The XRD of both the fabrics was done within the 2θ range of 10° to 30° at the scan speed of 3° per minute at 25°C temperature, using Cu-K_α radiation of wavelength 1.5406Å. The diffraction profiles were obtained for individual samples. The XRD patterns are given in figure 4.27 and 4.28 for PP and NPP4 samples i.e. pure polypropylene filament and 0.7% nano silica in polypropylene filament respectively.

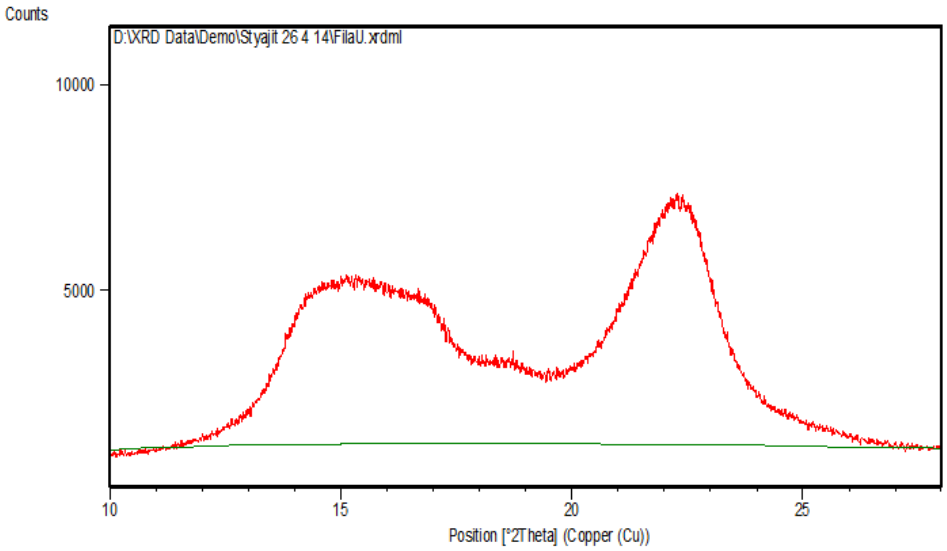

Pos. [°2θ]	Height [cts]	d-spacing [Å]	Area[cts*°2θ]	Rel. Int. [%]
16.2515	2950.48	5.44974	2325.38	48.08
18.9598	1571.51	4.67694	3731.00	25.61
22.8988	6136.10	3.88056	4711.30	100

Figure 4.27 XRD pattern of pure polypropylene filament (PP)

In the XRD pattern of PP sample, only two broad prominent features are observed, which is an indication of a predominantly amorphous structure. The feature at 2θ value of 22.8988° has the highest intensity followed by very broad feature with elevation at 16.2515° and 18.9598°.

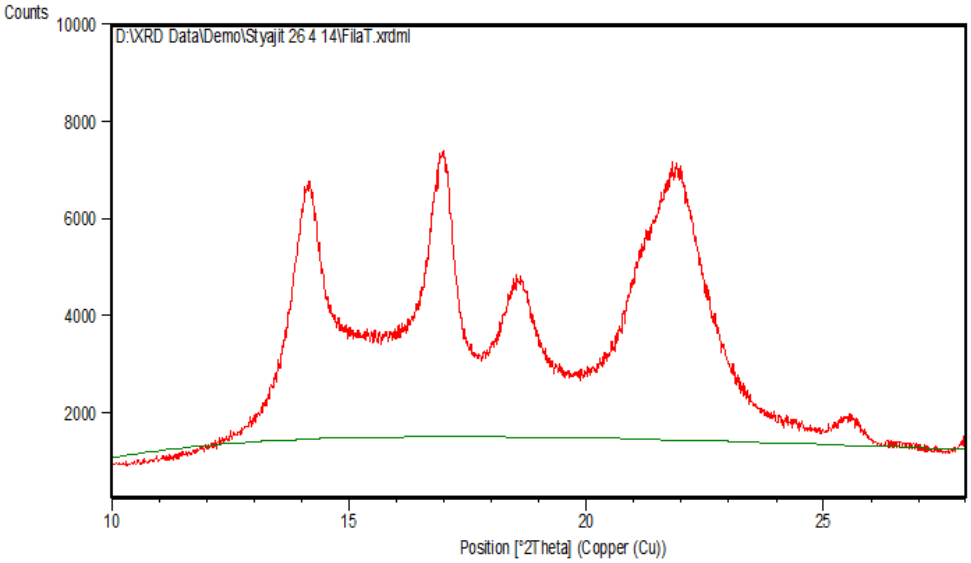

Pos. [°2θ]	Height [cts]	d-spacing [Å]	Area [cts*°2θ]	Rel. Int. [%]
14.176	4547	6.24270	5940.13	82.31
16.872	5524	5.25059	7770.83	100
18.339	2503	4.83392	2561.03	45.32
22.454	2778	3.95646	3164.23	50.29
25.479	675	3.49319	410.37	12.22

Figure 4.28 XRD pattern of polypropylene silica nanocomposite filament (NPP4)

Figure 4.28 shows the XRD pattern of NPP4 sample, which clearly shows the change in XRD pattern due to addition of silica nano particles. It shows some sharper features with high intensity. Five prominent and wide peaks are observed. The peak at 2θ value of 16.872° has the highest intensity followed by 14.176°, 22.454°, 18.339° and 25.479° in that order.

Addition of silica nano particles result into enhanced crystallinity, which can be seen from the appearance of multiple peaks in the treated samples. The presence of silica nano particles might be affecting the kinetics of the interaction between the polymer and silica nanoparticles to give better crystallinity. Similar results have been observed by Srisawat, et al. that due to addition of nano silica, the polypropylene crystallinity increases on account of nucleating effect [153].

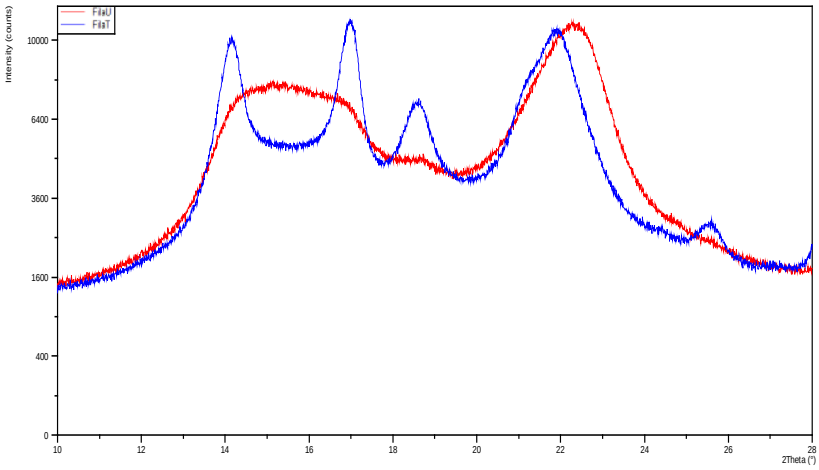

Figure 4.29 Combined XRD patterns of PP and NPP4 samples

The 'd' values for the observed diffraction peak of silica is in close agreement with those reported for corresponding standard samples as reported in JCPDS data file no. 84-0384. The peak corresponding to the d-value of 3.9518 Å is an exact match with the obtained data.

4.2.1.5 Thermal analysis

Table 4.10 Effect of SiO_2 concentration on melting point of PP and enthalpy of melting (ΔH)

Samples	SiO_2 Concentration (%)	Melting Point T_m (°C)	Enthalpy ΔH (J/g)	Crystallinity $=\left(\frac{\Delta H}{(1-w_f)\Delta H^*}\right) \times 100$ (%)
CS	0.00	162.40	82.97	39.70
NPP1	0.10	161.99	85.50	41.03
NPP2	0.30	162.94	87.96	42.62
NPP3	0.50	162.97	87.92	42.36
NPP4	0.70	161.63	90.52	43.75
NPP5	1.00	163.13	94.23	45.31
NPP6	1.25	162.45	82.92	40.28
NPP7	1.50	161.42	81.41	38.97

The thermal analysis was done on DSC 6000, by Perkin Elmer for all the samples. In the present study the concentration of nano silica selected was from 0.1% to 1.5%. The results of the analysis are reported in table 4.10 and the DSC curves are given in figure 4.26 (a to h).

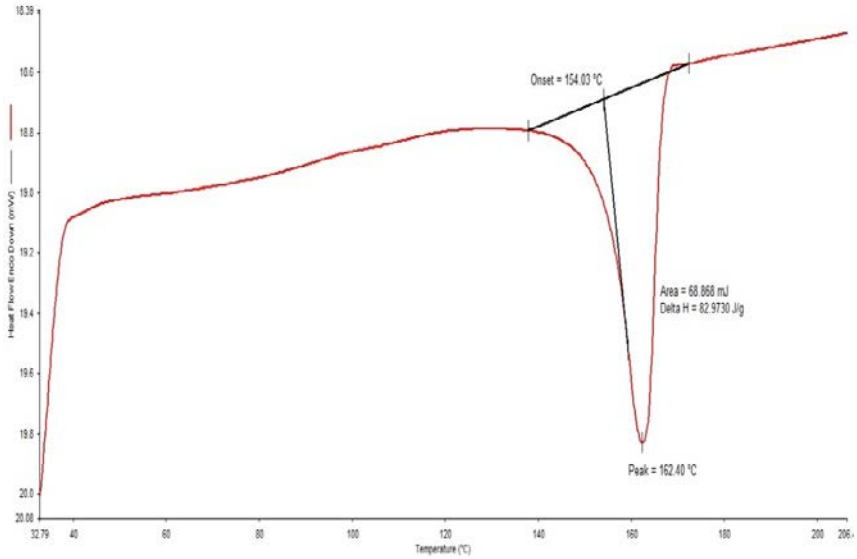

a) DSC curve of pure polypropylene filament (PP)

Figure 4.30 (a) shows the differential scanning calorimetry (DSC) curve of pure polypropylene filament. Here the pure polypropylene filament sample was heated at 10°C/min rate upto 300°C, in which it shows the melting temperature of the polypropylene filament as 162.4°C and the total heat required to melt i.e. enthalpy (ΔH) is 82.97 J/g, the % crystallinity calculated on the bases of enthalpy is 39.70%.

Figure 4.30 (b to h) shows the DSC curves of nanocomposite filaments of polypropylene and SiO_2 nano particles at different concentration levels like 0.1%, 0.3%, 0.5%, 0.7%, 1.0%, 1.25% and 1.5%. The melting temperature, enthalpy and % crystallinity of all filaments are given in table 4.10. The melting temperature of pure polypropylene filament is 162.4°C and there is no significant effect on melting temperature of all the nanocomposite filaments due to addition of silica nano particles. In case of polyamide film there was reduction in melting temperature at 1% silica concentration from 215°C to 209°C, which is explained in part-I. Even though there is agglomeration seen in 1%, 1.25% and 1.5% concentration sample of polypropylene nanocomposite filaments, there is no effect of this agglomeration on melting temperature like polyamide film.

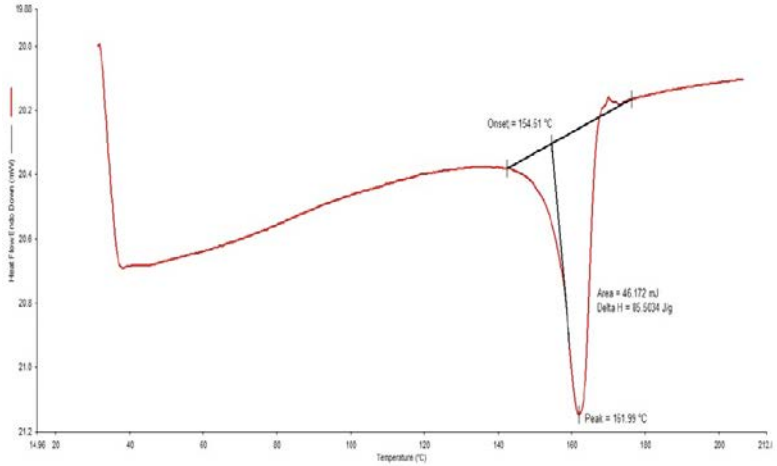

b) DSC curve of Polypropylene filament with 0.10% SiO_2 nanoparticles (NC - 2)

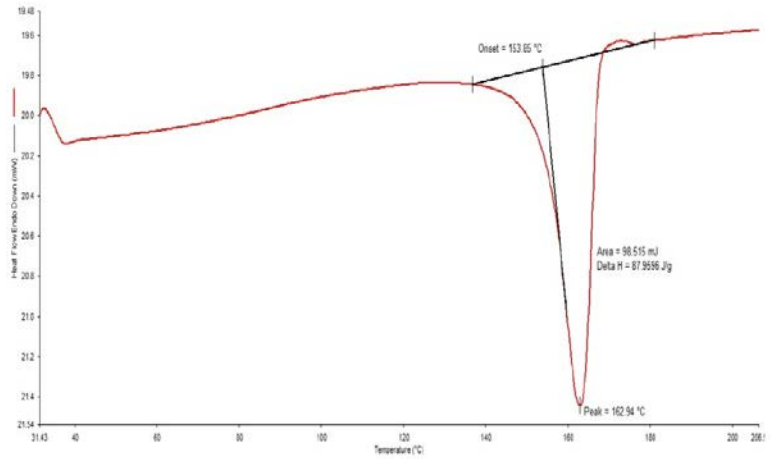

c) DSC curve of Polypropylene filament with 0.30% SiO_2 nanoparticles (NPP2)

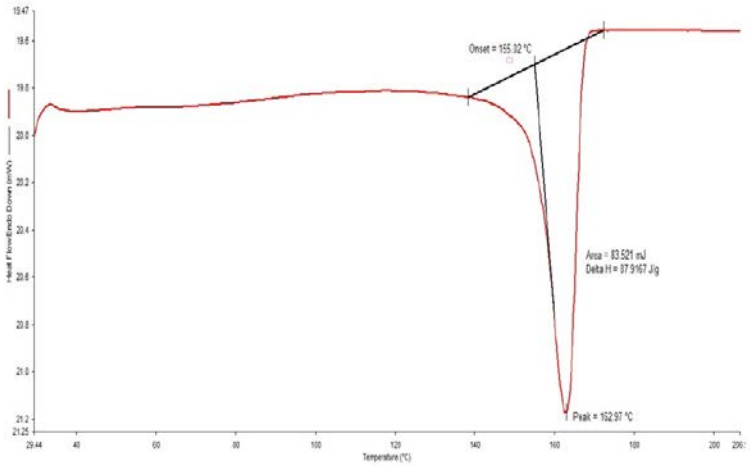

d) DSC curve of Polypropylene filament with 0.50% SiO_2 nanoparticles (NPP3)

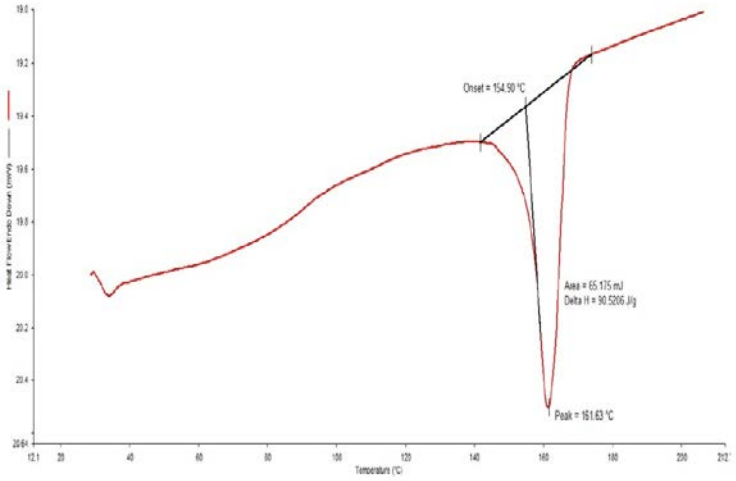

e) DSC curve of Polypropylene filament with 0.70% SiO_2 nanoparticles (NPP4)

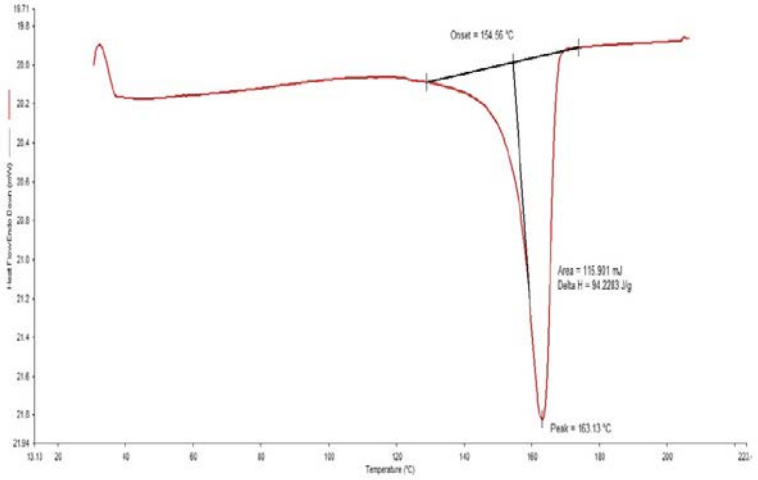

f) DSC curve of Polypropylene filament with 1.00% SiO_2 nanoparticles (NPP5)

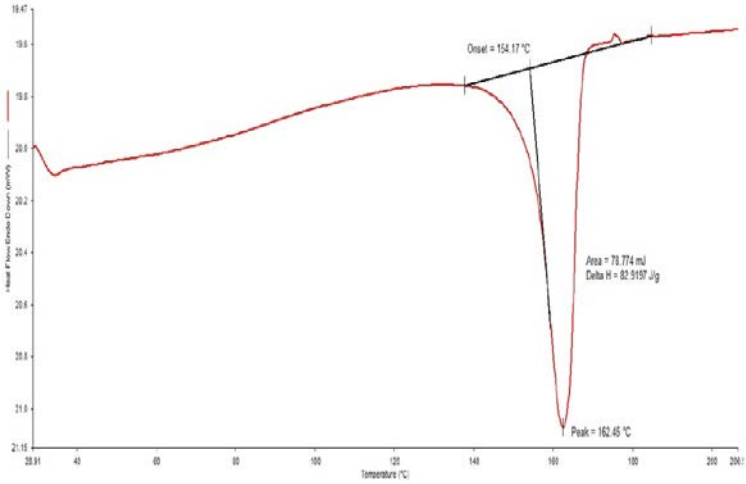

g) DSC curve of Polypropylene filament with 1.25% SiO_2 nanoparticles (NPP6)

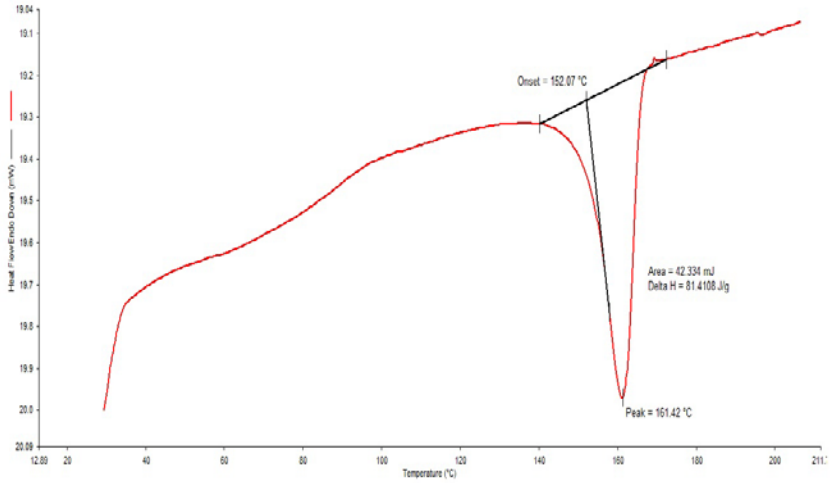

h) DSC curve of Polypropylene filament with 1.50% SiO_2 nanoparticles (NPP7)

Figure 4.30 DSC curves of pure polypropylene (a) and polypropylene silica nanocomposite filaments (b to h)

It can be seen from the table 4.10 that with increase in SiO_2 nanoparticles concentration the ΔH value (enthalpy) has increased. The increase is in direct proportion to the SiO_2 nanoparticle concentration in polypropylene matrix i.e. upto 1% concentration and thereafter decreases. The same has led towards the increase in crystallinity value of the nanocomposite filament yarns in the same proportion [154]. Altan et al. [137] had reported that the increase in crystallinity with the increased SiO_2 nanoparticles concentration in polypropylene matrix was mainly attributed to the nucleation role of nanoparticles used. The results obtained in the present research have also followed the same trend.

The percentage change in enthalpy is found increasing by 3.05%, 6.01%, 5.97%, 9.10% and 13.57% with 0.1%, 0.3%, 0.5%, 0.7% and 1.0% concentration of nano silica in polypropylene filament respectively as compare to pure polypropylene filament. This may be due to increase in concentration and uniform distribution of nano particles in polymer matrix, which can be seen from the SEM micrographs. At 1.25% and 1.5% concentration of silica nano particles, the crystallinity is found reducing by 0.06% and 1.88% respectively as compare to pure polypropylene filament. This may be due to agglomeration of nano silica in polymer matrix and thus may not be allowing the formation of crystals, which has also seen in tenacity property, where with increase in concentration i.e. from 1%, the

tenacity is found reducing. This agglomeration of silica nano particles can also be seen from the SEM micrographs.

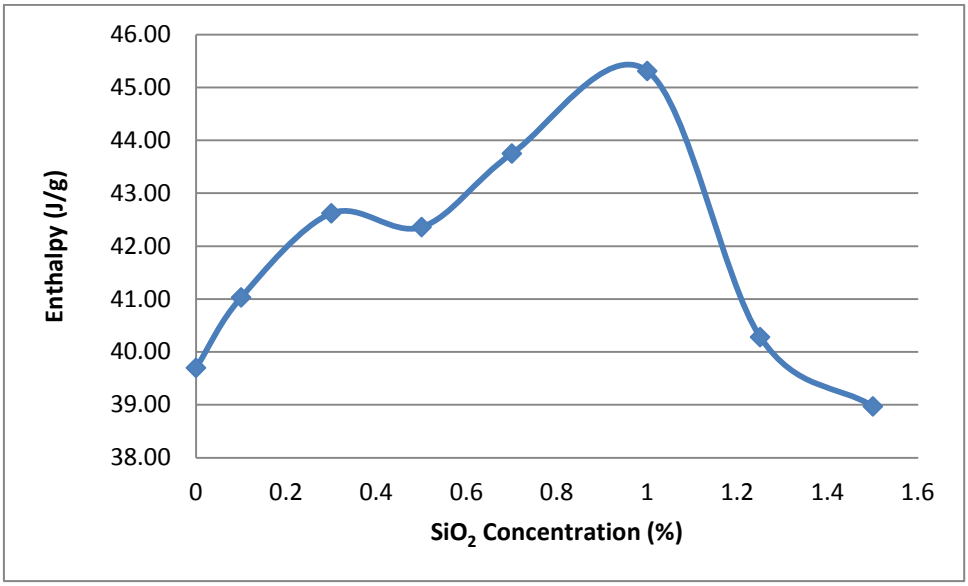

Figure 4.31 Effect of SiO_2 concentration on enthalpy of PP filament

The percentage change in crystallinity is found increasing by 3.35%, 7.36%, 6.70%, 10.20% and 14.13% with 0.1%, 0.3%, 0.5%, 0.7% and 1.0% concentration of nano silica in polypropylene filament respectively as compare to pure polypropylene filament. This may be due to increase in concentration and uniform distribution of nano particles in polymer matrix, which can be seen from the SEM micrographs. The XRD pattern also showing the increased number of peaks and their intensity also, this is an indication of increase in crystallinity. At 1.25% concentration of silica nanoparticles, the rise in crystallinity percentage is only 1.46% as compare to pure polypropylene filament, which is much less rise compare to lesser concentrations of nano particles polypropylene filaments. But at 1.5% concentration of silica nano particles the crystallinity is found reducing by 1.84% as compare to pure polypropylene filament. This may be due to agglomeration of nano silica in polymer matrix and thus may not be allowing bindings of polymer. This agglomeration of silica nano particles can also be seen from the SEM micrographs.

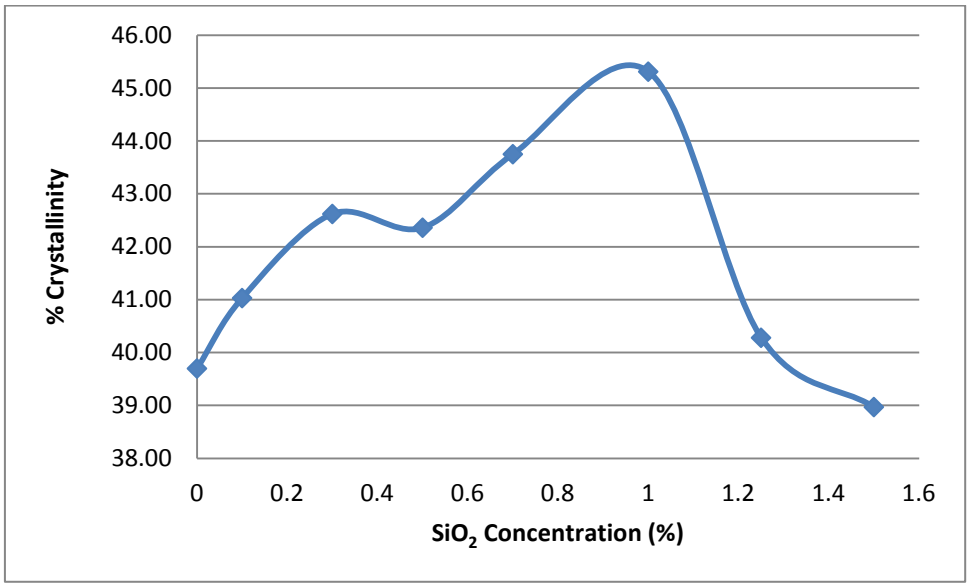

Figure 4.32 Effect of SiO_2 concentration on % crystallinity of PP filament

4.2.2 MECHANICAL PROPERTIES

The effect on mechanical properties i.e. tensile, young's modulus and work of rupture due to incorporation of silica nanoparticles in polypropylene filaments is studied here. The silica nanoparticles were added in different proportions as 0.1, 0.3, 0.5, 0.7, 1.0, 1.25 and 1.5 percentages on weight bases.

4.2.2.1 Tensile strength

The tensile test was performed on Llyod LRX tensile testing machine and the stress strain curves of various sample tested are summarized in table 4.11 and shown in figure 4.33 below.

Table 4.11 Effect of SiO_2 nano particles on tensile property of polypropylene filaments

SAMPLES	SiO_2 Concentration (%)	Average Linear Density (Denier)	Maximum Load in gm	Tenacity in gm/den	% Elongation
CS	0	2123.3	584.24	0.323	265.29
NPP1	0.1	1572.53	641.94	0.375	380.2
NPP2	0.3	616.79	288.63	0.464	585.51
NPP3	0.5	999.75	388.4	0.488	218.39
NPP4	0.7	677.84	364.66	0.542	286.93
NPP5	1	1806.3	634.29	0.299	365.38
NPP6	1.25	1717.6	438.66	0.279	311.82
NPP7	1.5	1742.9	498.5	0.288	206.48

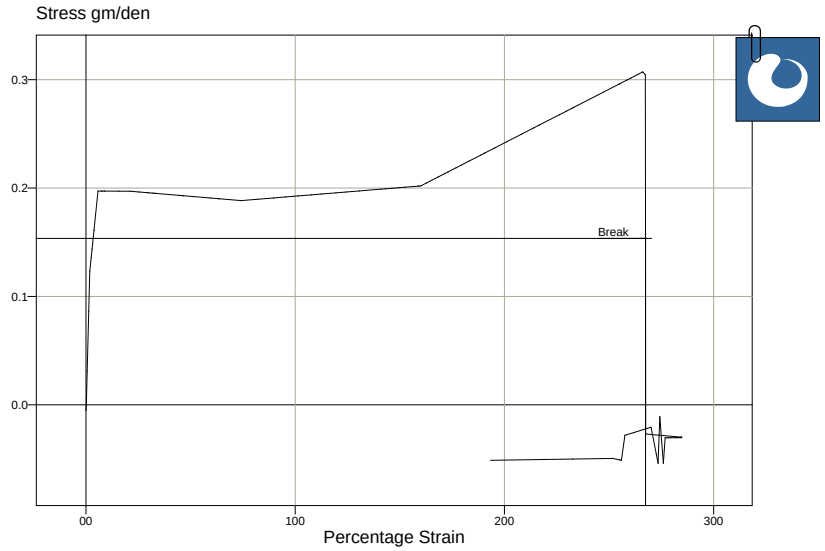

a) Pure Polypropylene filament (PP)

It is apparent from the results given in table 4.11 that as the concentration of silica nano particles increases, the strength of filament also increases. It may be due to the increased concentration of SiO_2 nanoparticles and stiff structure of silica particles, better dispersion and surface adhesion between the silicone dioxide and the polymer matrix causes

improvement in the tensile property of polypropylene filaments [137]. Nano particles in polymer structure impart stiffness to the polymer upto 0.7% concentration but beyond this concentration of SiO_2 the dispersion as well as surface adhesion between the nano particles and polymer structure may be getting disturbed, which result in decrease in tensile strength from 1% concentration and above [137].

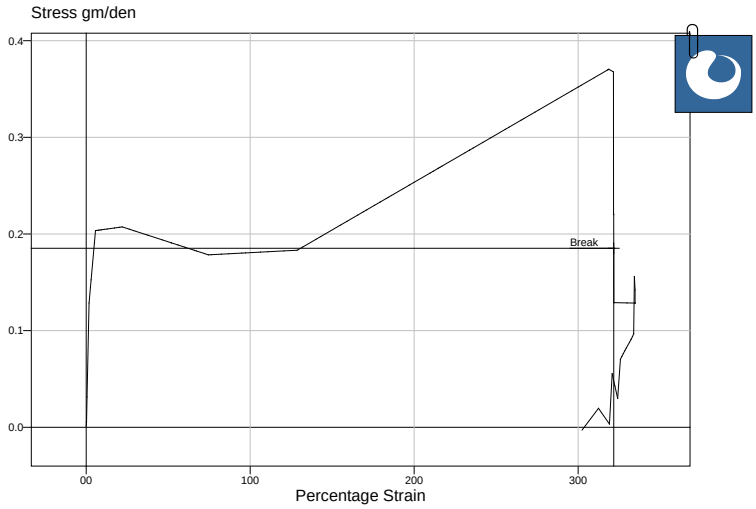

a) Polypropylene filament with 0.1% SiO_2 nanoparticles (NPP1)

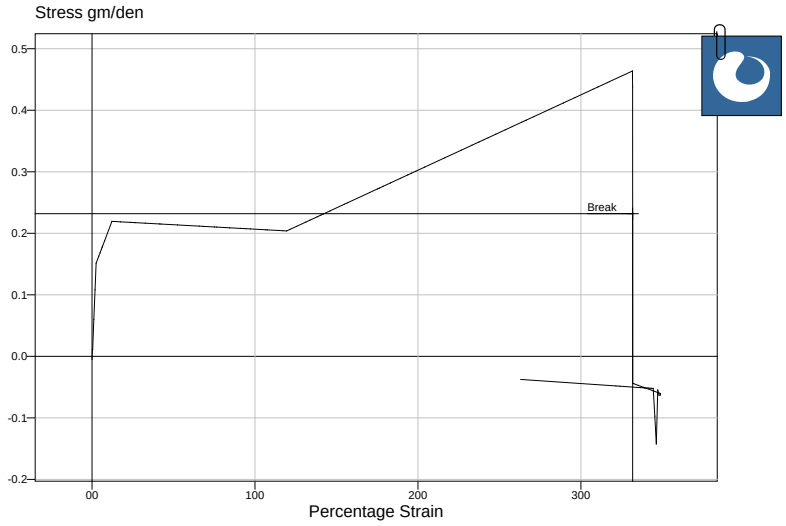

b) Polypropylene filament with 0.3% SiO_2 nanoparticles (NPP2)

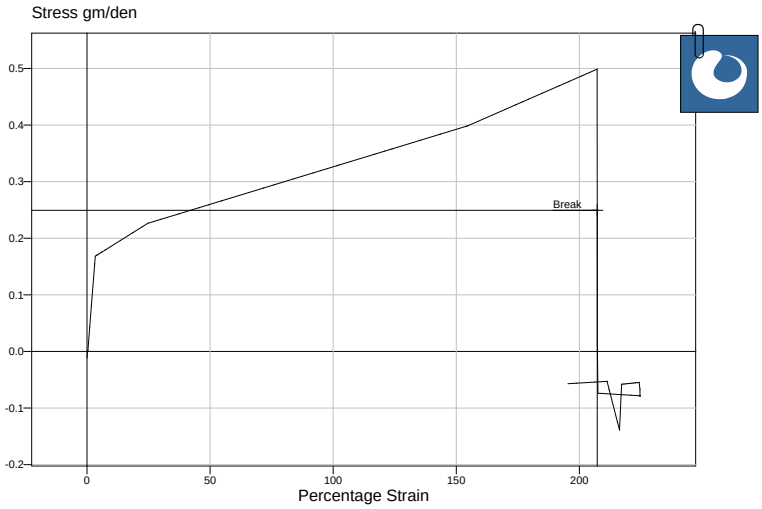

c) Polypropylene filament with 0.5% SiO_2 nanoparticles (NPP3)

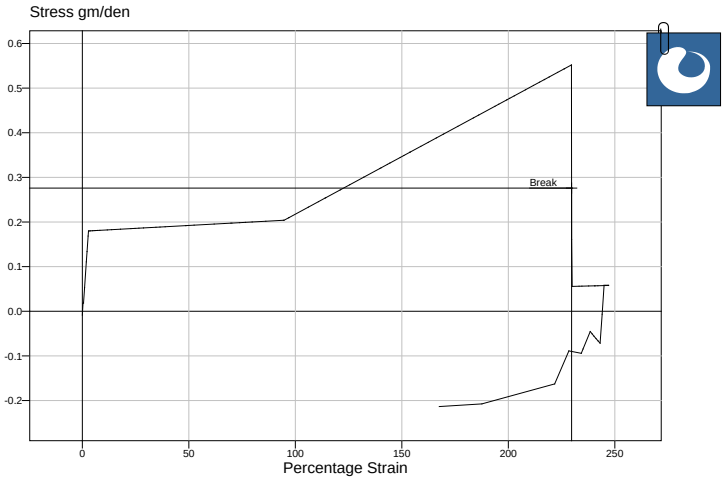

d) Polypropylene filament with 0.7% SiO_2 nanoparticles (NPP4)

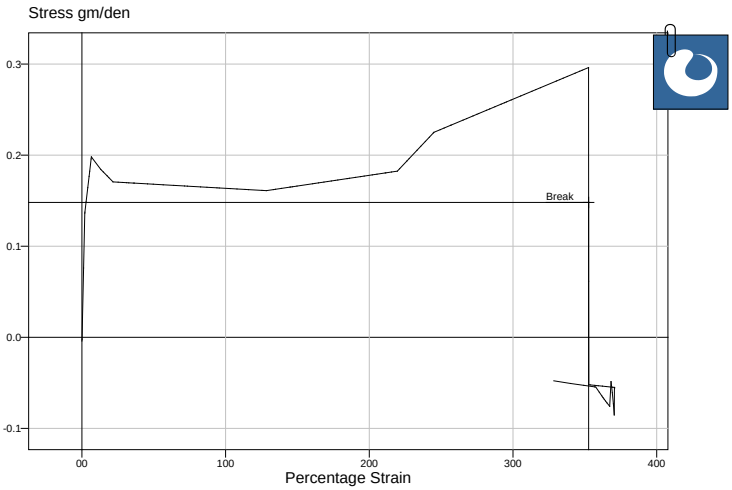

e) Polypropylene filament with 1% SiO_2 nanoparticles (NPP5)

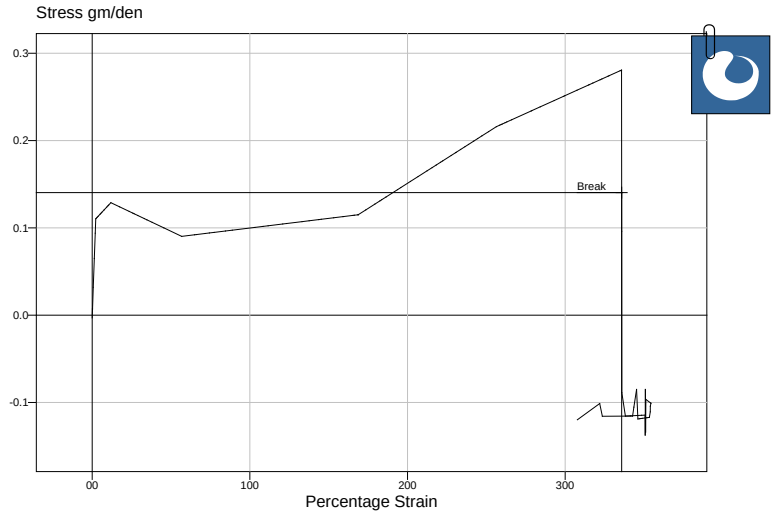

f) Polypropylene filament with 1.25% SiO_2 nanoparticles (NPP6)

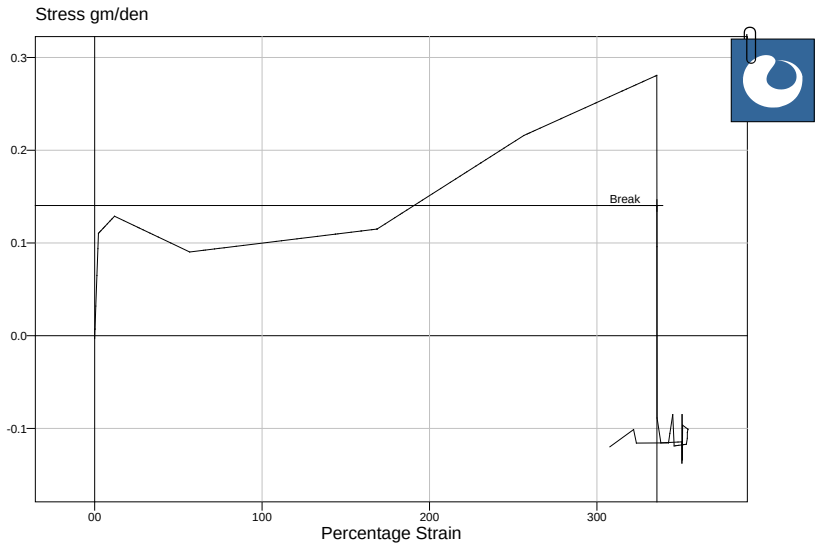

g) Polypropylene filament with 1.5% SiO_2 nanoparticles (NPP7)

Figure 4.33 Stress strain behavior of pure polypropylene (a) and polypropylene/SiO_2 nanocomposite filaments (b to h)

The percentage change in tenacity is found increasing by 16.10%, 43.65%, 51.08% and 67.8% with 0.1%, 0.3%, 0.5% and 0.7% concentration of nano silica in polypropylene filament respectively as compare to pure polypropylene filament as shown in figure 4.30. This may be due to increase in concentration and uniform distribution of nano particles in polymer matrix, which can be seen from the SEM micrographs [137]. It is also supported by the XRD pattern of NPP4 sample i.e. 0.7% nano silica concentration polypropylene filament, in which it has been observed that due to addition of nano silica the crystalline

peaks has increased. Above 0.7% concentration, it is observed that the tenacity decreases by 37.73%, 17.54% and 22.17% with 1%, 1.25% and 1.5% concentration of nano silica in polypropylene filament respectively as compare to pure polypropylene filament. This may be due to agglomeration of nano silica in polymer matrix and thus degrades the tenacity of nano composite polypropylene filaments, this agglomeration of silica nano particles can also be seen from the SEM micrographs [134].

Generally, tensile properties such as tensile strength, stress at break increases while elongation decreases [135, 136]. The increase in strength is seen upto 0.7% concentration of silica nano particles. This may be due to the uniform distribution and incorporation of silica nano particles in polypropylene polymer matrix. Above 0.7% concentration of silica nano particles, it has observed that the strength of filament decreases. This may be due to agglomeration of nano particles which may not be allowing to form compact structure [134].

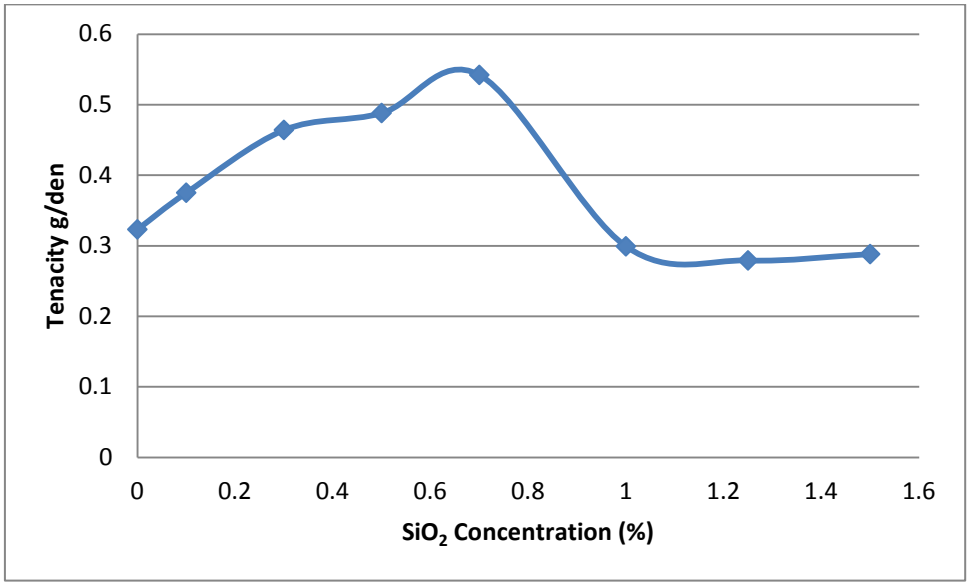

Figure 4.34 Tenacity of pure polypropylene and polypropylene silica nanocomposite filament

The load elongation curves of these undrawn pure polypropylene and silica nano composite polypropylene filaments are shown in figure 4.33 (a to h). The neck phenomenon is observed in all polypropylene filaments, which may be due to slow spinning speed i.e. 400 mpm, caused into amorphous structure. Overall each curve may be divided into three regions. In the first region, the load elongation relationship is approximately linear and the deformation is more or less reversible i.e. elastic nature. The load then reaches a maximum

and falls slightly. After this, filament deforms plastically under constant load conditions and the deformation is not recoverable. The material draws through a neck and the reduced cross-sectional area spreads through the neck through the whole length of the specimen. Finally, as the breaking point is approached, the stress rises sharply with a small increment in strain, signifying strain hardening before catastrophic failure occurs [155].

The increase in tensile strength of nano composites might be due to the phenomenon of reinforcement effect at nanoscopic level. All the samples under consideration are low oriented yarns. So, they need further drawing before application, which will alter its tensile behavior further.

4.2.2.2 Young's modulus and work of rupture

Table 4.12 Effect of nano silica on young's modulus and work of rupture

Sample	% Concentration of nano SiO_2	Young's Modulus (g/den)	Work of rupture at maximum load (kgf.mm)
PP	0.0	0.030	69.28
NPP1	0.1	0.031	29.03
NPP2	0.3	0.045	33.11
NPP3	0.5	0.050	39.97
NPP4	0.7	0.052	78.22
NPP5	1.0	0.027	54.14
NPP6	1.25	0.010	61.85
NPP7	1.5	0.029	39.14

The table 4.12 and figure 4.35 show the young's modulus (Meredith's method) of pure polypropylene filament and nano silica loaded polypropylene filaments. The pure polypropylene filament is showing lower young's modulus i.e. 0.030 g/den than the silica loaded polypropylene nanocomposite filaments i.e. 0.031, 0.045, 0.050 and 0.052 g/den for 0.1%, 0.3%, 0.5% and 0.7% concentration of nano silica particles in polypropylene filament. Above 0.7% concentration i.e. 1%, 1.25% and 1.5%, the drop in young's modulus to 0.027, 0.010 and 0.029 g/den is observed.

The young's modulus is found increased with addition of silica nano particles and also there is increase in young's modulus with increase in percentage loading of silica nano particles i.e. upto 0.7% concentration. It means that initially the load bearing capacity of nanocomposite filament increases with addition of silica nanoparticles. Above 0.7% concentration of silica nano particles, the drop in young's modulus is observed. This drop may be due to agglomeration of silica nano particles, which may not be allowing to form compact structure. Due to which the structure would become brittle and can break easily, which has also been supported by reduced tenacity of these filaments.

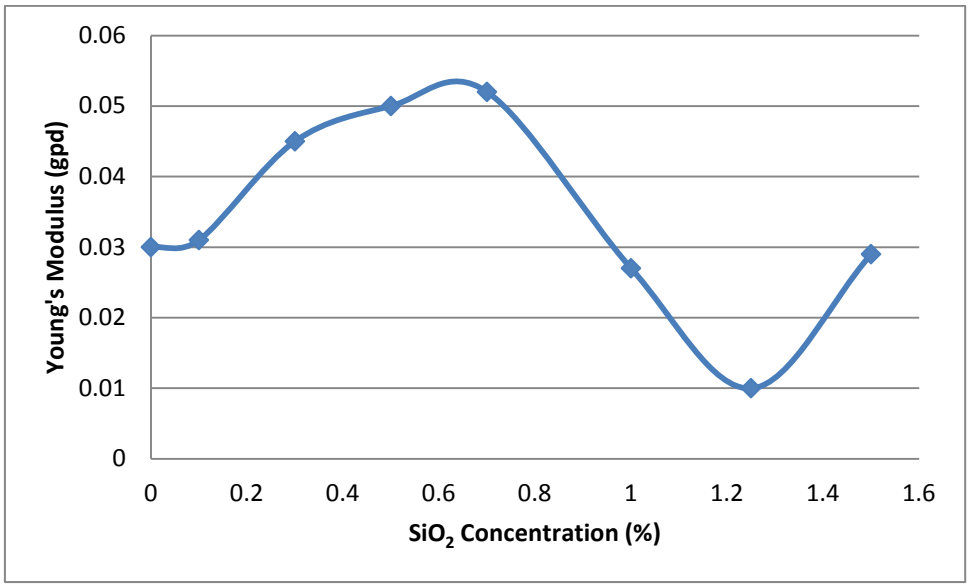

Figure 4.35 Effect of nano silica on young's modulus of treated and untreated polypropylene filaments

The work of rupture is energy or work required to break the specimen, it is a measure of the "toughness" of the material. The area under the load-elongation curve represents the work done in stretching the material to breaking point. The work of rupture value indicates the resistance of the material [148]. Table 4.12 and figure 4.36 show the work at maximum load, of pure polypropylene filament and nano silica loaded polypropylene filaments. The work required to break the pure polypropylene filament (PP) is 69.28 kgf.mm. Sample NPP1, NPP2 and NPP3 are showing reduced work of rupture at maximum load as compare to PP sample, which means that to

break these samples less energy is required. Sample NPP4 i.e. 0.7% concentration of nanosilica is showing increased work of rupture i.e. more energy is required to break this sample which means that this sample became more tough and also overall this sample is showing good property in all aspects i.e. tenacity and young's modulus. Above 0.7% concentration sample again there is reduction in work of rupture, it may be due to agglomeration of nano particles and making the filament brittle and break easily with less energy, it may be due to agglomeration of nano particles, agglomeration can be seen from the SEM micrograph in figure 4.20 to 4.22. Overall the work of rupture of the NPP4 sample of 0.7% nano silica loaded polypropylene filament is showing rise as compare to all other samples. Higher nano silica loaded polypropylene filament would not be allowing the material to become compact due to agglomeration of the nano particles and becoming more brittle, which would be hindering the development of compact structure. Similar trend has been observed in case of polyamide silica nanocomposite films, in which due to addition of silica nano particles the strength, young's modulus has found increasing upto 0.7% concentration and thereafter there is decrease in these properties observed.

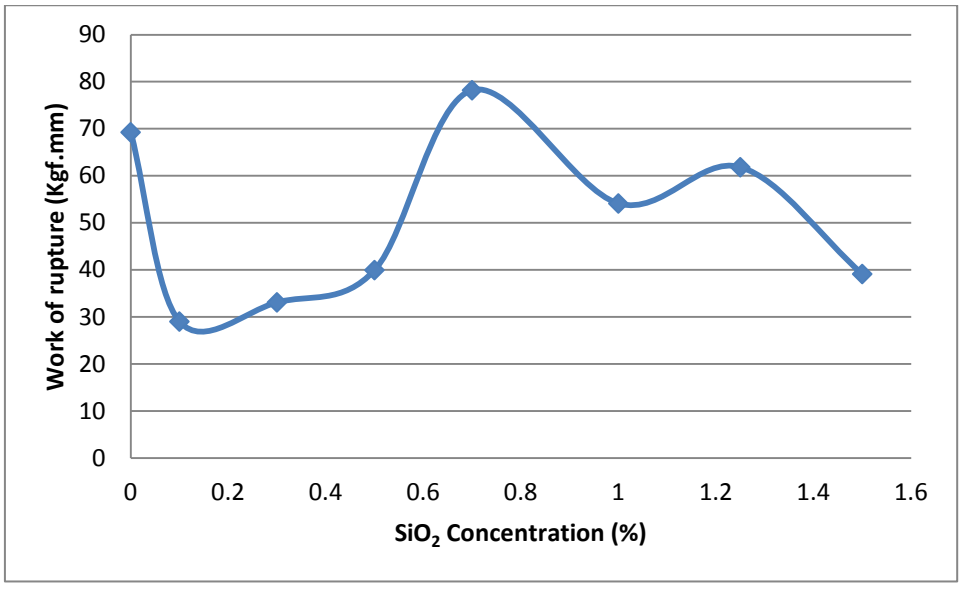

Figure 4.36 Effect of nano silica on work of rupture of treated and untreated polypropylene filaments

4.3 PART – III: POLYMER SILICA NANOCOMPOSITE FABRIC

Polymer Silica nanocomposite fabrics were prepared by incorporating different quantities of silica nano particles to polymeric fabric i.e. polyester fabric by pad-dry-cure method. The prepared nanocomposite fabrics were analyzed in terms of change in their structural and mechanical properties. Then the comparison was done with the pure polyester fabric.

In this part, the basic polymer was changed to polyester in fabric form, and the concentration of silica nano particles is kept as 1 gpl, 2.5 gpl and 5 gpl. The polyester fabric with different proportions of silica nanoparticles were prepared by pad-dry-cure method. The evaluation of prepared polymer silica nanocomposite fabric was done in terms of their structural properties through SEM, FTIR, XRD and DSC techniques. Nanocomposite fabrics were also evaluated for changes in their mechanical properties and compared with the pure polyester fabric. The nomenclature used during discussion for the samples prepared is as given in table 4.13.

Table 4.13 Compositions of polypropylene SiO_2 nanocomposite filament

Sr. No.	SAMPLE	COMPOSITIONS
1	PT	Polyester fabric without SiO_2
2	NPT1	Polyester fabric with 1 gpl SiO_2
3	NPT2	Polyester fabric with 2.5 gpl SiO_2
4	NPT3	Polyester fabric with 5 gpl SiO_2

PT: polyester, NPT: Nano silica loaded polyester

4.3.1 STRUCTURAL ANALYSIS

4.3.1.1 Surface morphological analysis through SEM

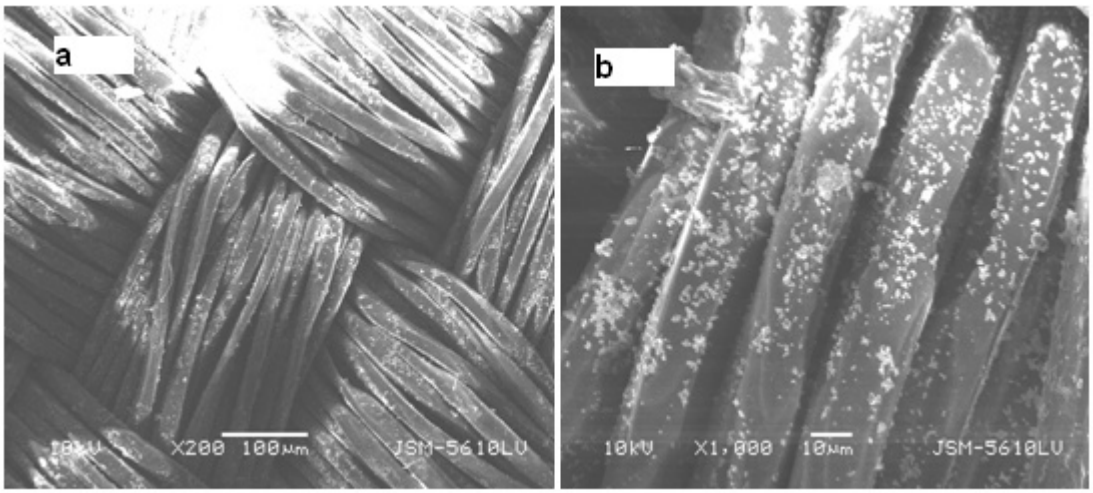

Figure 4.37 SEM microphotographs of polyester fabric treated with silica nano particles

The surface morphology of the treated polyester fabric sample was observed on scanning electron microscopy. The result is shown in figure 4.37, the nano scale silica particles can be clearly seen well distributed on the surface of polyester sample. The particle size plays a primary role in determining their adhesion to the fibre. It is reasonable to expect that the largest particle agglomerates will be easily removed from the fibre surface, while the smaller particle will penetrate deeper and adhere strongly into the fabric matrix. As reported by Wang et. al [41] in their study in 2004 that nano particles have large surface area to volume ratio, which makes it easy for them to attach to fibres or fabrics and increase the durability of the functions imparted by the particles.

4.3.1.2 FTIR spectral analysis

The chemical compositions of the treated and untreated polyester fabrics were evaluated using Fourier transform infrared spectroscopy (FTIR) Nicolet is10 FT-IR Spectrometer (Thermo Scientific). IR characterization absorption peaks of untreated and treated fabrics are shown in figure 4.38 and 4.39 respectively.

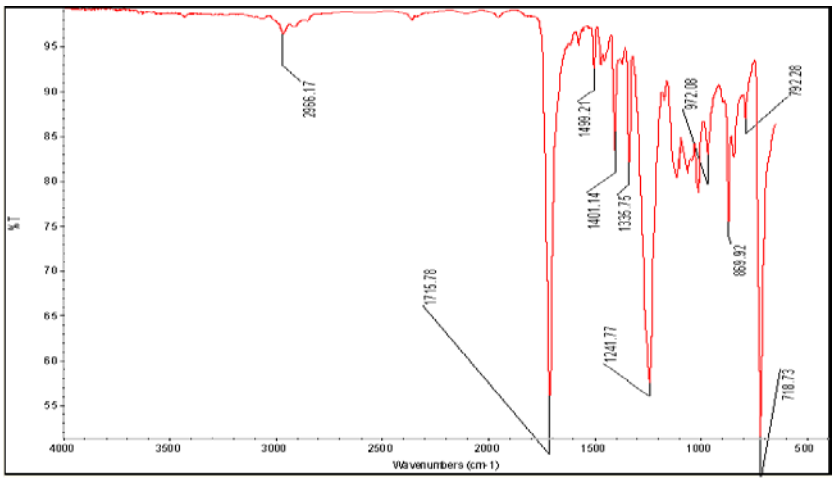

Figure 4.38 IR absorption peaks of untreated polyester fabric (PT)

Table 4.14 and figure 4.38 represents the IR characterization absorption peak of pure polyester fabric, from which it can be seen that the peaks associated were 2966 cm^{-1} shows C-H stretching, 1715 cm^{-1} shows C=O vibration, 1499 cm^{-1} shows skeletal ring stretching vibration of aromatic and hetero aromatic ring, 1401 cm^{-1} of aromatic ring, 1335 cm^{-1} & 1021 cm^{-1} shows carboxylic ester or anhydride, 1021 cm^{-1} indicates the presence of O=C–O–C or secondary alcohol, 1241 cm^{-1} shows C-O stretch alcohols carboxylic acid, 972 cm^{-1} is of C=C stretching, 869 cm^{-1} peak shows five substituted H in benzene, 792 cm^{-1} shows C-H stretching in aromatic ring and 718 cm^{-1} shows C-H rock alkane. The main structure of the polyester sample had ester, alcohol, anhydride, aromatic ring and heterocyclic aromatic rings. Alcohol was able to react with anhydride and produce ester groups. This is a reason that there is still alcohol and anhydride as residual reactants left in the polyester. The peak at 1409 cm^{-1} corresponded to the aromatic ring which is a stable group. It was the characteristic absorption peak of PET. The peak at 1715 cm^{-1} was assigned to the ester group.

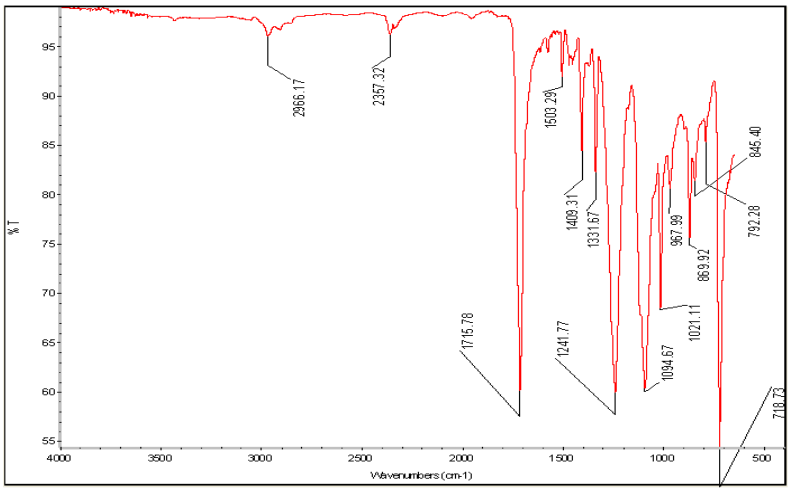

Figure 4.39 IR absorption peaks of treated polyester fabric (NPT3)

Peaks shown by pure polyester fabric are identical in polyester silica nanocomposite fabric as shown in figure 4.39, additionally the nanocomposite fabric shown the peaks of silica at 845 cm^{-1} corresponds to Si-O-Si [143] bending vibration, band at 1094 cm^{-1} correspond to asymmetric stretching vibration of Si-O-Si [144, 86] band, Si-C stretching belongs to 2357 cm^{-1} [140].

Table 4.14 FTIR characterization peaks of pure polyester and polyester/Silica nanocomposite fabric

Groups	**Wave number (cm^{-1})**	
	PT	**NPT3**
C-H rock alkane	718	718
C-H stretching in aromatic ring	792	792
Si-O-Si bonds vibration		845
H in benzene	869	869
C=C stretching	972	967
Carboxylic ester or anhydride, O=C-O-C or secondary alcohol	1021	1021

Si-O-Si asymmetric stretching vibration band		1094
C-O stretch alcohols carboxylic acid	1241	1241
Carboxylic ester or anhydride	1335	1331
Aromatic ring (PET)	1401	1409
Skeletal ring stretching vibration of aromatic and hetero aromatic ring	1499	1503
C=O stretch (strong), unsaturated ester group (polyester)	1715	1715
Si-C stretching		2357
C-H stretching	2966	2966

4.3.1.3 X-ray diffraction analysis

The characterization of treated and untreated polyester fabrics was done using PANalytical XRD. The XRD of both the fabrics was done within the 2θ range of 10° to 30° at the scan speed of 3°C per minute at 25°C temperature, using Cu-K_α radiation of wavelength 1.5406 Å. The diffraction profiles were obtained for individual samples. The X-Ray Diffractometer X'pert Pro PANalytical, Singapore make was used. The XRD patterns are given in figure 4.40 and 4.41 for PT and NPT3 samples i.e. pure polyester fabric and 5 gpl nano silica in polyester fabric, respectively.

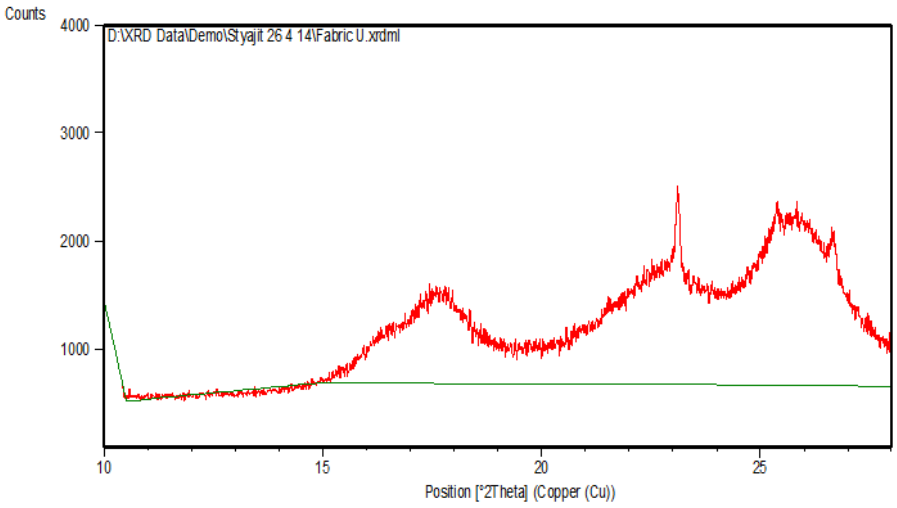

Pos. [°2θ]	Height [cts]	d-spacing [Å]	Area [cts*°2θ]	Rel. Int. [%]
17.66	854	5.09492	1650.99	62.13
23.11	719	3.87573	92.96	100
25.89	1179	3.45912	1203.79	87.52
26.6	981	3.41702	438.67	82.27

Figure 4.40 XRD pattern of pure polyester fabric (PT)

XRD pattern of PT sample as shown in figure 4.40 shows semi crystalline state of the material. Four prominent features are observed. One distinct crystalline peak is observed due to which the semi crystalline nature of polyester fibre may be considered. Some broadness in peak is also observed in rest of the peaks, but they by and large denote the amorphous nature of fibre. The peak at 2θ value of 23.11° has the highest intensity followed by 25.89°, 26.6° and 17.66° and these peaks are indicative of polyester polymer [156].

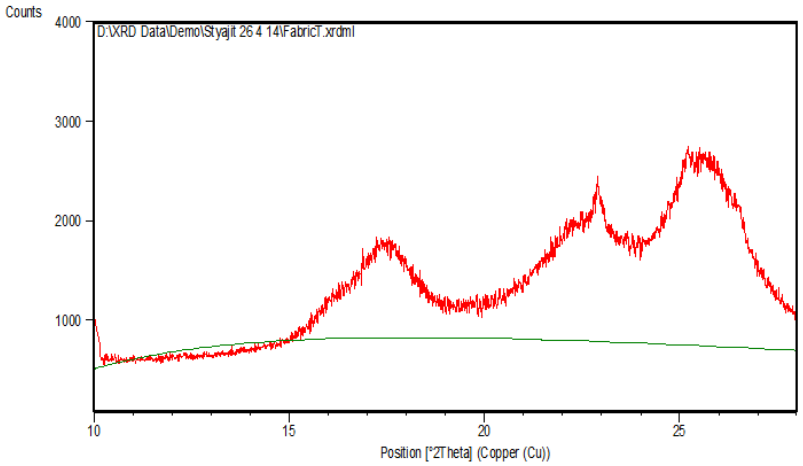

Pos. [°2θ]	Height [cts]	d-spacing [Å]	Area [cts*°2θ]	Rel. Int. [%]
17.2642	813	5.11714	1116.17	66.67
22.9302	1108	3.91579	1407.17	83.27
25.7797	1525	3.50489	3012.15	100
26.0695	309	3.44348	62.95	81.48

Figure 4.41 XRD pattern of polyester silica nanocomposite fabric (NPT3)

The incorporation of silica nano particles lead to the development of some kind of force which drifts the atomic planes, such that the d-value increases. From the figure 4.42 it can be seen that the intensities in the treated sample is on the lower side compared to the untreated samples. There is a shift in the peak 2θ values towards the lower side in general, indicating a change in d-values across the range, to the same extent. Hence, the presence of silica nano particles affects the structure of material in terms of atomic plane spacing. The SEM micrographs show the incorporation of silica nano particles well dispersed on the surface of fabric. The d-values for the observed diffraction peak of silica is in close agreement with those reported for corresponding standard samples as reported in JCPDS data file 84-0384. Here the peak corresponding to the d-value of 3.4224 Å is in agreement.

Sosa et. al [129] reported that as each crystalline material including the semi crystalline polymers as well as metal and metal oxide particles and layered silicate nano particles have a characteristic atomic structure, it will diffract X-ray in a unique characteristic diffraction order or pattern.

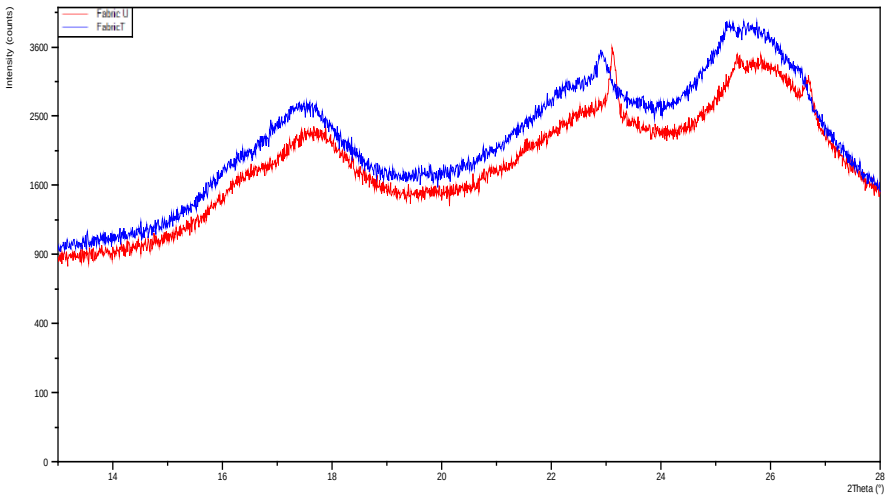

Figure 4.42 Combined XRD patterns of PT and NPT3 samples

4.3.1.4 Thermal analysis

Differential scanning calorimetry (DSC) was done to study the effect of incorporation of nano silica particles on thermal behavior of polyester fabric, which is shown in figure 4.43 and 4.44.

Table 4.15 Enthalpy (ΔH) of treated and untreated polyester fabric

Sr. No.	Concentration of nano silica (g/lt)	Melting Temperature °C	Enthalpy (ΔH) (J/g)
1	0.0	251.72	67.77
2	5.0	251.71	71.47

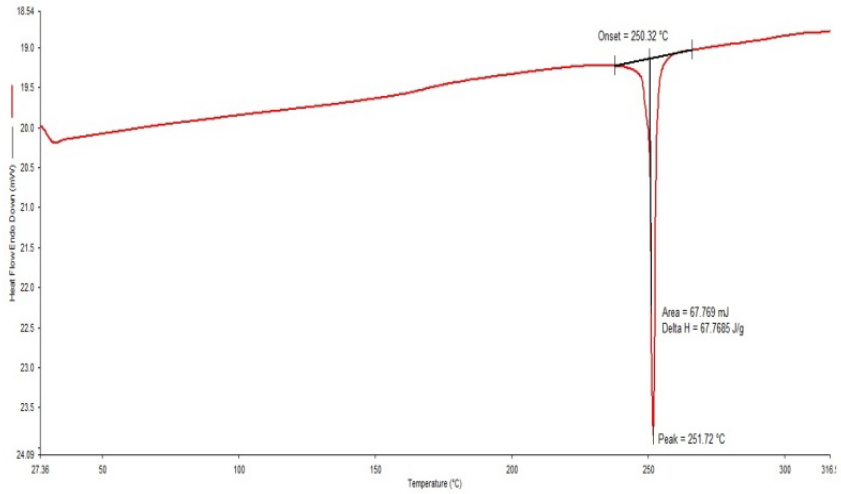

Figure 4.43 DSC curve of pure polyester fabric (PT)

Table 4.15 shows the melting temperature and enthalpy (ΔH) values of treated and untreated fabrics determined by DSC. Figure 4.43 shows the thermal behavior of pure polyester fabric. The melting temperature of polyester is 251.72°C and the enthalpy required to melt the pure polyester is 67.77 J/g. Figure 4.44 shows the thermal behavior of 5 gpl silica treated polyester silica nanocomposite fabric. The melting temperature of silica treated polyester fabric is 251.71°C, so there is no effect on melting temperature due to addition of silica nano particles. The enthalpy required to melt silica treated polyester fabric is 71.47 J/g. Due to nano silica treatment the rise in

enthalpy is by 5.46%. This rise in enthalpy may be due to nanoscopic level of silica, hence inducing better thermal stability to the fabric. Altan et. al [137] has made similar observation for polypropylene and polyester, being thermoplastic fibre may behave in the same manner due to the coating of nano SiO_2 particles. Similar observations are observed in earlier parts like in case of polyamide film and polypropylene filament, due to addition of silica nanoparticles the enthalpy required to melt the film/filament has also increased and there is no change in melting temperature due to addition of silica nanoparticles.

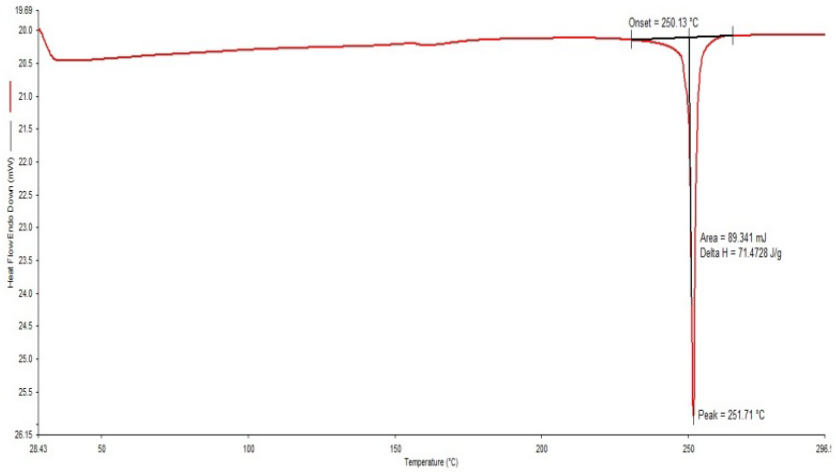

Figure 4.44 DSC curve of polyester fabric treated with 5gpl nano silica (NPT3)

4.3.2 MECHANICAL PROPERTIES

Treated and untreated polyester fabrics were evaluated for the change in their mechanical properties in terms of tensile strength, young's modulus, work of rupture, tearing strength and crease recovery angle. The treatment was carried out by pad-dry-cure method at different levels of concentration i.e.1gpl, 2.5gpl and 5gpl of silica nano particles.

4.3.2.1 Tensile strength

Table 4.16 Tensile strength of polyester fabric

Sample	Concentration of nano silica (g/lt)	Tensile strength (Kgf)		Stress Kgf/mm^2		Strain %	
		Warp way	Weft way	Warp way	Weft way	Warp way	Weft way
PT	Untreated sample	99.84	73.86	23.77	17.59	31.46	34.2
NPT1	1.0	101.7	77.66	24.21	18.49	29.61	39.89
NPT2	2.5	103.4	82.15	24.62	19.56	30.72	40.67
NPT3	5.0	104.9	85.04	24.98	20.25	31.20	36.74

Gauge length = 200 mm, Thickness of fabric = 0.21 mm, Width of fabric = 20 mm, Cross sectional area = 4.2 mm^2

The treated and untreated polyester samples were tested on Lloyd LRX tensile strength tester and the results are shown in table 4.16 and their tensile behavior is shown in figures 4.45 to 4.49. The untreated polyester fabric is showing 23.77 and 17.59 kgf/mm^2 stress in warp and weft way respectively. The stress value of warp direction is higher than the weft direction stress of polyester fabric. It may be due to the density of warp yarns is higher than the weft yarns i.e. 36 ends/cm, and 28 picks/cm respectively.

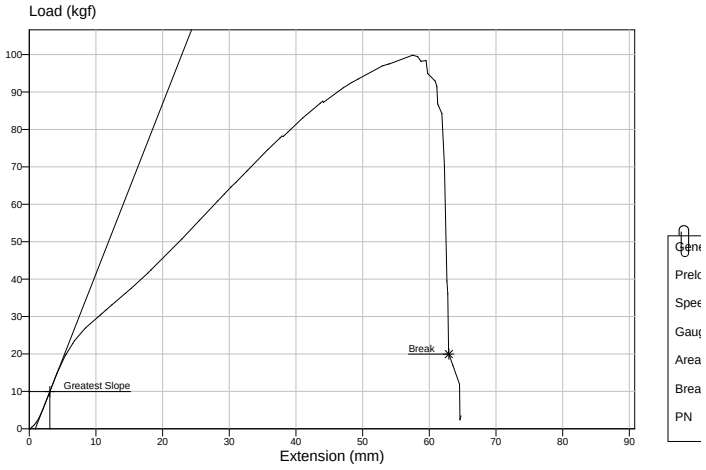

Figure 4.45 Load elongation behavior of pure polyester fabric (warp way)

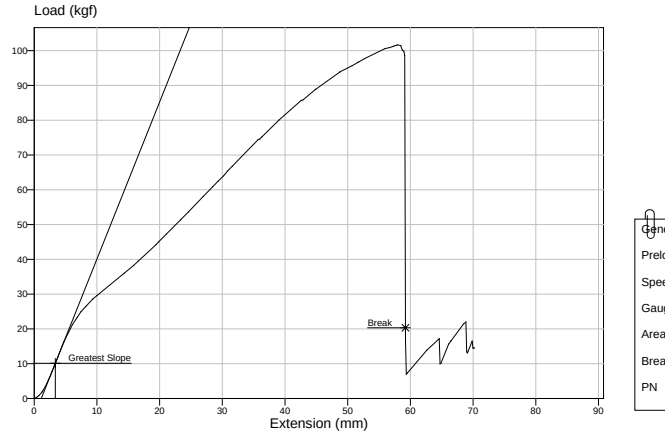

Figure 4.46 Load elongation behavior of 5 gpl polyester fabric (warp way)

Due to the treatment of nano silica in different concentrations to polyester fabric, the stress values in warp and weft direction are 24.21, 24.62 & 24.98 kgf/mm^2 and 18.49, 19.56 and 20.25 kgf/mm^2 respectively. The treatment of silica nano particles to the polyester fabric increases the stress property in warp as well as weft directions. This increase in strength may be due to binding caused by introduction of silica nano particles into the polymer matrix. The warp tensile strength is higher than the weft tensile strength because generally in warp, stronger yarns are used due to high stresses gets induced during weaving in the warp yarns as compare to the weft yarns and also the density of warp is higher than the weft yarns as explained above.

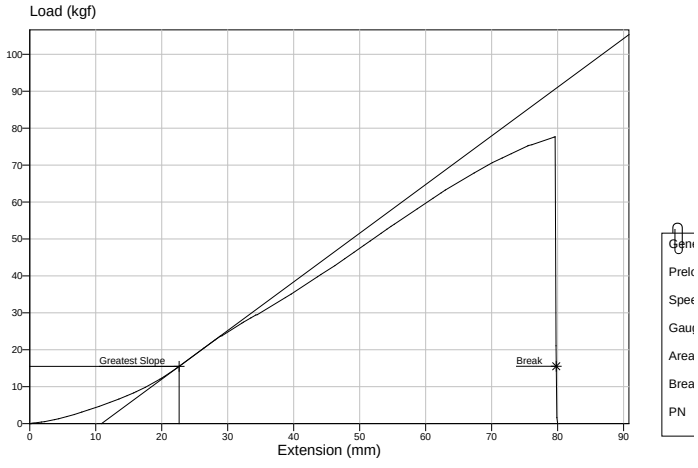

Figure 4.47 Load elongation behavior of pure polyester fabric (weft way)

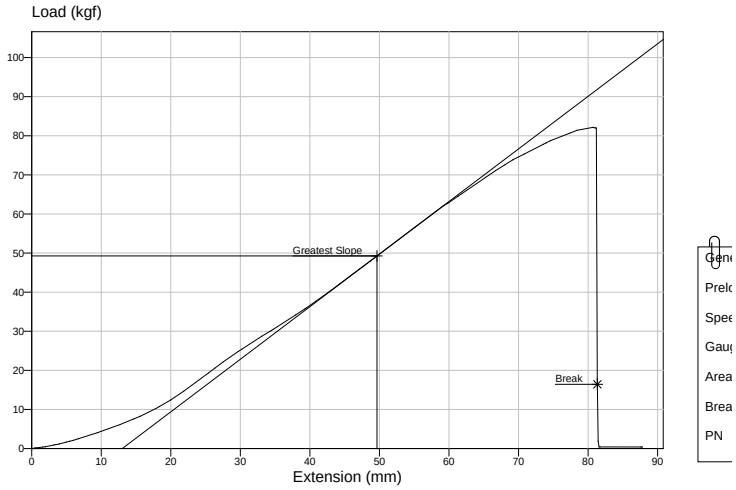

Figure 4.48 Load elongation behavior of 5 gpl polyester fabric (weft way)

The tensile strength is found increasing in both the directions as the concentration of silica nano particles increased. The percentage strain of warp and weft direction has not affected significantly due to the nano silica treatment. But the overall strain percentage of polyester fabric in weft direction is higher than the warp direction strain. This may be due to the less weaving tension in weft yarns during weaving, which may cause high crimp into the weft yarns.

The results are further supported by Mohltig et. al [22] 2005 reported that the possibility to increase the mechanical properties to be considered it as industrial nano reinforced fibre by treating the finished fabric with SiO_2 coating.

4.3.2.2 Young's modulus and work of rupture

The table 4.17 shows the young's modulus of untreated polyester fabric and nano silica treated polyester fabric. The young's modulus is calculated on the bases of Meredith's method. The untreated polyester fabric is showing 1.55 kgf/mm^2 young's modulus in warp direction and 0.44 kgf/mm^2 in weft direction. The warp direction young's modulus is higher than weft direction young's modulus, which means that the warp yarns are more stiffer than weft yarns, i.e. warp yarns can take more load with less deformation as compare to weft yarns. The young's modulus of nano silica treated polyester fabric in warp and weft directions is 1.51, 1.53 and 1.57 kgf/mm^2 and 0.41, 0.41 and 0.40 kgf/mm^2 respectively. Due to addition of nano silica particles

there is no significant change in young's modulus is observed in warp as well as weft direction. The young's modulus of polyester fabric in warp direction is higher than weft direction. The reason could be the same as given for the untreated polyester sample.

Table 4.17 Effect of nano silica on young's modulus and work of rupture of polyester fabric.

Sample	Concentration of nano SiO_2 (g/lt)	Young's Modulus in (kgf/mm^2)		Work of rupture at maximum load (kgf.mm)	
		Warp way	Weft way	Warp way	Weft way
PT	0.0	1.55	0.40	3475.3	2904.7
NPT1	1	1.51	0.41	3748.6	3123.7
NPT2	2.5	1.53	0.41	3853.1	3289.3
NPT3	5	1.57	0.40	3997.8	3424.8

The "toughness" of the material is measured in terms of work of rupture of the material. The area under the load-elongation curve represents the work done in stretching the material to breaking point. The work of rupture value indicates the resistance of the material [148]. Table 4.17 shows the work at maximum load, of untreated polyester fabric and nano silica treated polyester fabrics. The work required to break the untreated polyester fabric (PT) is 3475.3 kgf.mm in warp direction and 2904.7 kgf.mm in weft direction. The work required to break the polyester fabric in warp direction is higher than the weft direction, which means that the warp direction polyester fabric is tougher than weft direction. As the work of rupture is a product of breaking load and elongation, the reason of high work of rupture in warp direction polyester fabric as compare to weft direction may be due to high breaking load required to break the polyester fabric in warp direction as compare to weft direction and the elongation at break of warp is less than weft direction polyester fabric but the difference in breaking load is much high as compare to the difference in elongation property of warp and weft direction polyester fabric.

The sample NPT1, NPT2 and NPT3 are showing increase in work of rupture to 3748.6, 3853.1 and 3997.8 kgf.mm in warp direction and 3123.7, 3289.3 and 3424.8 kgf.mm in weft direction as compare to PT sample, which means that to break treated samples high energy is required. The nano particles could be enhancing the work property of polyester fabric in both the directions. The work of rupture of polyester fabric in warp direction is higher than weft direction. The reason is same as above as higher breaking load required to break the polyester fabric in warp direction as compare to weft direction and the elongation at break of warp is less than weft direction polyester fabric but the difference in breaking load is much high as compare to the difference in elongation property of warp and weft direction polyester fabric.

4.3.2.3 Tearing strength

The treated and untreated samples were tested on Elmendorf tearing tester. Table 4.18 shows result of tearing strength of treated and untreated polyester fabric. Untreated polyester fabric tearing strength is 4352 and 3840 gf in warp and weft directions respectively. Here the warp direction tearing strength is higher than the weft direction tearing strength of polyester fabric. The reason could be high density of warp i.e. 36 ends/cm as compare to 28 picks/cm of weft. The treated samples, NPT1, NPT2 and NPT3 are showing minor improvement in tearing strength as compare to untreated sample. Also it is observed that as the concentration of silica nano particles increases, there is only 1 to 2 percentage increase in tearing strength, which is very minute. So, it can be interpreted that incorporation of nano silica particles does not affect the tearing strength of polyester fabric in both warp and weft direction. This may be due to the smaller size of the particle which may not be helping to improve tearing property.

Table 4.18 Tearing Strength of polyester fabric

Sr. No.	Concentration of nano silica (g/lt)	Tearing Strength (gf)	
		Warp way	Weft way
1	Untreated sample	4352	3840
2	1	4388	3856
3	2.5	4412	3880

4	5	4458	3902

4.3.2.4 Crease recovery angle

The crease recovery test is a measure the ability of a fabric to resist creasing. The magnitude of this crease recovery angle is an indication of the ability of a fabric to recover from creasing [157].

Table 4.19 Crease Recovery Angle of Polyester fabric

Sr. No	Concentration of nano silica (g/lt)	Warp way		Weft way	
		30 Sec	60 Sec	30 Sec	60 Sec
1	Untreated sample	140	147	105	110
2	1	142	147	109	114
3	2.5	145	148	110	116
4	5	147	151	113	119

The treated and untreated samples were tested on crease recovery angle tester and the results are shown in table 4.19. The crease recovery angle of untreated polyester fabric for warp way for 30 seconds and 60 seconds are 140° and 147° respectively. The weft way crease recovery angle for 30 seconds and 60 seconds are 105° and 110° respectively. The warp way crease recovery is higher than the weft way and as the time increases i.e. from 30 sec. to 60 sec. the recovery angle has increased in both the directions. Due to the treatment of silica nano particles in different concentrations as 1 gpl, 2.5 gpl and 5 gpl, the crease recovery angle has increased to 142, 145 & 147 and 147, 148 & 151 for 30 seconds and 60 seconds of warp way polyester fabric respectively. The weft way crease recovery angles are 109, 110 & 113 and 114, 116 & 119 for 30 seconds and 60 seconds respectively.

The result shows minor improvement in crease recovery angle of the treated samples i.e. warps way and weft way. The crease recovery angle is found increasing as the concentration of nano silica is increased. Overall the crease recovery angle in warp way is higher than the weft way in both treated and untreated samples. The silica nano particles because of their small size can enter in between the polymer molecules and perhaps act as filler or cross linking agent which also contributes to the load sharing phenomenon during load application to the material. Unlike chemical cross linking

which cause an improvement in crease recovery angle at the cost of imparting some rigidity in the material to an extent depending on the extent of cross linking. The incorporation of nano silica particle remains quite gentle in this regard. There was little improvement in the property which proves that the particles penetrated in between the polymer chain molecules, do not interfere much to the polymer flexibility. Also the crease recovery property of fabric improves with increase in the concentration of silica nano particles [158].